8-2012

An Analysis of the Redox Properties and Stability of Chlamydomonas reinhardtii Cytochrome F, Cytochrome C6, and Mutants thereof

Nicole Lynn Vanderbush
University of Arkansas, Fayetteville

AN ANALYSIS OF THE REDOX PROPERTIES AND STABILITY OF *CHLAMYDOMONAS REINHARDTII* CYTOCHROME F, CYTOCHROME C_6, AND MUTANTS THEREOF

AN ANALYSIS OF THE REDOX PROPERTIES AND STABILITY OF *CHLAMYDOMONAS REINHARDTII* CYTOCHROME F, CYTOCHROME C_6, AND MUTANTS THEREOF

A dissertation submitted in partial fulfillment
Of the requirements for the degree of
Doctor of Philosophy in Cell and Molecular Biology

By

Nicole Lynn Vanderbush
Shorter University
Bachelor of Science in Biology, 2006

August 2012
University of Arkansas

ABSTRACT

This body of work presents mutagenesis studies conducted on two c-type cytochromes from *Chlamydomonas reinhardtii*. Cytochrome f, a unique c-type cytochrome, is investigated in regards to its redox potential, the dependence of the redox potential, and the thermal stability of the protein. The mutations made were Y1F, Y9F, Y160F, Y160L, R156L, and R156K. The residues that were mutated surround the heme. It was found that, relative to the wild-type, only the Y160L and R156 mutants showed any difference in midpoint potential at pH 7. Wild-type and mutants both had a midpoint potential that was dependent upon pH indicating that none of the investigated residues are responsible for the alkaline transition seen in cytochrome f. The stability of each of the mutants also did not vary from that of the wild-type protein. The arginine mutants were unsuitable to be investigated by current methods in regards to the pH dependence of the midpoint potential and stability.

Cytochrome c_6, a typical class I, c-type cytochrome, and the mutants K29I and K57I were investigated in the same manner as was cytochrome f along with CD spectral studies. The K29 and K57 residues are found in the vicinity of the heme. In regards to the midpoint potential of the mutants at pH 7, they were found to be lower than that for the wild-type protein. The midpoint potential for both the wild-type and mutants was found to be independent of pH as far as pH 10. The melting temperature of the mutants, when examined, was also lower than that of the wild-type indicating a lower relative stability of the mutants when compared to the wild-type. CD spectroscopy was done to investigate if an aromatic residue in the vicinity of the heme is responsible for the negative Cotton effect seen in the oxidized spectrum. The residue in *Chlamydomonas reinhardtii* cytochrome c_6 is a tryptophan that is not co-facially oriented with respect to the heme. The absence of the Cotton effect provides further evidence that for the presence of a negative Cotton effect there must be an aromatic residue in the vicinity and it must be co-facially oriented with respect to the heme.

This Dissertation is approved for recommendation
to the Graduate Council.

Dissertation Director:

_____
(Dr. Dan Davis)

Dissertation Committee:

_____
(Dr. Frank Millett)

_____
(Dr. Bill Durham)

_____
(Dr. Mack Ivey)

DISSERTATION DUPLICATION RELEASE

I herby authorize the University of Arkansas Libraries to duplicate this thesis when need for research and/or scholarship.

Agreed_____
(Nicole Lynn Vanderbush)

Refused_____
(Nicole Lynn Vanderbush)

ACKNOWLEDGEMENTS

I would like to thank God and my family for being my support throughout my life to get me to this point. I would also like to thank Dr. Chuck Pearson who was my main guidance and support during my undergraduate and offered much needed advice and sanity throughout graduate school.

I would like to thank Dr. Lois Geren and Marylyn Davis for all of their help in the lab and the support they showed me during my struggles in the lab and in life. It was such a blessing to have not only one, but two moms away from home.

I would like to thank my dissertation committee, Dr. Frank Millett, Dr. Bill Durham, and Dr. Mack Ivey, for all the teaching and guidance they provided me during this process. It is a privilege to be able to learn from great minds.

Lastly, I have to thank my dissertation advisor Dr. Dan Davis. I could not have had a better advisor. I cannot imagine anyone better suited to have helped my through this process and be so supportive of me. I only hope one day that I can be the teacher that he is.

TABLE OF CONTENTS

Page

List of Figures

Figure **Page**

LIST OF TABLES

Tables **Page**

CHAPTER 1 – INTRODUCTION

The vast majority of earth's energy is derived from the light of the sun through the process of photosynthesis. Photosynthesis is the conversion of light energy into chemical energy stored in the form of carbohydrates. The chemical equation given to describe the sum of the reactions that occur in photosynthesis is given as:

$$\text{Light} + CO_2 + H_2O \rightarrow (CH_2O) + O_2$$

This simple equation represents the sum of a number of complex energy transducing reactions performed by a set of proteins located within the cells of plants, algae, and some forms of bacteria during oxygenic photosynthesis. The equation should be modified by removing O_2 as a product to account for the reactions of anoxygenic photosynthesis, a type of photosynthesis that occurs in anoxygenic photosynthetic bacteria in which no molecular oxygen is generated because of the lack of the ability of the organisms to extract electrons from water (Berg et al. 2002). Figure 1.1 shows the comparison of oxygenic and anoxygenic photosynthesis.

Oxygenic photosynthesis is divided into the light dependent reactions and the light independent reactions. The light dependent reactions consist of a series of electron and proton transfer reactions that take place within the chloroplasts of higher plants and algae. The chloroplast is a double membrane bound organelle that contains a system of thylakoids, or flattened sacks, found in stacks called grana which are connected by stroma lamella. This system of thylakoids is found in a dense liquid matrix called the stroma contained within the chloroplast's inner membrane as seen in Figure 1.2 (Whitmarsh J. and Godvinjee 2001). Located inside, around, and within the membrane of the thylakoid are a set of proteins that can function to utilize the energy of light. The absorption of light results in the excitation of electrons and the subsequent energetic downhill transfer of the electrons through the chain of proteins associated with the membrane. Photons of light are absorbed by a number of pigment molecules such as alpha and beta chlorophyll along with carotenoids and beta-carotene, termed antennae pigments, and are subsequently transferred to a special pair of chlorophyll molecules located at the reaction centers of photosystem I and Photosystem II, P700 and P680 respectively. When the photon reaches the special pair it results in the excitation of electrons at the reaction centers (Berg et al. 2002).

Figure 1.1: Illustration of the differences and similarities between oxygenic and anoxygenic photosynthesis (Blankenship 1992).

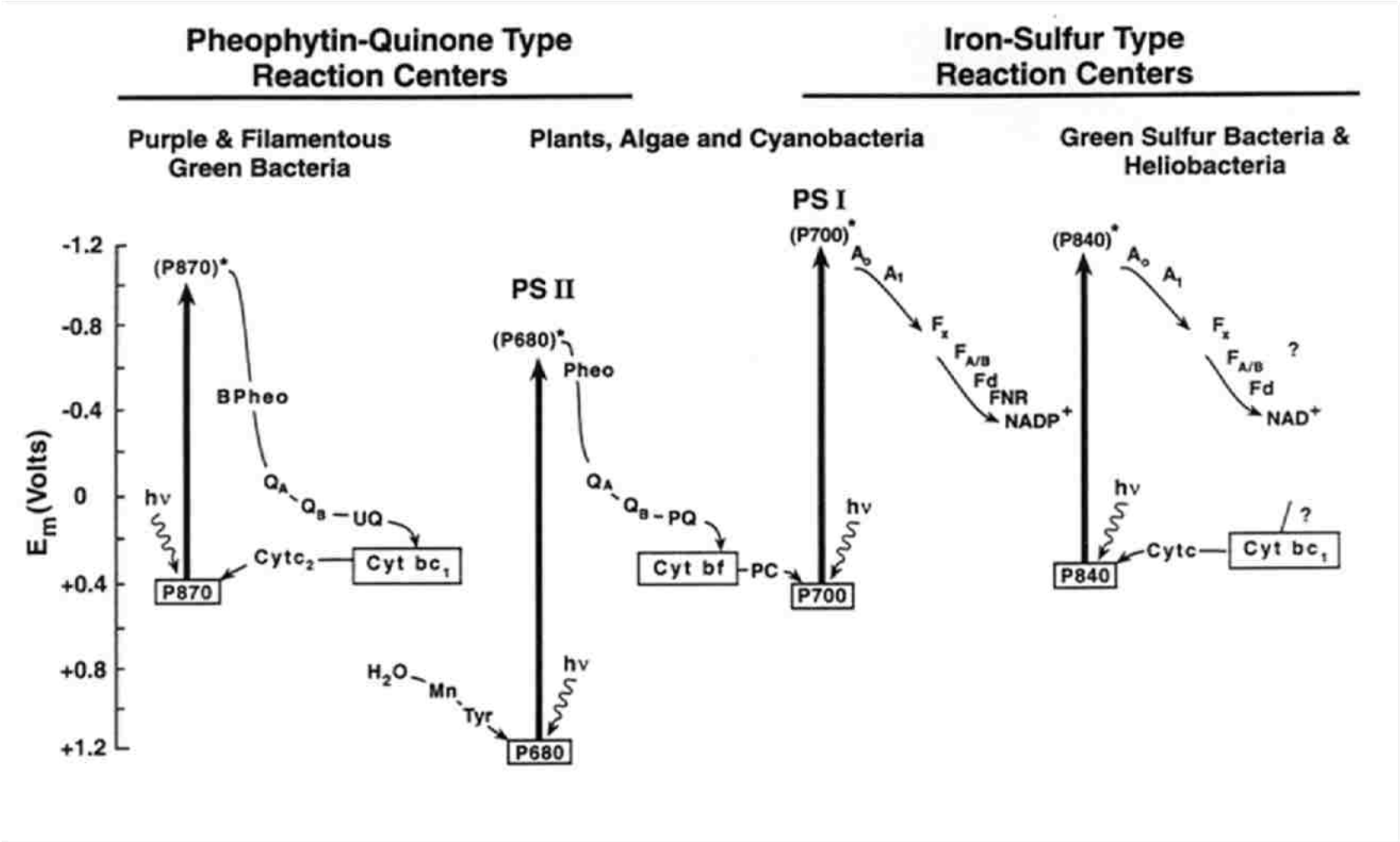
Pheophytin-Quinone Type Reaction Centers
Iron-Sulfur Type Reaction Centers
Purple & Filamentous Green Bacteria
Plants, Algae and Cyanobacteria
Green Sulfur Bacteria & Heliobacteria
PS I
PS II
E_m(Volts)
-1.2
-0.8
-0.4
0
+0.4
+0.8
+1.2
(P870)*
BPheo
Q_A Q_B – UQ
hν
$Cytc_2$
Cyt bc_1
P870
(P680)*
Pheo
Q_A Q_B – PQ
Cyt bf
PC
H_2O Mn Tyr
P680
(P700)*
A_o A_1
F_x
$F_{A/B}$
Fd
FNR
$NADP^+$
P700
(P840)*
?
NAD^+
Cytc
P840

Figure 1.2: A typical chloroplast. (*a*) Schematic diagram of a higher plant chloroplast. (*b*) Electron micrograph of a chloroplast (L. Taiz, E. Zeiger 2006).

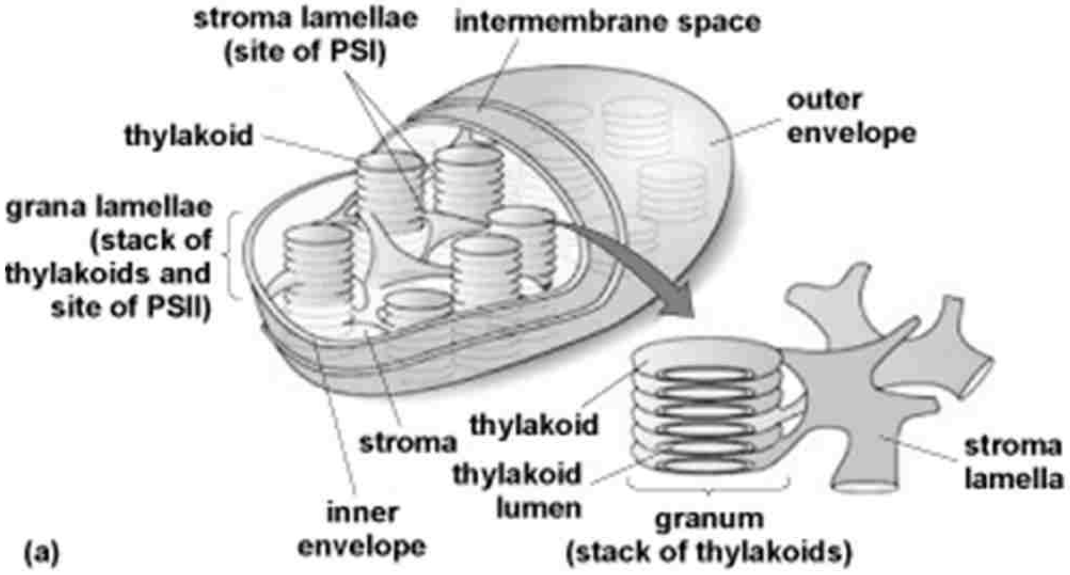
stroma lamellae
(site of PSI)
intermembrane space
outer
envelope
thylakoid
grana lamellae
(stack of
thylakoids and
site of PSII)
stroma
thylakoid
thylakoid
lumen
stroma
lamella
inner
envelope
granum
(stack of thylakoids)
(a)

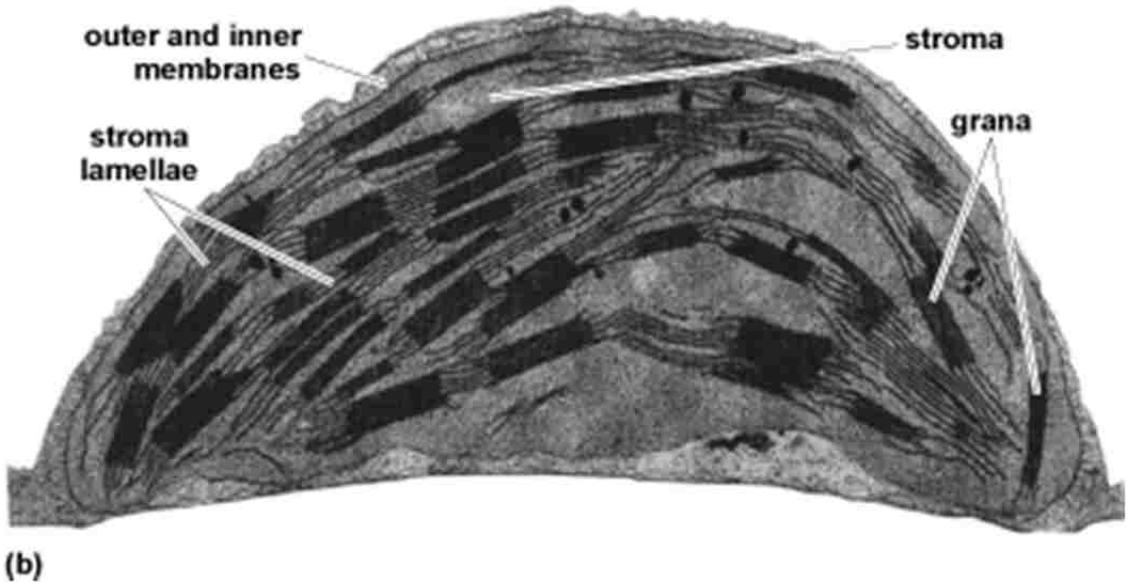
outer and inner
membranes
stroma
grana
stroma
lamellae
(b)

In cyclic electron transport the excited state electron at photosystem II is transferred through a series of molecules: the intermembrane plastoquinone molecules, the membrane bound b_6f complex, and the luminal mobile protein plastocyanin before arriving at the photosystem I reaction center where it replaces an excited electron that was concurrently excited and transferred through the mobile stromal protein ferredoxin, the peripheral stromal protein ferredoxin, and ferredoxin /NADP oxidoreductase where it is used to convert $NADP^+$ into NAPDH. The electron lost from the photosystem II reaction center is replaced by the splitting of a water molecule resulting in the evolution of molecular oxygen and the contribution of hydrogen ion to the luminal side of the membrane. An electrochemical gradient in the form of a hydrogen ion gradient is also produced across the membrane of the thylakoids during the process of the electron transport. Proton translocation across the membrane is coupled to the electron transport during the reduction of plastoquinone by photosystem II on the stromal side of the membrane and the cytochrome b_6f complex's reaction with plastoquinone on the luminal side of the membrane where the plastoquinone molecule is oxidized. This results in the release of hydrogen ions into the lumen of the thylakoid. The hydrogen ion gradient generated by the electron transport reactions is utilized by the ATP synthase to phosphorylate ADP creating ATP. Both the NADPH and the ATP generated by the light dependent reactions of photosynthesis are utilized in the light independent reactions to fix atmospheric carbon dioxide into organic carbohydrate molecules which are able to be used as the source of energy for heterotrophic organisms. A depiction of both the process of the photosynthetic electron transport through the membrane associated molecules and the generation and utilization of the hydrogen ion gradient are shown in Figure 1.3 (Berg et al. 2002).

Electron carriers like those seen in the redox chain of photosynthesis are generally metal ion complexes and aromatic groups. The electron transfer proteins seen in photosynthesis contain metal ion centers or metal ion complexes in the form of hemes, quinones, flavins, copper, and iron-sulfur clusters. The tertiary structure of the proteins in which the metal centers are bound determines the specific environment around the metal center and therefore influences its potential to transfer electrons. Each of the proteins found in the photosynthetic electron transport chain has a very specific conformation that surrounds the metal centers and gives them their characteristic redox potential allowing them to function in the specific place in the photosynthetic electron transport chain. The structures of the proteins that are

present in the electron transport chain have been evolutionarily fine tuned to allow them utilize the energy of the sun and turn it into chemical energy that can be used to support (heterotrophic) life (Rogers and Moore 1988, Paoli et al. 2002). The following body of work focuses on two heme proteins found within the redox chain: cytochrome f, the luminal domain of the cytochrome b_6f complex, and the second is cytochrome c_6, a protein that can function in place of plastocyanin in lower species.

In this work we will attempt to define how the specific environments that surround the heme of a protein influence its midpoint potential and the dependence of that midpoint potential on pH. We will also investigate the thermal stability of the proteins in this study. Mutations to residues surrounding the heme that remove the interaction of the residue with the heme will allow us to describe the importance of the residue to the characteristics of the wild-type protein. In the case of the unique cytochrome f this may even lead to elucidation of the residue responsible for the dependence of the midpoint potential on pH seeing as it is not the same as the classic case of mitochondrial cytochrome c. This work will also provide an initial characterization of the cytochrome c_6 from *C. reinhardtii.* We have attempted to express the protein in the same expression system as cytochrome f for expression in *E. coli*. Further characterization of the protein in terms of spectral characteristics, midpoint potential and its dependence on pH, and the thermal stability of the protein has also been conducted. The two mutants presented in the study are residues surrounding the heme and interacting with the heme. Both of the mutated residues are suggested to function as ligand replacements at high pH as seen in mitochondrial cytochrome c. Through mutation of the residues we will be able to see if this is the case. We will also be able to see if the residues contribute to the redox potential and thermal stability of the protein. The last study using circular dichroism spectroscopy may help to determine whether or not an aromatic amino acid in the presence of the heme needs to be co-facially oriented with respect to the heme to observe a negative peak in the oxidized spectrum.

Figure 1.3: Light-dependent reactions of photosynthesis at the thylakoid membrane (L. Taiz, E. Zeiger 2006).

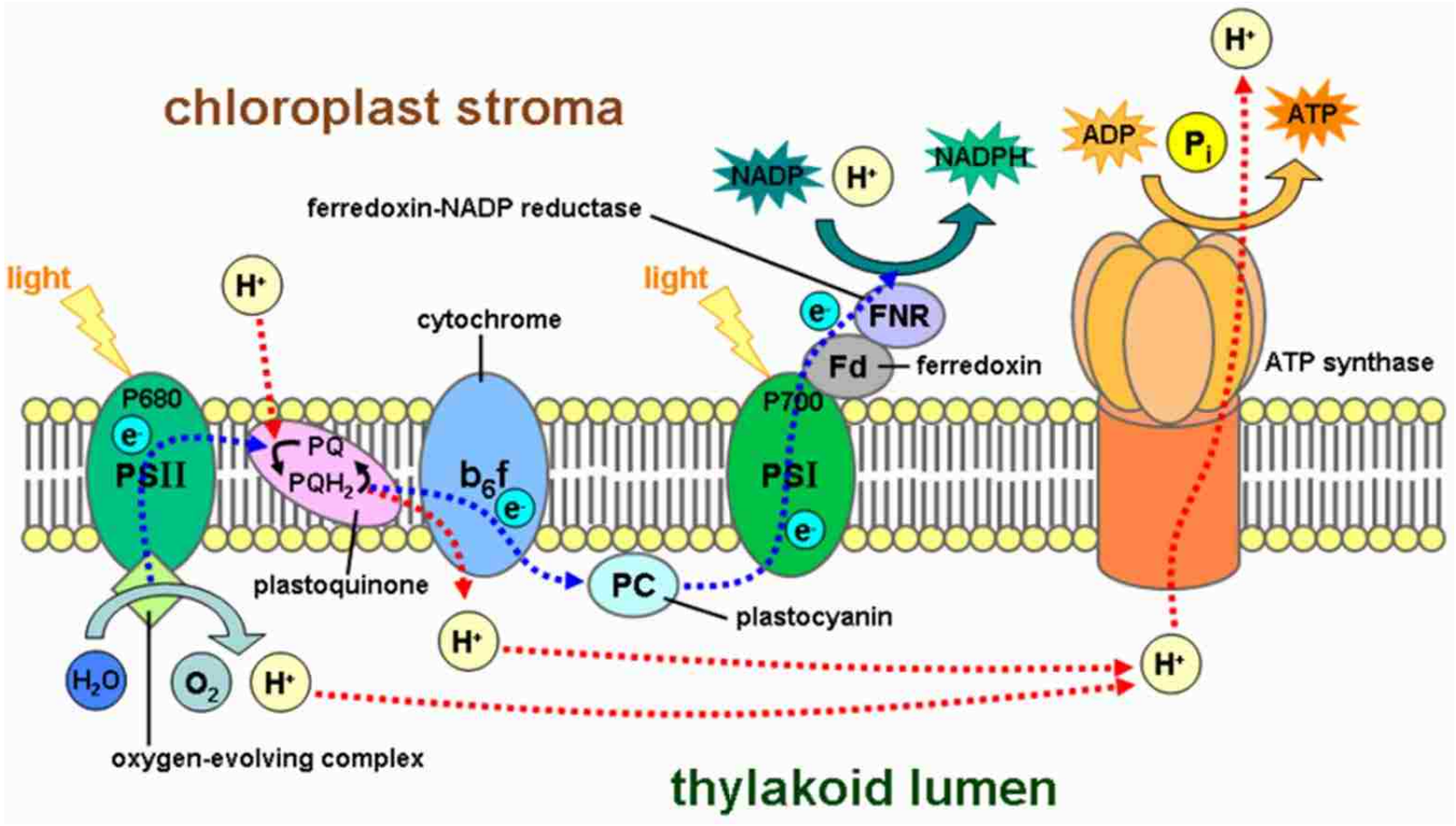
chloroplast stroma
H+
ADP
Pi
ATP
NADP
H+
NADPH
ferredoxin-NADP reductase
light
H+
cytochrome
light
e-
FNR
Fd
ferredoxin
ATP synthase
P680
e-
PSII
PQ
PQH2
b6f
e-
P700
PSI
e-
plastoquinone
PC
plastocyanin
H+
H+
H2O
O2
H+
oxygen-evolving complex
thylakoid lumen

CHAPTER 2 – BACKGROUND

2.1 THE CYTOCHROME B_6F COMPLEX

The cytochrome b_6f complex is a dimeric, 220 kD, membrane bound complex found in the thylakoid membrane. Its function is analogous to that of the cytochrome bc_1 complex of the mitochondrial respiratory electron transport chain as it oxidizes the plastoquinol pool and reduces a mobile electron carrier. The complex couples the electron transport to hydrogen ion transport across the thylakoid membrane. The transport of hydrogen ions results in the buildup of an electrochemical gradient that will be utilized by the ATP-synthase in the production of ATP (Baniulis et al. 2008). Figure 2.1.1 shows the x-ray crystal structure of the b_6f dimer from the cyanobacterium *Mastigocladus laminosum.* Structural determinations of the complex from cyanobacteria and algae reveal identical compositions of the cytochrome b_6f complex (Kurisu et al. 2003, Stroebel et al. 2003, Baniulis et al. 2009). The complex contains four large subunits (cytochrome b_6, cytochrome f, the Rieske iron-sulfur protein, and subunit IV) as well as four smaller subunits (PetG, PetL, PetM, and PetN), and a number of prosthetic groups (plastoquinone, chlorophyll, beta carotene, four hemes, and an 2FE-2S iron-sulfur cluster) per monomeric unit (Stroebel et al. 2003, Kurisu at al. 2003).

2.2 CYTOCHROME F

Cytochrome f, the luminal domain of the cytochrome b_6f complex , is reduced by the Rieske iron-sulfur protein and reduces either the blue copper protein plastocyanin or cytochrome c_6 in lower species under low copper conditions (Kerfeld and Krogmann 1998, Gorman and Levine 1965). Cytochrome f is analogous in function to the cytochrome c_1 of the cytochrome bc_1 complex of the mitochondrial respiratory electron transport chain. The protein is a c-type cytochrome of about 28 kD. The protein possesses a heme c prosthetic group that is covalently bound to the protein through two cysteine residues, Cys21 and Cys24 (Chi 2000).

Figure 2.2.1: X-ray crystal structure of the dimeric cytochrome b_6f complex from the cyanobacterium *Mastigocladus laminosum* showing subunits and prosthetic groups (Kirusu et al. 2003).

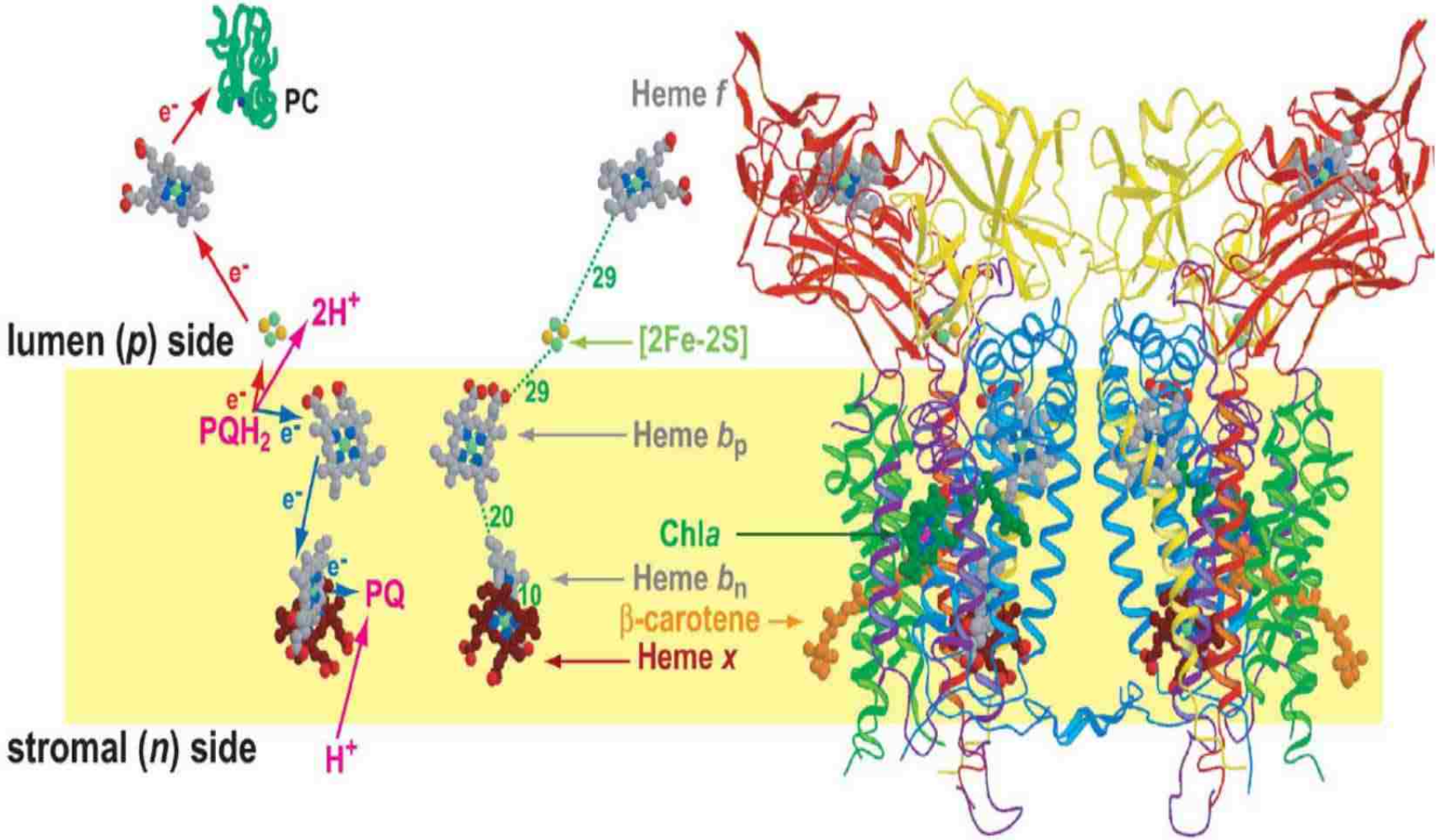
PC
e-
e-
2H+
lumen (p) side
e-
PQH2
e-
e-
e-
PQ
H+
stromal (n) side
Heme f
29
[2Fe-2S]
29
Heme bp
20
10
Heme bn
Chla
β-carotene
Heme x

The redox potential of the protein ranges from 345 mV to 395 mV and has been shown to be pH dependent (Metzger et al. 1997, Martinez et al. 1996). Cytochrome f has variable isoelectric points between species. The isoelectric has been seen to range from 4.4 in some cyanobacterium up to 8.8 in the algae *Cyanophora paradoxa* (Kerfeld and Krogman 1998, Hervás et al. 2003).

The cytochrome f gene, *petA*, is a chloroplast encoded gene. The apo-protein is encoded by an 867 nucleotide sequence and is present in one copy in the genome. The translated precursor apo-protein contains a 31 residue expansion that functions as a luminal targeting peptide. Once the protein reaches the lumen of the thylakoid the targeting sequence is cleaved, and the protein is anchored to the thylakoid membrane (Kallas et al. 1988, Choquet et al. 2003). Figure 2.2.2 shows the sequence of the apo cytochrome f gene with the leader sequence removed and then linked to the pel B leader sequence.

The crystal structure determined for *Chlamydomonas reinhardtii* cytochrome f has been resolved to 2.0 angstrom resolution. The crystal structure solved was for the truncated version of the protein lacking a 33 residue extension that comprises the c-terminal alpha helix that functions to anchor the protein to the membrane. This truncated version is redox active and retains the same redox potential as that of the complete protein. Unlike mitochondrial cytochrome c_1, cytochrome f predominately consists of beta-sheet secondary structure. Another unique feature of the protein is the axial ligation of the heme. In typical c-type cytochromes the axial ligands to the heme are methionine and histidine. The axial ligands in cytochrome f, however, are the alpha amino group of the N-terminal residue and histidine 25 (Chi et al. 2000, Pettigrew and Moore 1987). Yet another unique feature of the protein is that unlike its functional analogue the single domain cytochrome c_1, cytochrome f consists of two domains. The smaller of the two domains is made up of four major and 3 minor beta strands, and the large domain has an immunoglobulin-like fold with alpha helices flanking. The heme is situated in the large domain near the connection to the small domain. The crystallized unit contains three monomers although this is functionally insignificant because of the fact that the protein belongs to dimeric cytochrome b_6f complex. The crystal structure also contains an internal water chain that extends through the protein and has been proposed to function as a proton wire that may be involved in the proton transfer pathway to the Rieske iron-sulfur protein and is important for the specific environment around the heme of the protein that

contributes to its specific midpoint potential (Chi et al. 2000, Sainz et al. 2000). Figure 2.2.3 shows the crystal structure representation showing the heme and the large and small domains.

A number of conserved residues in the heme vicinity of cytochrome f are investigated in this body of work. They are illustrated in Figure 2.2.4. The mutations made to cytochrome f are as follows: Y1F, Y9F, Y160F, Y160L, R156L, and R156K. The Y1F and Y9F mutants remove the ability of the residues to be ionizable by replacing the tyrosine residue with a phenylalanine residue which does not contain an ionizable hydroxyl group. The Y160F mutant removes both the aromatic character of the residue and the ability to hydrogen bond to a propionate group of the heme, and the Y160L mutant retains the aromatic character of the residue but eliminates its capacity to form a hydrogen bond. The R156L mutation removes the positive charge of the residue so that it no longer can interact electrostatically with the heme propionate, and the R156K mutant reinstates the positive charge to allow an electrostatic interaction but removes the specificity of the residue conformation (Chi et al. 2000). Figure 2.2.4 shows the residues of interest surrounding the heme in cytochrome f from *Chlamydomonas reinhardtii*.

The pKa of a residue in a protein may change due to other residues in the area being protonated or deprotonated, small conformational shifts in the protein, or conformations of flexible hydroxyl groups. Previous studies have examined the dependence of redox potential on pH of wild-type cytochrome f from turnip (Metzger et al. 1997, Martinez et al. 1996). Both of these studies used potentiometric titration to determine the redox potential of cytochrome f at various pH's. The studies conducted in 1996 and 1997 showed that the cytochrome f from turnip is pH dependent and has a pKa value around 8.5. In their discussion of their results they predicted that residues Y1, Y160, and R156 would not contribute to the pKa value of around 8.5.

In her computational studies, M. Gunner suggests that the residues Y1 and Y9 may play a role in the pH dependence and pKa of transition for cytochrome f (Hauser et al. 2004, Alexov and Gunner 1997). The Y160 and R156 residues which both interact with surface exposed heme propionates are also considered in this study. The Y160 residue interacts with a heme propionate group via a hydrogen bond involving the phenolic hydrogen of the residue (Chi et al. 2000). The interaction between the propionate group and R156 is an electrostatic interaction between the positively charged residue and the

negatively charged propionate group. These residues are of interest in this study to due to their proximity and interaction with the heme and even though not specifically predicted to have an effect on the pH dependence of the redox potential or the pKa of transition by M. Gunner may influence the redox potential and its pH dependence (Metzger et al. 1997, Martinez et al. 1996).

Figure 2.2.2: Nucleotide and protein sequence of the region of the pUCF2 containing gene encoding the luminal domain of the apo cytochrome f from *Chlamydomonas reinhardtii* with the leader sequence removed and then linked to the pel B leader sequence (Soriano et al. 1998).

pelB Leader Sequence

```
ATG AAA TAC CTG CTG CCG ACC GCT GCT GCT GGT CTG CTG CTC CTC GCT GCC CAG CCG
 M   K   Y   L   L   P   T   A   A   A   G   L   L   L   L   A   A   Q   P

GCG ATG GCC
 A   M   A
```

Pet A-Sequence Encoding C. reinhardtii Cytochome f Mature Form

```
  1                   5                  10                  15
TAC CCT GTA TTT GCA CAA CAA AAC TAC GCT AAC CCA CGT GAG GCT AAT GGT CGT ATT
 Y   P   V   F   A   Q   Q   N   Y   A   N   P   R   E   A   N   G   R   I

 20                  25                  30                  35
GTA TGT GCA AAC TGT CAC TTA GCG CAA AAA GCA GTT GAA ATC GAA GTA CCA CAA GCT
 V   C   A   N   C   H   L   A   Q   K   A   V   E   I   E   V   P   Q   A

     40                  45                  50                  55
GTT TTA CCT GAT ACT GTT TTT GAA GCT GTT ATT GAA CTT CCA TAC GAT AAA CAA GTT
 V   L   P   D   T   V   F   E   A   V   I   E   L   P   Y   D   K   Q   V

         60                  65                  70                  75
AAA CAA GTT TTA GCT AAT GGT AAA AAA GGT GAC TTA AAC GTT GGT ATG GTT TTA ATT
 K   Q   V   L   A   N   G   K   K   G   D   L   N   V   G   M   V   L   I

             80                  85                  90                  95
TTA CCA GAA GGT TTT GAA TTA GCA CCA CCA GAT CGC GTT CCG GCA GAA ATT AAA GAA
 L   P   E   G   F   E   L   A   P   P   D   R   V   P   A   E   I   K   E

    100                 105                 110
AAA GTT GGT AAC CTT TAC TAC CAA CCA TAC AGT CCA GAA CAA AAA AAT ATT TTA GTT
 K   V   G   N   L   Y   Y   Q   P   Y   S   P   E   Q   K   N   I   L   V

115                 120                 125                 130
GTT GGT CCA GTT CCA GGT AAA AAA TAC AGT GAA ATG GTA GTA CCT ATT TTA TCT CCA
 V   G   P   V   P   G   K   K   Y   S   E   M   V   V   P   I   L   S   P

    135                 140                 145                 150
GAT CCT GCT AAA AAT AAA AAC GTT TCT TAC TTA AAA TAT CCT ATT TAT TTT GGT GGT
 D   P   A   K   N   K   N   V   S   Y   L   K   Y   P   I   Y   F   G   G

        155                 160                 165                 170
AAT CGT GGT CGT GGT CAA GTA TAT CCA GAT GGT AAA AAA TCA AAC AAC ACT ATT TAC
 N   R   G   R   G   Q   V   Y   P   D   G   K   K   S   N   N   T   I   Y

            175                 180                 185                 190
AAC GCA TCA GCA GCT GGT AAA ATT GTA GCA ATC ACA GCT CTT TCT GAG AAA AAA GGT
 N   A   S   A   A   G   K   I   V   A   I   T   A   L   S   E   K   K   G

    195                 200                 205
GGT TTT GAA GTT TCA ATT GAA AAA GCA AAC GGT GAA GTT GTT GTA GAC AAA ATC CCA
 G   F   E   V   S   I   E   K   A   N   G   E   V   V   V   D   K   I   P

210                 215                 220                 225
GCA GGT CCT GAT TTA ATT GTT AAA GAA GGT CAA ACT GTA CAA GCA GAT CAA CCA
 A   G   P   D   L   I   V   K   E   G   Q   T   V   Q   A   D   Q   P

        230                 235                 240                 245
TTA ACA AAC AAC CCT AAC GTT GGT GGT TTC GGT CAG GCT GAA ACT GAA ATT GTA
 L   T   N   N   P   N   V   G   G   F   G   Q   A   E   T   E   I   V

    250
TTA CAA AAC CCT GCT CGT ATT CAA (Artificially introduced STOP codon)
 L   Q   N   P   A   R   I   Q
```

Figure 2.2.3: *Chlamydomonas reinhardtii* cytochrome f: file 1CFM downloaded from the Protein Data Bank edited in DS ViewerPro 5.0 by Accelrys Inc. The heme shown in ball and stick format (black).

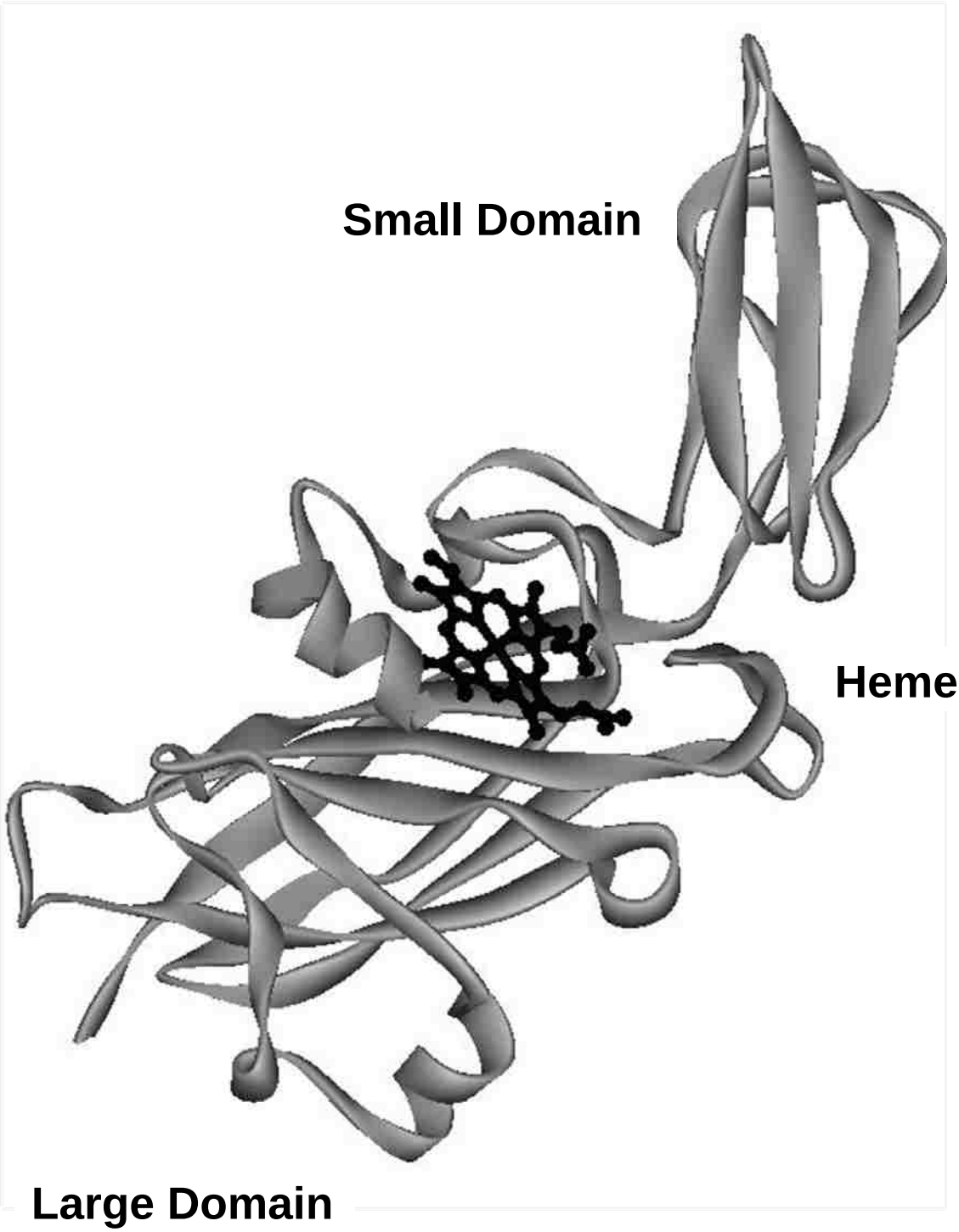
Small Domain
Heme
Large Domain

Figure 2.2.4: *Chlamydomonas reinhardtii* cytochrome f: file 1CFM downloaded from the Protein Data Bank edited in DS ViewerPro 5.0 by Accelrys Inc. The heme portion and residues Y160, Y1, Y9, and R156 are shown in ball and stick format.

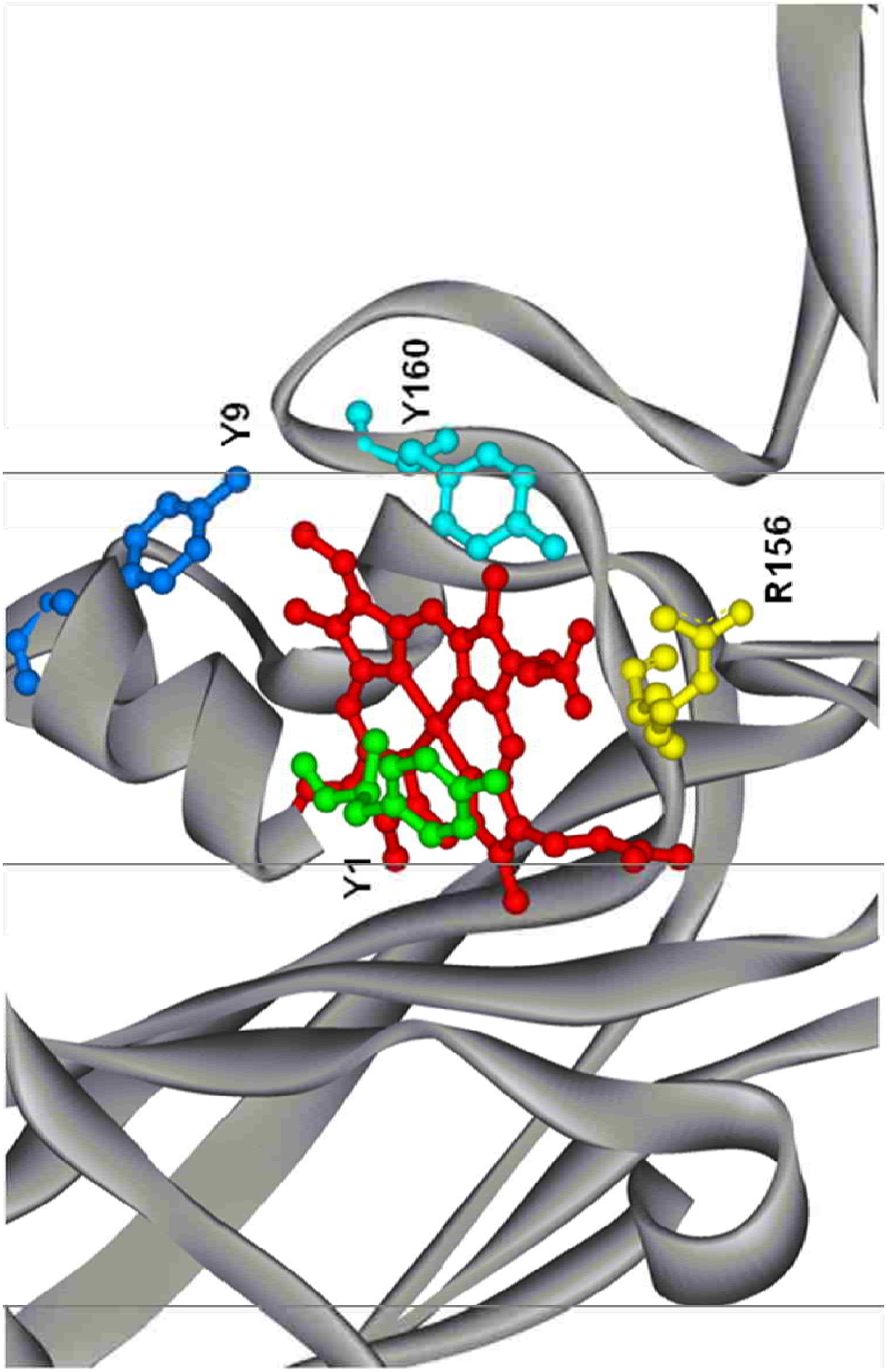
Y9
Y160
R156
Y1

2.3 CYTOCHROME C_6

Cytochrome c_6 is a small mobile electron transfer protein found in cyanobacteria and certain types of algae. It is located in the lumen of the thylakoid, and its function is analogous to that of mitochondrial cytochrome c in the respiratory electron transport chain. It functions in photosynthesis by transporting electrons from cytochrome f of the cytochrome b_6f complex to photosystem I (Kerfeld and Krogmann 1998, Navarro et al. 2004). Also like mitochondrial cytochrome c, it is a c-type cytochrome possessing a covalently bound c-type heme with histidine and methionine serving as the axial ligands to the heme iron. The mature polypeptide is slightly smaller than that of the cytochrome c from mitochondria and is comprised of 83-91 amino acids (Kerfeld et al.1995).

Although cytochrome c_6 resembles mitochondrial cytochrome c in respect to size, fold, and function, it shares a number similarities with the blue copper protein plastocyanin. Plastocyanin and cytochrome c_6 carry out the exact same function in photosynthesis with plastocyanin functioning solely in higher plants. Both proteins are both utilized in lower species but are not known to function at the same time. Cytochrome c_6 is expressed and replaces plastocyanin under situations of low copper availability. The two proteins are very similar in size, isoelectric point, and redox potential subsequently allowing them to function in the same role in photosynthesis without have any sequence similarity or and any similarity in secondary structure. Both cytochrome c_6 and plastocyanin have a molecular weight of about 10.5 kD and although the isoelectric point of both proteins is known to vary greatly between species, ranging from about 3.8 to 9.3 for cytochrome c_6, it remains consistent for each of the proteins in any given species (Kerfeld and Krogmann 1998). The secondary structure of cytochrome c_6 is primarily alpha helical whereas that of plastocyanin is beta barrel. The redox potential of cytochrome c_6 from species studied is found to range between 335 mV and 390 mV. It is similar to that of plastocyanin and has been shown to be pH dependent (Campos et al. 1993, Worall et al. 2007). Even though the secondary structures of cytochrome c_6 and plastocyanin differ, the charged and hydrophobic patches on the surfaces of the proteins which allow them to interact with their reaction partners, the cytochrome b_6f complex and photosystem I, are similar (Kerfeld and Krogmann 1998).

The gene that codes for cytochrome c_6 is present in one copy in the genome of *Chlamydomonas reinhardtii* and can be seen along with the amino acid sequence in Figure 2.3.2. The transcribed portion of the gene consists of 2.6 kilobase pairs and includes both the 852 nucleotide extension upstream of the start site and 495 downstream of the poly-adenylation signal. The gene contains two introns. Regulation is mostly at the transcriptional level, and expression levels of mRNA are influenced by copper availability. The regulation in response to copper availability allows for the exchange of function between cytochrome c_6 and plastocyanin (Hill et al. 1991).

Figure 2.3.1: *Chlamydomonas reinhardtii* cytochrome $_6$ gene and amino acid sequences (Hill et al. 1991).

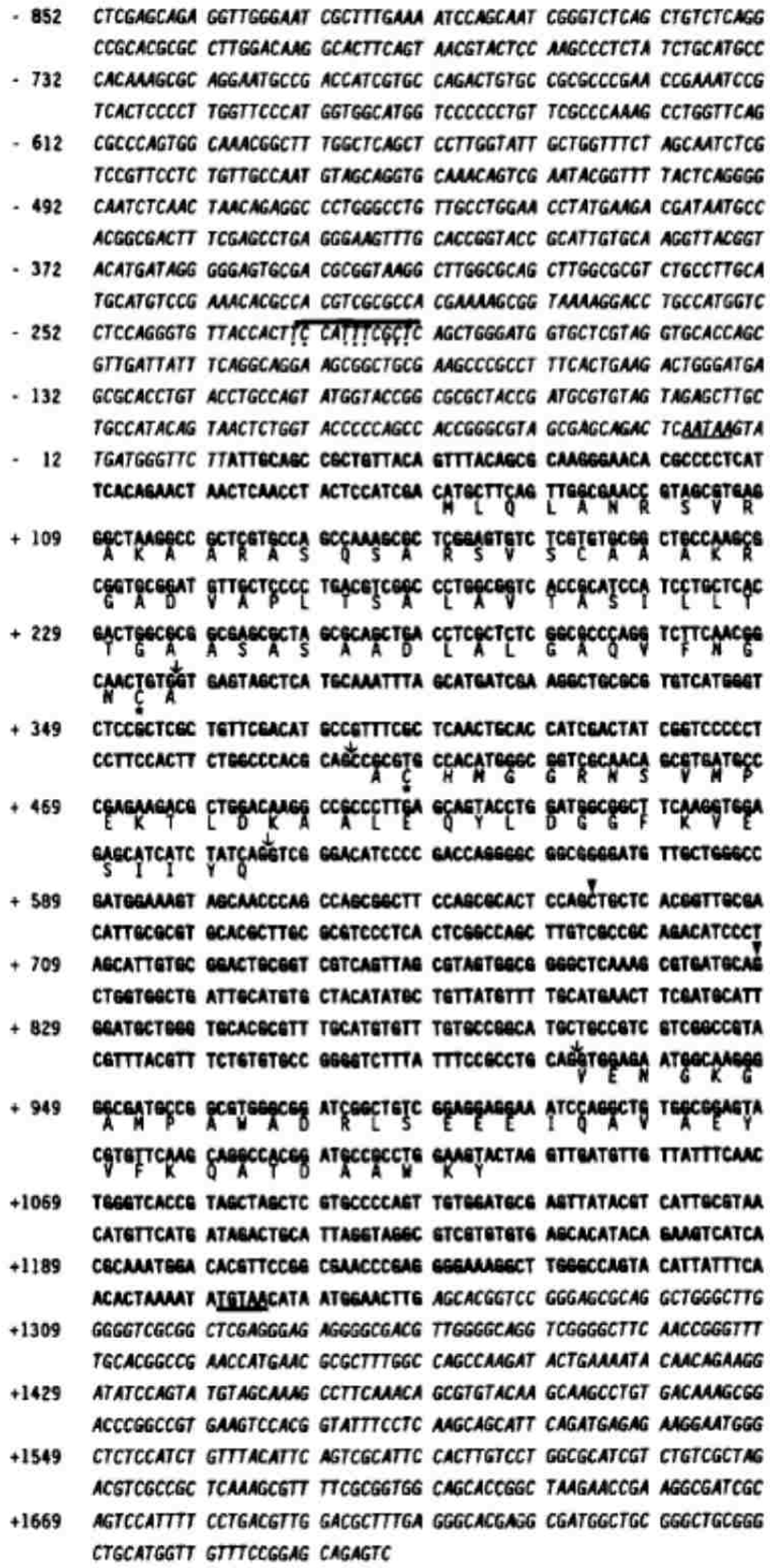

The first crystal structure determined for cytochrome c_6 was at 3.0 angstrom resolution and came from the cyanobacterium *Anacystis nidulans*. The next structures to follow revealed the structure in better detail being at 1.9 angstrom resolution for *Chlamydomonas reinhardtii* and 1.2 angstrom resolution for cytochrome c_6 from *Monoraphidium braunii* (Kerfeld and Krogmann 1998). Since then a number of structures have been determined from various organisms including the green algae *Scenedesmus obliqus*, the brown alga *Hizikia fusiformis*, the red alga *Porphyra yezoensis*, and the cyanobacteria *Arthrospira maxima* and *Synechococcus elongates* (Schnackenberg et al. 1999, Akazaki et al. 2008, Yamada et al. 2000, Sawaya et al. 2001, and Beissinger et al. 1998). The structure from *Chlamydomonas reinhardtii,* of which the proteins discussed in this volume are from, is similar in structure to other class I, c-type cytochromes. It is mostly alpha helical with four alpha helices, helix I comprised of residues 3 through 14, helix II residues 33 – 39, helix III residues 46 – 55, and helix IV residues 69 – 85. The molecule also contains turns and a double stranded anti-parallel beta sheet located in the most highly conserved region of the protein sequence near the methionine axial ligand to the heme which is comprised of residues 54 - 63. Figure 2.3.2 displays the secondary structure as well as the heme prosthetic group.

The protein was crystallized in two different isoforms. A number of cytochrome c_6 molecules from various organisms including *Anthropsira maxima, Monoraphidium braunii*, and *Scenedensmus obliqus* have been found to crystallize with various isoforms. (Sawaya et al. 2001, Campos et al. 1993, Schnackenberg et al. 1999). This is thought to be the result of differences in post-translational modifications which are known to occur due to responses to alterations in light intensity and other changed environmental parameters during photosynthesis (Kerfeld et al. 1995). The cytochrome c_6 of *Chlamydomonas reinhardtii,* as well as those from other organisms, appears to oligomerize in the crystal forms. Form 1 is dimeric and the second form is trimeric. The heme environment found in the cytochrome c_6 molecule is primarily hydrophobic in nature. The heme exposure to the solvent in the crystal structure for *Chlamydomonas reinhardtii* is limited to one edge of the heme ring and the D propionate oxygen atoms. The non-polar environment around the heme contains only three charged residues which flank the heme crevice. These residues are lysines 29 and 57 and aspartic acid 41 the first two of which are interest in the present studies. The two lysine residues are conserved in cytochrome c_6. The K57 residue

is known to be important to generate the electrostatic potential on the surface near the heme near the binding site for the interaction partners of the molecules based on molecular dynamic simulations (Haddadian and Gross 2005). Lysine 29 forms a salt-bridge with the D propionate oxygen atoms, and lysine 57 hydrogen bonds to buried water molecule in the structure. Both of these residues have been suggested to influence the redox potential of the protein and have also been suggested as potential ligand replacements during the alkaline transition of the protein (Kerfeld et al. 1995, Beissinger et al. 1998, Sawaya et al. 2001, Ying et al. 2009, Campos et al. 1993, Dikiy et al. 2002). Figure 2.3.3 shows the protein with the residues of interest highlighted, and Figure 2.3.4 shows a sequence alignment demonstrating the conservation of the K29 and K57 residues.

Figure 2.3.2: *Chlamydomonas reinhardtii* cytochrome c_6: file 1CYJ downloaded from the Protein Data Bank edited in DS ViewerPro 5.0 by Accelrys Inc. Showing the alpha helices and the heme portion (black) which is shown in ball and stick format.

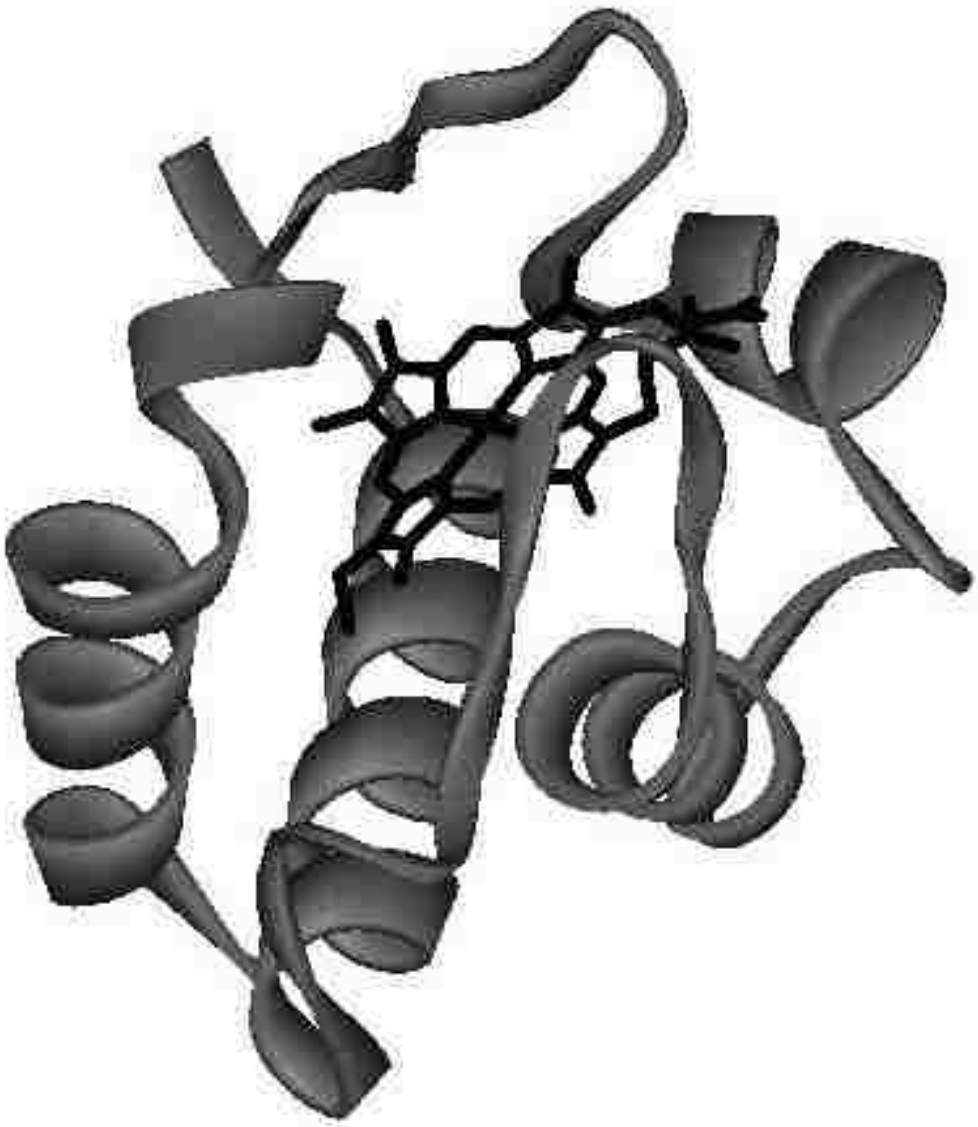

Figure 2.3.3: *Chlamydomonas reinhardtii* cytochrome c_6: file 1CYJ downloaded from the Protein Data Bank edited in DS ViewerPro 5.0 by Accelrys Inc. The heme portion (red) and residues K29 (green) and K57 (blue) shown in ball and stick format.

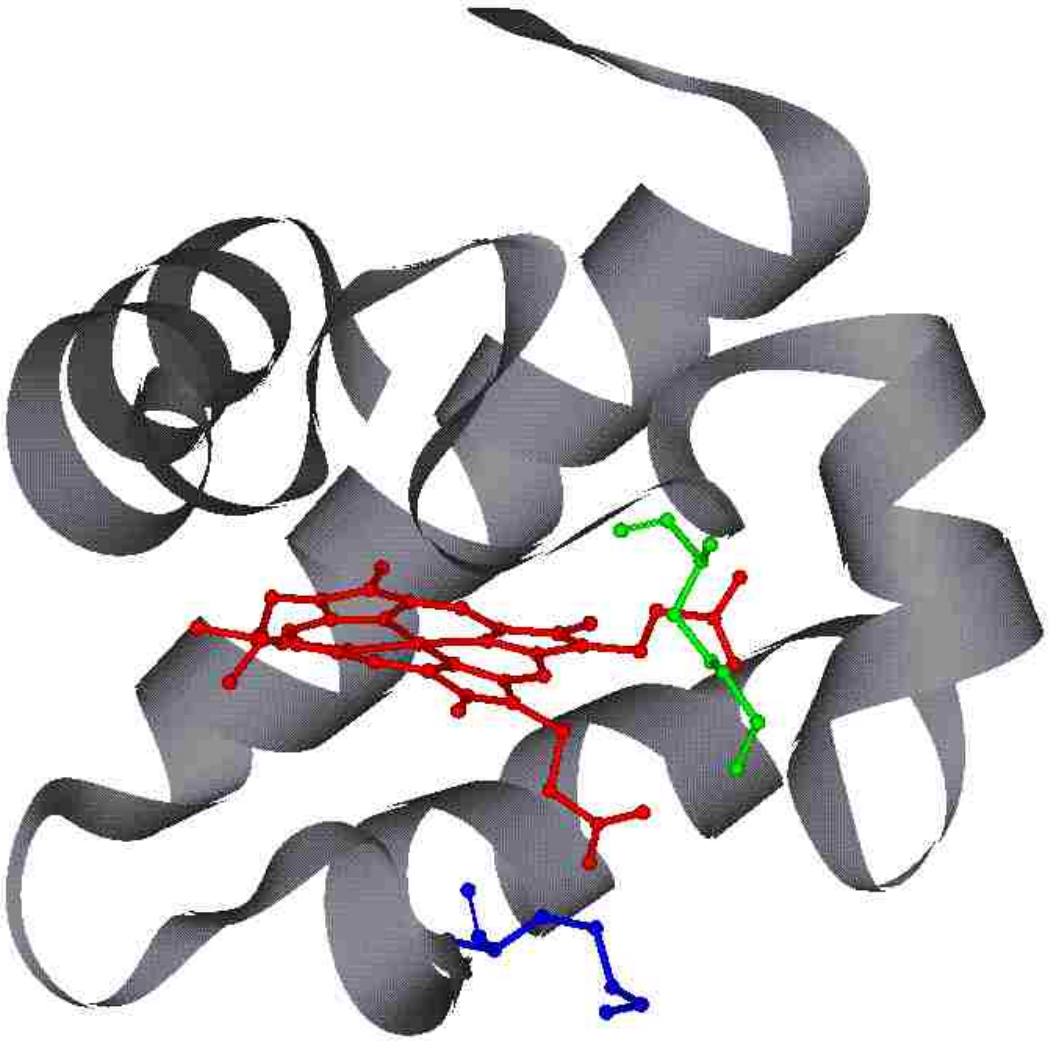

Figure 2.3.4 Sequence alignment of cytochromes c_6 using ClustalW with K29 and K57 highlighted in red and the one invariant of K29 in blue (Hill et al. 1991, Dikiy et al. 2002, Okamoto et al. 1987, Steiner et al. 2000, Genoscope 2008, Oku et al. 2003, Kadokure et al. 1998, Nakamura et al. 2003, Maeda et al. 2006, Copeland et al. 2005, Mejean et al. 2010, Worrall et al. 2007, Kerfeld et al. 2002, Lucas et al. 2008, Li et al. 2008, Copeland et al. 2008).

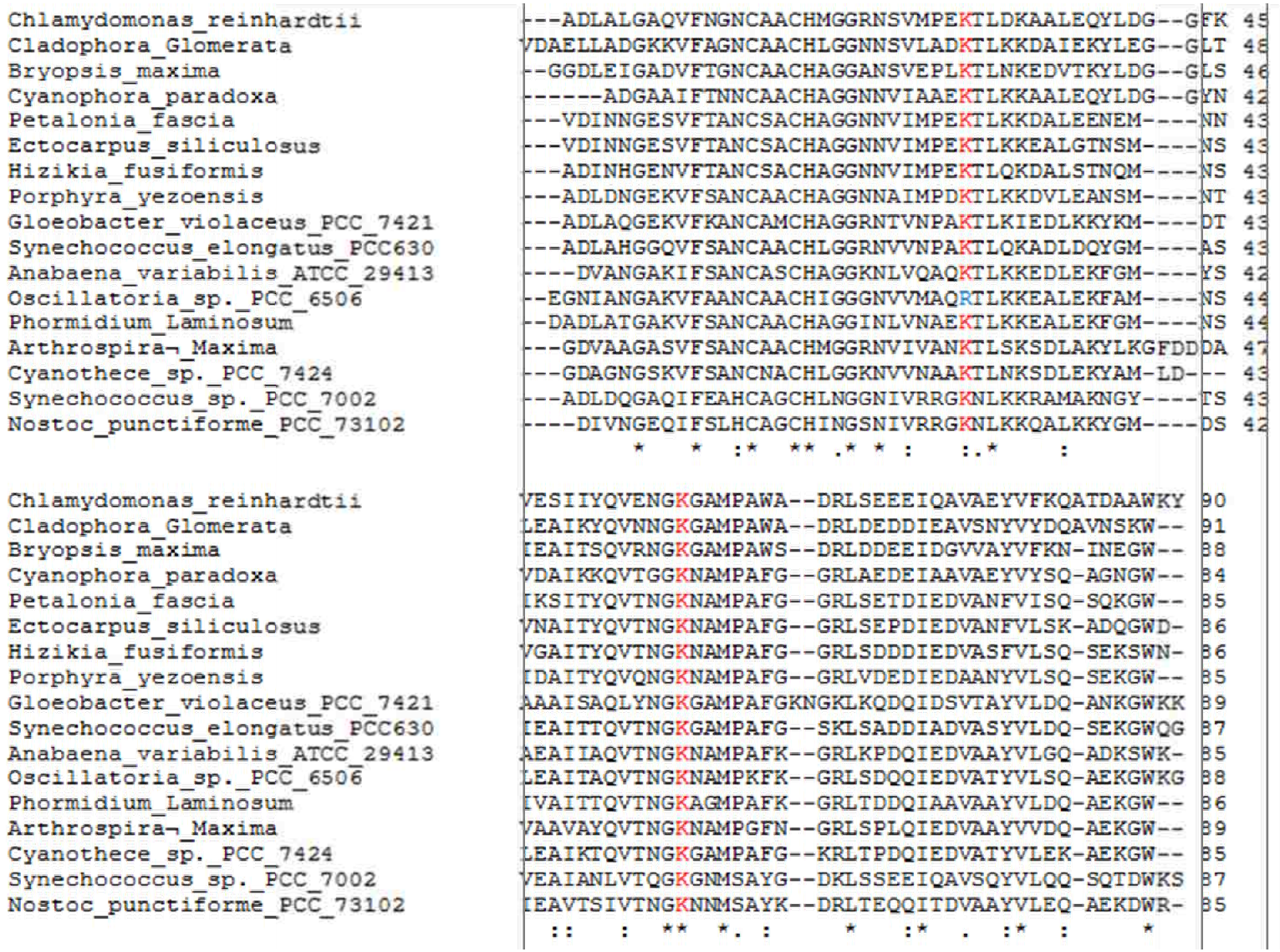
Chlamydomonas_reinhardtii ---ADLALGAQVFNGNCAACHMGGRNSVMPEKTLDKAALEQYLDG--GFK 45
Cladophora_Glomerata VDAELLADGKKVFAGNCAACHLGGNNSVLADKTLKKDAIEKYLEG--GLT 46
Bryopsis_maxima --GGDLEIGADVFTGNCAACHAGGANSVEPLKTLNKEDVTKYLDG--GLS 46
Cyanophora_paradoxa ------ADGAAIFTNNCAACHAGGNNVIAAEKTLKKAALEQYLDG--GYN 42
Petalonia_fascia ---VDINNGESVFTANCSACHAGGNNVIMPEKTLKKDALEENEM----NN 43
Ectocarpus_siliculosus ---VDINNGESVFTANCSACHAGGNNVIMPEKTLKKEALGTNSM----NS 43
Hizikia_fusiformis ---ADINHGENVFTANCSACHAGGNNVIMPEKTLQKDALSTNQM----NS 43
Porphyra_yezoensis ---ADLDNGEKVFSANCAACHAGGNNAIMPDKTLKKDVLEANSM----NT 43
Gloeobacter_violaceus_PCC_7421 ---ADLAQGEKVFKANCAMCHAGGRNTVNPAKTLKIEDLKKYKM----DT 43
Synechococcus_elongatus_PCC630 ---ADLAHGGQVFSANCAACHLGGRNVVNPAKTLQKADLDQYGM----AS 43
Anabaena_variabilis_ATCC_29413 ----DVANGAKIFSANCASCHAGGKNLVQAQKTLKKEDLEKFGM----YS 42
Oscillatoria_sp._PCC_6506 --EGNIANGAKVFAANCAACHIGGGNVVMAQRTLKKEALEKFAM----NS 44
Phormidium_Laminosum --DADLATGAKVFSANCAACHAGGINLVNAEKTLKKEALEKFGM----NS 44
Arthrospira¬_Maxima ---GDVAAGASVFSANCAACHMGGRNVIVANKTLSKSDLAKYLKGFDDDA 47
Cyanothece_sp._PCC_7424 ---GDAGNGSKVFSANCNACHLGGKNVVNAAKTLNKSDLEKYAM-LD-- 43
Synechococcus_sp._PCC_7002 ---ADLDQGAQIFEAHCAGCHLNGGNIVRRGKNLKKRAMAKNGY----TS 43
Nostoc_punctiforme_PCC_73102 ----DIVNGEQIFSLHCAGCHINGSNIVRRGKNLKKQALKKYGM----DS 42
Chlamydomonas_reinhardtii VESIIYQVENGKGAMPAWA--DRLSEEEIQAVAEYVFKQATDAAWKY 90
Cladophora_Glomerata LEAIKYQVNNGKGAMPAWA--DRLDEDDIEAVSNYVYDQAVNSKW-- 91
Bryopsis_maxima IEAITSQVRNGKGAMPAWS--DRLDDEEIDGVVAYVFKN-INEGW-- 88
Cyanophora_paradoxa VDAIKKQVTGGKNAMPAFG--GRLAEDEIAAVAEYVYSQ-AGNGW-- 84
Petalonia_fascia IKSITYQVTNGKNAMPAFG--GRLSETDIEDVANFVISQ-SQKGW-- 85
Ectocarpus_siliculosus VNAITYQVTNGKNAMPAFG--GRLSEPDIEDVANFVLSK-ADQGWD- 86
Hizikia_fusiformis VGAITYQVTNGKNAMPAFG--GRLSDDDIEDVASFVLSQ-SEKSWN- 86
Porphyra_yezoensis IDAITYQVQNGKNAMPAFG--GRLVDEDIEDAANYVLSQ-SEKGW-- 85
Gloeobacter_violaceus_PCC_7421 AAAISAQLYNGKGAMPAFGKNGKLKQDQIDSVTAYVLDQ-ANKGWKK 89
Synechococcus_elongatus_PCC630 IEAITTQVTNGKGAMPAFG--SKLSADDIADVASYVLDQ-SEKGWQG 87
Anabaena_variabilis_ATCC_29413 AEAIIAQVTNGKNAMPAFK--GRLKPDQIEDVAAYVLGQ-ADKSWK- 85
Oscillatoria_sp._PCC_6506 LEAITAQVTNGKNAMPKFK--GRLSDQQIEDVATYVLSQ-AEKGWKG 88
Phormidium_Laminosum IVAITTQVTNGKAGMPAFK--GRLTDDQIAAVAAYVLDQ-AEKGW-- 86
Arthrospira¬_Maxima VAAVAYQVTNGKNAMPGFN--GRLSPLQIEDVAAYVVDQ-AEKGW-- 89
Cyanothece_sp._PCC_7424 LEAIKTQVTNGKGAMPAFG--KRLTPDQIEDVATYVLEK-AEKGW-- 85
Synechococcus_sp._PCC_7002 VEAIANLVTQGKGNMSAYG--DKLSSEEIQAVSQYVLQQ-SQTDWKS 87
Nostoc_punctiforme_PCC_73102 IEAVTSIVTNGKNNMSAYK--DRLTEQQITDVAAYVLEQ-AEKDWR- 85

Although cytochrome c_6 is found in a number of lower species, it is not present in higher plants where the role of electron transport from the cytochrome b_6f complex to Photosystem I has been taken over solely by plastocyanin. The switch is thought to have occurred due to the fact that land plants typically have a better and more constant source for copper and have lost the selective pressure that would demand the retention of cytochrome c_6 as a functioning part of the proteome. However, an analogous protein to cytochrome c_6 was found in 2002 during a yeast two hybrid experiment looking for interaction partners for the chloroplast immunophilin protein in *Arabidopsis thaliana.* It was noted that the sequence was present in a number of higher species in addition to *Arabidopsis thaliana* (Gupta et al. 2002, Wastl et al. 2002). These initial studies determined that there was one copy of the gene in the genome.

A comparison between the sequence of the newly discovered protein named cytochrome c_{6A} and the cytochrome c_6 sequences reveals a 12 amino acid insertion in the sequence of cytochrome c_{6A} (Gupta et al. 2002). The extension contains 2 cysteine residues that after the elucidation of the crystal structure were found to form a disulfide bridge. The gene codes for a mono-heme protein with histidine and methionine serving as axial ligands to the heme. The fold is that of a typical class I, c-type cytochrome and is able to be superimposed upon structures of cytochrome c_6 with the exception of the 12 amino acid extension insertion which forms a loop between helices II and III and extends into helix III (Chida et al. 2006). Figure 2.3.5 shows a structure alignment of cytochrome c_{6A} and cytochrome $c_{6.}$ The spectrum is typical for that of a cytochrome and contains an alpha peak being located at 553 nm.

So far there is no conclusive evidence for its exact role in the cell. The 12 amino acid extension gives rise to differences in the properties of cytochrome c_6 and cytochrome c_{6A} that rule out the possibility for cytochrome c_{6A} to function in photosynthesis such as its redox potential. Cytochrome c_{6A} was found to have a midpoint potential of 140 mV (Molina-Heredia et al. 2003). With such a low potential it is impossible for it to function in the place of plastocyanin in higher plants due to the fact that it would be unable to oxidize the cytochrome b_6f complex. Homology modeling also reveals a difference between cytochrome c_6 and cytochrome c_{6A} in charge distribution around the binding site for the interaction with the redox partners of cytochrome c_6 indicating that the electrostatic interaction would also altered (Howe

et al. 2002). In 2004 the protein was also found in the green algae *Chlamydomonas reinhardtii* (Wastl et al. 2004). This meant that the evolutionary step from cytochrome c_6 to cytochrome c_{6A} happened early. A duplication event and the 12 amino acid extension is likely to have occurred in algae.

Figure 2.3.5: Superimposition of A. thaliana cytochrome c6A (red) and red alga P. yezoensis cytochrome c6A (blue) (Chida et al. 2006).

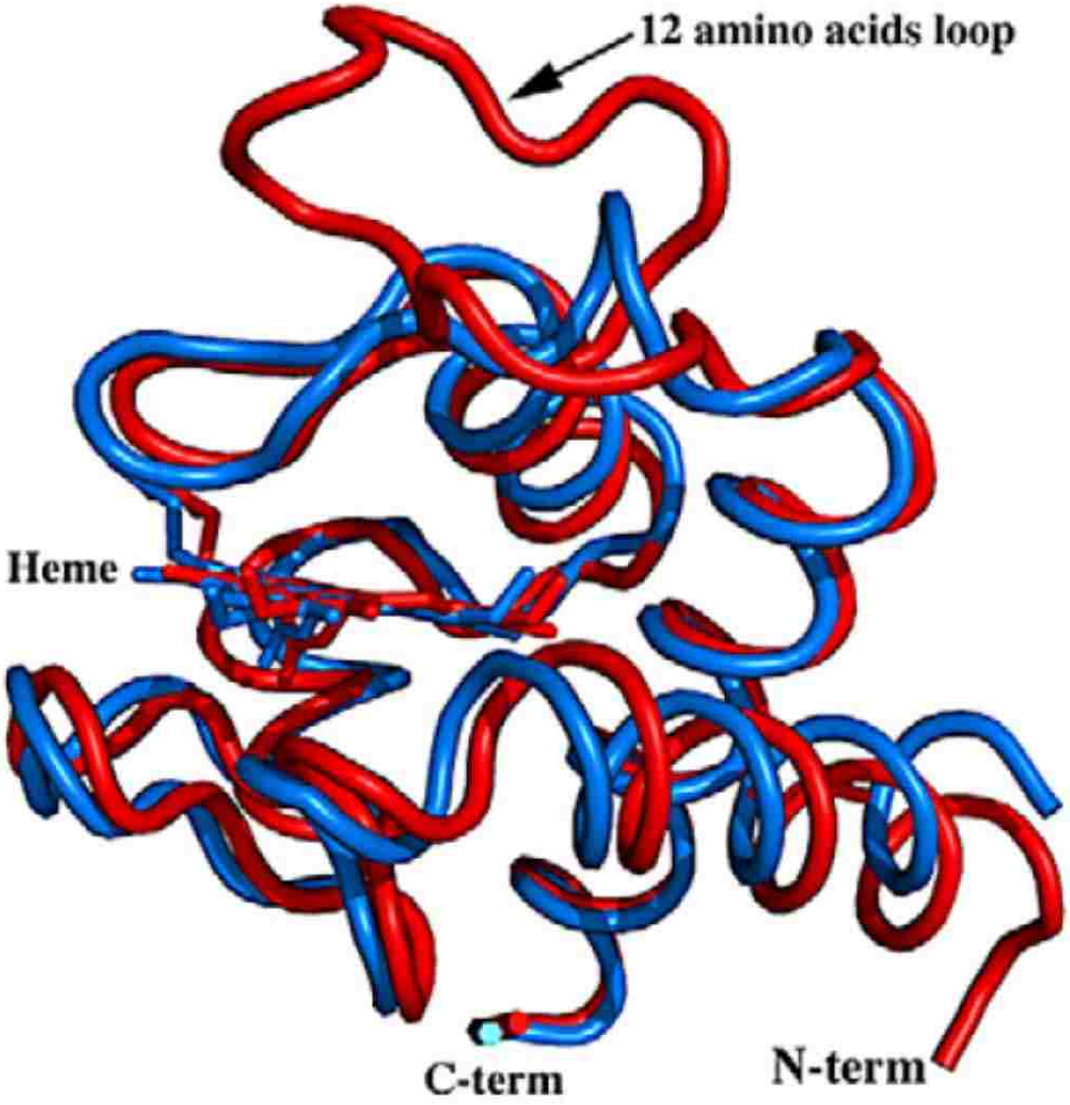
12 amino acids loop
Heme
C-term
N-term

CHAPTER 3 – MATERIALS AND METHODS

3.1 CYTOCHROME C_6 PLASMID CONSTRUCTION

The incorporation of the cytochrome c_6 gene from *Chlamydomonas reinhardtii* into the pUCF2 plasmid was performed by Marylyn Davis. The synthetic gene constructed was based on the gene sequence from Hill et al. 1991 displayed in Figure 3.1.1. The leader sequence and introns were removed, and the codons were substituted to reflect the codon bias of E. coli. NcoI, EcoR1, and Kpn1 restriction sites were also added for the use in introducing the sequence into the plasmid. An expression system utilizing the C. reinhardtii cytochrome f gene-containing plasmid pUCF2, previously obtained from G. Soriano and W.A. Cramer from Purdue University, was developed in which a single base mutation at the end of the pelB leader sequence introduced an NcoI site. Subsequent cleavage with NcoI/EcoR1 removed the cytochrome f gene which was then replaced by the NcoI/EcoR1 portion of the designer gene.

3.2 MUTAGENESIS

Mutagenesis was used to create the cytochrome f mutant plasmids Y160F, Y160L, Y1F, Y9F, R156L, and R156K and the cytochrome c_6 mutant plasmids K29I and K57I. The mutagenesis was done using the Quickchange II Site-Directed Mutagenesis Kit from Stratagene (Stratagene 2004). The plasmid Y160F was prepared by Bryan Bishop, and the Y160L plasmid was constructed by Ashwini Bhise. The cytochrome f Y1F, Y9F, and R156L were created in the summer of 2005 during the Research Experience for Undergraduates program. The primers for all mutants were designed based on sequence length, compatibility of the melting temperatures, and minimizing the chance of hairpin conformations able to be formed by the primers. The primers were ordered from Integrated DNA technologies. The sequences of the primers that were used for the creation of the cytochrome f R156K, and the cytochrome c_6 mutants K29I and K57I are shown in Figure 3.2.1. The procedures for the mutagenesis are outlined in Figure 3.2.2.

Figure 3.1.1: Sequence of the designer gene for Chlamydomonas reinhardtii cytochrome c_6 (Hill et al. 1991).

```
cc atg gcg gat ctg gcg ctg ggc gcg cag gtg ttt aac ggc aac tgt gcg gcg
   M   A   D   L   A   L   G   A   Q   V   F   N   G   N   C   A   A
 NcoI

tgc cat atg ggc ggt cgc aac agc gtg atg ccg gaa aaa acc ctg gat aaa gcg
 C   H   M   G   G   R   N   S   V   M   P   E   K   T   L   D   K   A

gcg ctg gaa cag tat ctg gat ggc ggc ttt aaa gtg gaa agc att att tat cag
 A   L   E   Q   Y   L   D   G   G   F   K   V   E   S   I   I   Y   Q

gtg gaa aac ggg aaa ggc gcg atg ccg gcg tgg gcg gat cgc ctg tcg gaa gaa
 V   E   N   G   K   G   A   M   P   A   W   A   D   R   L   S   E   E

gaa att cag gcg gtg gcg gaa tat gtg ttt aaa cag gcc acc gat gcg gcg tgg
 E   I   Q   A   V   A   E   Y   V   F   K   Q   A   T   D   A   A   W


aaa tat tag tag aat tcg gta cc
 K   Y  stop
              EcoR1    Kpn1
```

Figure 3.2.1: Primer sequences for the cytochrome f R156K, cytochrome c_6 K29I, and cytochrome c_6 K57I mutagenesis.

Cytochrome f R156K

Forward: 5’ - GGT GGT AAT CGT GGT AAA GGT CAA GT

Reverse: 5’ – CCA TCT GGA TAT ACT TGA CCT TTA CCA

Cytochrome c_6 K29I

Forward: 5’ - GTG ATG CCG GAA ATA ACC CTG GAT AA

Reverse: 5’ – CGC CGC TTT ATC CAG GGT TAT TTC CG

Cytochrome c_6 K57I

Forward: 5’ - GAA AAC GGG ATA GGC GCG ATG CCG G

Reverse: 5’ – CGC CCA CGC CGG CAT CGC GCC TAT C

Figure 3.2.2: Protocol for site-directed mutagenesis (Stratagene 2004).

MUTAGENESIS PROCEDURE

1.) Pulse centrifuge primers for a couple of seconds

2.) Add 0.8 mL of sterile water to the primers

3.) To tubes containing 1 mL of sterile water add 5 µL of primer

4.) Measure the absorbance at 260 nm (this will equal 1 for 33 µg/mL of single stranded DNA)

5.) Multiply the absorbance at 260 nm by 33 to get the DNA concentration in µg/mL in the cuvette

6.) Multiply the result of 5.) by 200 to get the concentration of DNA in the stock solution

7.) Make a dilution of the primers to 63 µg/mL by adding sterile water giving a final volume of 200 µL

8.) Add 36 µL of sterile water, 2 µL of forward primer, 2 µL of reverse primer, 5 µL of 10x Pfu reaction buffer, 1.5 µL dNTP, 2.5 µL plasmid, and 1 µL of Pfu DNA polymerase

9.) Pulse centrifuge for a couple seconds and then place into the thermal cycler

10.) Add 1 µL of Dpn1 restriction enzyme to digest parental DNA

11.) Gently mix and pulse centrifuge

12.) Incubate for 1 hour at 37ºC

13.) Add 5 µL of Dpn1 treated DNA and 50 µL of E. coli XL-1 Blue supercompetent cells to a pre-chilled sterile Falcon tube.

14.) Incubate on ice for 30 minutes

15.) Heat pulse at 42ºC for 45 seconds then place back on ice for 2 minutes

16.) Add 0.5 mL of NZY^+ broth and incubate for 1 hour at 37 ºC

17.) Plate the contents of the tube on a plate containing ampicillin and incubate overnight at 37ºC

18.) Colonies from these plates will be used to do plasmid preps

3.3 TRANSFORMATION

Transformations were conducted in order to do plasmid preps. The mutant or wild-type plasmids were transformed into *E. coli* cells (MV1190 or XL1B strain). 2.0 µL of the selected plasmid was combined with 25 µL of competent E. coli cells in a pre-chilled Falcon tube. The tube was incubated of ice for 30 minutes then heat pulsed at 42ºC for a period of 2 minutes before being returned to ice for 2 more minutes. 0.5 mL of 2xYT broth was added to the tube and incubated at 37 ºC for 1 hour. The contents of the tube were then plated and selectively grown on 2xYT agar plates containing ampicillin or chloramphenical.

3.4 PLASMID PREPS

A plasmid prep was performed to create a stock of plasmid and was done by taking individual colonies from the transformed plates and growing them up in tubes containing 0.5 mL of 2xYT liquid growth media containing 5 µL of 0.27 M ampicillin overnight at 37ºC. Isolation of the plasmids was done using the Wizard Plus Minipreps DNA Purification System (Promega 2002). The procedures for the purification of the plasmids are shown in Figure 3.4.1. The plasmids were sequenced by the DNA sequencing facility at the University of Arkansas in the poultry science division to confirm the presence of the mutation.

3.5 EXPRESSION THROUGH CO-TRANSFORMATION

The mutant or wild-type plasmids were co-transformed along with the pEC86 plasmids into *E. coli* cells (MV1190 or XL1B strain). The cell strains are protease containing which is necessary due to the design of the expression system where the pelB leader sequence directs the exportation of the protein to the periplasm of the cell where the protein is bound to the heme. The proteases are necessary to cleave the leader sequence. This system allows for easier separation during purification as only the periplasmic contents will be recovered from harvesting. Co-expression of this plasmid in conjunction with a pEC86 plasmid containing the ccmA-H cytochrome

Figure 3.4.1: Protocol for plasmids isolation (Promega 2002).

PLASMID ISOLATION PROCEDURE

1.) Pellet cells from the overnight growth in eppendorf tubes by centrifuging for 20 seconds

2.) Discard the supernatant and resuspend the cells in 150 µL of Cell Suspension Buffer

3.) Add 150 µL of Cell Lysis solution, mix well

4.) Place sample in a 37ºC water bath for 2-3 minutes

5.) Add 150 µL of Neutralization solution. This will precipitate the chromosomal DNA.

6.) Place sample on ice for 10 minutes

7.) Centrifuge the sample for 5 minutes

8.) Transfer the supernatant to new eppendorf tubes

9.) Add 1 mL of DNA binding resin and place sample on ice for 5 minutes

10.) Attach a minicolumn to a syringe and transfer the sample to the minicolumn

11.) Wash the column with 2 mL of Wash solution then centrifuge to remove remaining Wash solution

12.) Add 50 µL of sterile water at 70ºC to the column

13.) Place the column in a new eppendorf tube and centrifuge in order to release the sample into the tube.

14.) Store recovered plasmids at -80ºC

maturation genes for the covalent attachment of the heme to the cytochrome resulted in successful production of the protein and incorporation of the heme into the protein. To accomplish the co-transformation 2.0 µL of the pEC86 plasmid and 2.0 µL of the desired plasmid were combined with 25 µL of competent E. coli cells in a pre-chilled Falcon tube. The tube was incubated of ice for 30 minutes then heat pulsed at 42ºC for a period of 2 minutes before being returned to ice for 2 more minutes. 0.5 mL of 2xYT broth was added to the tube and incubated at 37 ºC for 1 hour. The contents of the tube were then plated and selectively grown on 2xYT agar plates containing ampicillin and chloramphenical.

3.6 GROWTH

The cells were grown according to Soriano (Soriano et al. 1998). Colonies were selected after the 24 hour period, placed in 5 mL of 2xYT liquid growth media containing 5 µL of 0.27 M ampicillin and 2.5 µL of 0.15 M chloramphenicol, and grown aerobically at 37ºC for 24 hours. The tube cultures were then placed in 1.8 liters of LB medium inoculated with 0.054 mM ampicillin, 0.06 mM chloramphenicol, 1 mM KNO_3, and 0.25 mM IPTG and grown semi-anaerobically for 22 hours at 37ºC.

3.7 HARVESTING

The cells were harvested and the protein was released by osmotic shock using a STE buffer (20% sucrose, 30 mM Tris-Cl, 1 mM EDTA, pH 7.5) according to procedures outlined by Soriano (Soriano et al. 1998). Cells were pelleted by centrifuging at 9,000 rpm for 15 minutes. The pellet was resuspended in about 100 mL of the STE buffer then stirred vigorously on ice for 15 minutes. The cells were again pelleted by centrifuging at 10,000 rpm for 15 minutes. The supernatant was discarded. The pellet was resuspended in about 100 mL of ice cold water to release the contents of the periplasm. The sample then stirred on ice vigorously for another 15 minutes. The cells were pelleted by centrifugation at 10,000 rpm for 15 minutes and the soluble portion was labeled and stored at 20ºC. The yield of both proteins was conducted by taking the absorbance at the alpha peak and dividing that by the extinction coefficient (26 mM^{-1} for cytochrome f and 23.3 mM^{-1} for cytochrome c_6) then multiplying by the milliliters of culture and the molecular weight of the protein (27.9 kDa for cytochrome f and 10.4 kDa for cytochrome c_6) and

divide by the number of liters of growth media. This gives a yield in mg of protein per liter of growth media.

3.8 PURIFICATION

Identical procedures were used for the purification of both cytochrome f and cytochrome c_6. The soluble fraction recovered from the osmotic shock was first applied to a Whatman DE-53 diethylaminoethyl anion exchange column, rinsed with 100 mL of 10 mM Tris, pH 7.0 then eluted off of the column with a 0.0- 10 mM Tris buffer at pH 7.0, 0.2M NaCl gradient created with a gradient maker. Fractions of about 4 mL were collected. The fractions were read using an Agilent 8453 Diode Array Spectrophotometer and monitoring the absorbance at 280 nm, 421 nm, and 554 nm. Fractions determined to contain the protein were pooled and concentrated to 5 mL using Amicon-Centriprep concentrators with a molecular weight cut off of 10,000 Da. The concentrate was passed through a Sephadex G-100 gel filtration column that had been equilibrated with 10mM Tris buffer, pH 7.0. Ellution of the protein was achieved by the use of 10 mM Tris, pH 7.0. The fractions collected, read, pooled, and concentrated to 10 mL were then purified further on a Waters HPLC using a BioRad Q12 anion exchange column with a 5 mM phosphate, pH 7.0 to 500 mM phosphate, pH 7.0 gradient. The sample was considered pure when (absorbance at the alpha peak / absorbance at 280 nm) ≥ 0.8. Further preparation of the sample for experimental use was based on the procedure to be performed and is described in the appropriate section.

3.9 REDOX TITRATIONS

Completion of sample preparation prior to redox titrations consisted of the exchange of the protein into 5 mM phosphate buffer at pH 7.0 and concentrated to 5 μM. Using the ratio of reagent grade Potassium Ferricyanide (Fe) to Potassium Ferrocyanide (Fo), the midpoint potentials of the mutants were measured. Fe, which oxidizes the sample, was added to 1 mL of 5 μM purified cytochrome f. Fo was added in increments to reduce the sample. A few crystals of ascorbic acid and sodium dithionite were added at the end to ensure complete reduction of the sample. All additions were made according to Tables 3.1 and 3.2. The change in absorbance at 554 nm was used to monitor the change in the redox

state of cytochrome f and the change in absorbance at 553 nm was used for cytochrome c_6. Absorbance was measured with an Agilent 8453 Diode Array Spectrophotometer after each addition of Fe, Fo, ascorbic acid, and dithionite. According to the Nernst Equation (Eh = Eo – 59 log [(red)/(ox)]) the plot of log [(red)/(ox)] vs. Eh gives a midpoint potential equal to the redox potential where log [(red)/(ox)] = 0.0. Each run was plotted to determine the value for the potential.

These titrations were done at varying pH from 6.0 to 10.5 in increments of 0.5. The buffer used also varied with pH. For pH 6 through 7.5 a 100 mM phosphate buffer was used, for pH 8 through 10 a 10mM Tris buffer was used initially and then was changed to 100 mM to conserve ionic strength throughout the range of pH, and for pH 10.5 a 100 mM CAPS buffer was used. These buffers where chosen based on a previous study conducted by the Kramer lab (Soriano et al. 1998).

The pKa value determined for the protein was determined to be at the intersection of lines fitted to a plot of pH vs. midpoint potential. The first line was fitted to the data points that showed no significant drop in potential from the starting point (pH 6). The second line was fitted to the data where the redox potential began to fall off. The pH corresponding to the intersection of the resultant lines was taken as the pKa of transition for the protein

3.10 DIFFERENTIAL SCANNING CALORIMETRY

DSC runs for oxidized data were conducted using 1.1 mL, 0.5 -1 mg/mL samples of protein dialyzed against 3 portions of 100 mL of 0.1 M phosphate buffer, pH 7 and ferricyanide using Spectra/Por membrane MWCO of 6 – 8,000 (10 mM). Reduced data was collected after dialysis in buffer containing dithionite. Concentrations were determined using a difference spectrum. Buffer exchanges were done no sooner than every two hours. Buffer vs. buffer baselines were established for each run using degassed dialysis buffer from the third 100 mL portion. Degassed protein vs. buffer was used to conduct each run and obtain an unfolding profile. Runs were conducted using a temperature range of 10°C - 80°C for cytochrome f and 10°C – 110°C for oxidized cytochrome c_6 and 30°C – 130°C for reduced cytochrome c_6. Heating and cooling rates used were 0.5°C/min, 1°C /min, and 2°C/min. Data was analyzed using

Cpcalc software. In runs containing NDSB, 2 M NDSB was added to the protein sample post-dialysis to give a final concentration of 1 M NDSB.

3.11 CIRCULAR DICHROISM SPECTROMETRY

Circular dichroism has classically been used to elucidate secondary structure in proteins by examining the far UV region between 190 nm and 250 nm. However, this technique can also be utilized to observe alterations in the heme environment by focusing on the Soret or gamma-band region of 380nm – 440 nm (Myer 1985). Three milliliter samples of protein around 5 μM in concentration were dialyzed against 3, 300 mL portions of 100 mM phosphate buffer at pH 7 in 10,000 molecular weight cut off (10 mM) dialysis membranes from Spectra-por. Concentration was kept in the range where the Soret peak absorbance was below one. Additions of ferricyanide were made to the buffers in order to conduct oxidized runs, and sodium dithionite was added to the buffer in order to reduce the protein in the case of reduced runs. A UV-Vis spectrum was recorded for measurement of concentration and to ensure the absorbance at the Soret peak was less than 1. Samples were run on a JASCO-710 CD-spectropolarimeter. The parameters used for the experiment are as follows: bandwidth: 2 nm, sensitivity: 100 mdeg, response: 4 sec, range: 650 - 300 nm, scan mode: continuous, data pitch: 0.1 nm scan speed: 50 nm/min, step resolution, 0.5 nm, runs: 6. Baselines were obtained using the last change of dialysis buffer and FeCN or sodium ascorbate for the oxidized and reduced baselines respectively (Eades 1996, Scharlau 1998).

Tables 3.9.1 and 3.9.2: The following tables give a description of the concentrations and additions of oxidizing and reducing agents for redox potential measurements and corresponding Eh values for measurements made at pH's 6 – 9.5. for Table 3.1 and measurements made at pH's 10 and 10.5 in Table 3.2. Note: The second table also describes the titrations of the cytochrome f R156 mutants due to their low redox potentials.

Table 3.1

Addition	Calculated Eh Value
1µL of 100mM Potassium Ferricyanide	
1µL of 100mM Potassium Ferrocyanide	430 mV
1µL of 100mM Potassium Ferrocyanide	412 mV
2µL of 100mM Potassium Ferrocyanide	394 mV
2µL of 100mM Potassium Ferrocyanide	384 mV
2µL of 100mM Potassium Ferrocyanide	371 mV
2µL of 100mM Potassium Ferrocyanide	366 mV
10µL of 100mM Potassium Ferrocyanide	353 mV
10µL of 100mM Potassium Ferrocyanide	343 mV
10µL of 100mM Potassium Ferrocyanide	335 mV
10µL of 100mM Potassium Ferrocyanide	330 mV
A few crystals of ascorbic acid	
A few crystals of Sodium dithionite	

Table 3.2

Addition	Calculated Eh Value
1µL of 350mM Potassium Ferricyanide	
1µL of 350mM Potassium Ferrocyanide	389 mV
1µL of 350mM Potassium Ferrocyanide	371 mV
2µL of 350mM Potassium Ferrocyanide	353 mV
2µL of 350mM Potassium Ferrocyanide	343 mV
2µL of 350mM Potassium Ferrocyanide	335 mV
2µL of 350mM Potassium Ferrocyanide	330 mV
10µL of 350mM Potassium Ferrocyanide	312 mV
10µL of 350mM Potassium Ferrocyanide	302 mV
10µL of 350mM Potassium Ferrocyanide	294 mV
10µL of 350mM Potassium Ferrocyanide	289 mV
A few crystals of ascorbic acid	
A few crystals of Sodium dithionite	

CHAPTER 4 – RESULTS

4.1 GROWTH, EXPRESSION, AND SPECTRAL CHARACTERISTICS OF MUTANT AND WILD-TYPE CYTOCHROME F

The mutations made to the PUCF2 plasmid coding for cytochrome f include Y1F, Y9F, Y160F, R156L, and R156K. All of the residues investigated surround the heme. These mutations were made to investigate the effects of alterations made to the heme environment. The mutations were confirmed by DNA sequencing to ensure the correct mutation was made to the plasmid.

Spectral characteristics were observed to ensure the presence of the protein. A typical spectrum for *C. reinhardtii* cytochrome f in the reduced state includes an alpha peak at 554 nm, a beta peak at 524 nm, and a Soret peak at 421 nm. In the spectrum of the oxidized protein the broadening of the alpha and beta peaks is observed compared to that of the reduced protein, and the Soret peak is located at 411 nm. There is no peak located around 695 nm in the oxidized spectrum as seen in other c type cytochromes. This 695 nm band is indicative of a histidine-methionine coordination of the heme which is not the case in cytochrome f where the N-terminal α-amino group and histidine 25 serve as the axial ligands. Such is the case in previous examinations of the same protein done in our lab (Bhise 2006, Staiger 2007). An example of the reduced and oxidized spectra may be seen in Figure 4.1.1. The spectra of the mutant proteins are the same as that for the wild-type with the exception of the R156 mutants where the reduced Soret peak shows a shift from 554 nm to 553 nm and the oxidized Soret peak is shifted from 411 nm to 410 nm.

The position of the peaks of the wild-type and the mutants were monitored throughout the redox measurements. Some shifts were seen in the peaks of all the examined proteins and are represented in Tables 4.1.1, 4.1.2, and 4.1.3. The oxidized Soret peak tends to shift at high pH in both the wild-type and Y160F mutant. Shifts are also seen is the oxidized Soret peak in the Y1F and Y9F mutants as low as pH 7.0 and pH 8.5 respectively. The Y160L mutant shown in the next Table 4.1.2 shows shifts in the oxidized Soret peak at lower pH, shifts in the reduced Soret band at higher pH, shifts in the alpha band at extremely high pH, and shifts in the beta band throughout the entire range of pH's examined. All four peaks of the R156L mutant shown in Table 4.2.3 also shift throughout the entire range of pH examined.

The R156K mutant was not examined over a range of pH, but its spectra are similar in nature to that of the other R156 mutant R156L.

Both the wild-type and mutants were expressed in *E.coli* and grown semi-anaerobically. The wild-type and the mutants were also purified in the same manner by use of gel-filtration (G-100), anion exchange (DE-53), and HPLC anion exchange (Q-12). The absorbance spectra were used to monitor the purity of the samples through the process of purification. The absorbance at 280 nm was used to observe the presence of the entire population of proteins and the absorbance at the alpha peak was used to account for the population of cytochrome f within the sample as seen in Figure 4.1.2. All samples were considered pure when $A_{554}/A_{280} \geq 0.8$. The yield was also monitored using the absorbance at the alpha peak and the extinction coefficient of 26 $mM^{-1} \cdot cm^{-1}$. In the case of both of the R156 mutants the yield was notably lower: 0.5 – 1 mg/L for the R156L mutant and typically less than 0.6 mg/L for the R156K mutant as opposed to an average of 5 mg/L for the wild-type and the other mutants.

Figure 4.1.1: The absorbance spectra of 16 μM wild-type *C. reinhardtii* cytochrome f in 10 mM Tris buffer at pH 7 showing the reduced spectrum (black) with the alpha peak at 554 nm, the beta peak at 524 nm, and the Soret peak at 421 nm along with the oxidized spectrum (grey) showing the Soret peak at 411 nm along with the broadened alpha and beta peaks.

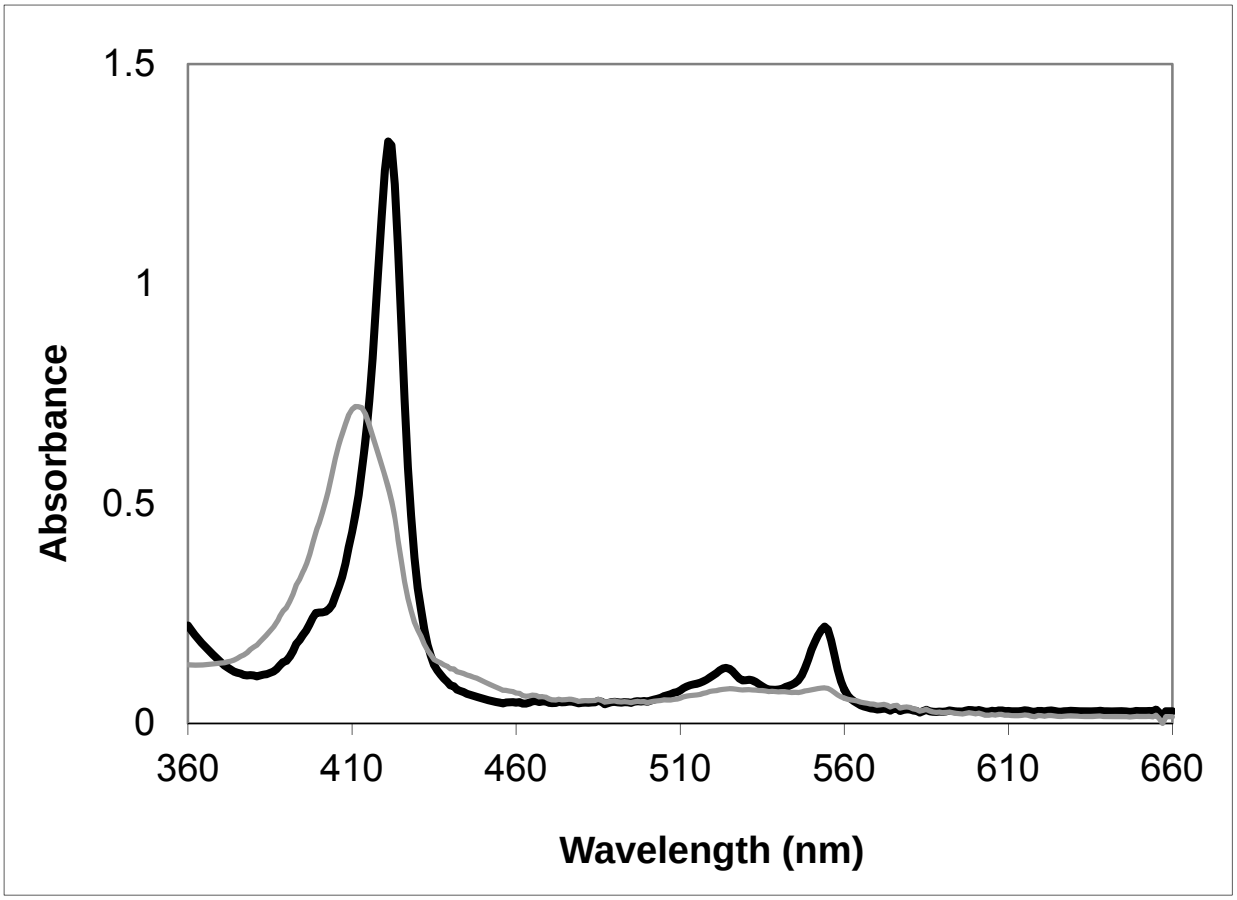
1.5
1
0.5
0
Absorbance
360
410
460
510
560
610
660
Wavelength (nm)

Table 4.1.1: Peaks of wild-type cytochrome f along with the Y160F, Y1F, and Y9F mutants as observed during redox titrations with shifted peaks in bold. Multiple entries are due to different value being observed during different titrations.

	alpha peak	beta peak	reduced Soret peak	oxidized Soret peak
Wt pH 6.0 - 9.0	554nm	524nm	421nm	411nm
Wt pH 9.5 - 10.5	554nm	524nm	421nm	**412nm**
Y160F pH 6.0 - 8.5	554nm	524nm	421nm	411nm
Y160F pH 9.0 - 10.5	554nm	524nm	421nm	**412nm**
Y1F pH 6.0 - 6.5	554nm	524nm	421nm	411nm
Y1F pH 7.0 -8.0	554nm	524nm	421nm	**410nm - 411nm**
Y1F pH 8.5	554nm	524nm	421nm	**412nm**
Y1F pH 9.0	554nm	524nm	421nm	**411nm - 412nm**
Y1F pH 9.5	554nm	524nm	421nm	**412nm**
Y1F pH 10.0 - 10.5	554nm	524nm	421nm	**412nm - 413nm**
Y9F pH 6.0 - 8.0	554nm	524nm	421nm	411nm
Y9F pH 8.5 - 9.0	554nm	524nm	421nm	**411nm - 412nm**
Y9F pH 9.5	554nm	524nm	421nm	**412nm**
Y9F pH 10.0	554nm	524nm	421nm	**411nm - 412nm**
Y9F pH 10.5	554nm	524nm	421nm	**412nm**

Table 4.1.2: Peaks of the cytochrome f Y160L mutant as observed during redox titrations with shifted peaks in bold. Multiple entries are due to different value being observed during different titrations.

	alpha peak (nm)	beta peak (nm)	reduced Soret peak (nm)	oxidized Soret peak (nm)
pH 6.0 - 7.0	554	524	421	**410**
pH 7.5	554	**523 - 524**	421	**410**
pH 7.5 + Dithionite	554	**524**	421	
pH 8.0	554	**523 - 524**	421	**410 - 411**
pH 8.0 + Dithionite	554	**523 -524**	421	
pH 8.5	554	**523 - 524**	421	**410 - 411**
pH 8.5 + Dithionite	554	524	421	
pH 9.0	554	**523 - 524**	421	411
pH 9.0 + Dithionite	554	**523 - 524**	421	
pH 9.5	554	524	421	411
pH 9.5 + Dithionite	554	**523**	421	
pH 10.0	554	524	**420 - 421**	411
pH 10.0 + Dithionite	554	**523 - 524**	**420 - 421**	
pH 10.5	**553 - 554**	524	**419 - 420**	411

Table 4.1.3: Peaks of the cytochrome R156L mutant as observed during redox titrations with shifted peaks in bold. Multiple entries are due to different value being observed during different titrations.

	alpha peak (nm)	beta peak (nm)	reduced Soret peak (nm)	oxidized Soret peak (nm)
pH 6.0	553	524	421	**409**
pH 6.0 + Dithionite	**552**	**523**	**419 - 420**	
R165L pH 6.5	553	524	**420**	**409**
pH 6.5 + Dithionite	**552**	**523**	**419**	
pH 7.0	553	**524 - 525**	**420 - 421**	**409 - 410**
pH 7.0 + Dithionite	**552 - 553**	524	**417 / 418 / 420**	
pH 7.5	553	524	421	**409 - 410**
pH 7.5 + Dithionite	**552 - 553**	**523 - 524**	**419 / 421**	
pH 8.0	553	524	**419 - 420**	410
pH 8.0 + Dithionite	553	**523**	**419 - 420**	
pH 8.5	553	524	**420**	**409 - 410**
pH 8.5 + Dithionite	553	524	**419**	
pH 9.0	**552 - 553**	524	**420**	410
pH 9.0 + Dithionite	553	**522 / 524**	**419**	
pH 9.5	**551 / 553**	**523 - 525**	**419**	**409**
pH 9.5 + Dithionite	**551 - 553**	**522**	**416 / 418**	
pH 10.0	**551**	**523 - 524**	**419**	**409**
pH 10.0 + Dithionite	**551**	**522**	**418**	
pH 10.5	**550**	**523**	**417**	**409**
pH 10.5 + Dithionite	**551**	**522**	**416**	

Figure 4.1.2: The absorbance spectra of wild-type *C. reinhardtii* cytochrome f in 10 mM Tris buffer at pH 7 showing the increase in the absorbance at the alpha peak relative to that of the 280 nm peak from 5 μM crude protein (thin black line), 4 μM protein after DE-53 anion exchange and 3 μM protein G-100 gel filtration columns (dashed line), and 3 μM after the Q-12 HPLC anion exchange column (dark black line).

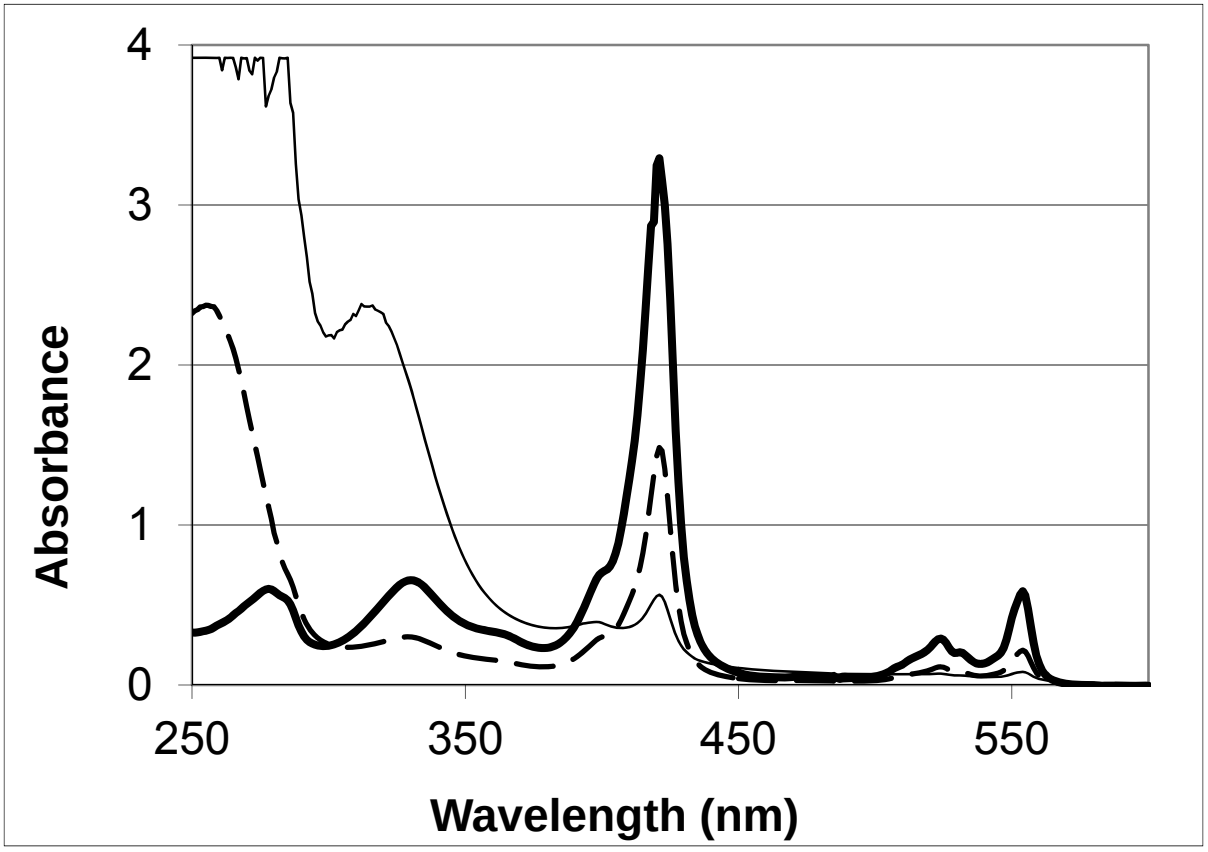
4
3
2
1
0
Absorbance
250
350
450
550
Wavelength (nm)

4.2 REDOX POTENTIALS OF MUTANT AND WILD-TYPE CYTOCHROME F AND THEIR DEPENDENCE UPON PH

The midpoint potentials were determined for the wild-type and mutants of cytochrome f by conducting titrations with a ferricyanide/ ferrocyanide couple of known potential. A straight line plot was generated by plotting the half cell potential (Eh) against the log of the fraction oxidized divided by the fraction reduced. The point at which the line crosses the X-axis gives the value for the midpoint potential of the protein. A summary of the average values at pH 7 and the number of calculated electrons transferred are displayed in Table 4.2.1. The wild-type cytochrome f was found to have a midpoint potential at pH 7 ($E_{m,7}$) of 380 ± 4 mV consistent with that of the literature values and previous values determined by our lab (Bhise 2006, Staiger 2007).

The mutants Y1F and Y9F when investigated were shown to have $E_{m,7}$'s of 384 ± 10 mV and 379 ± 1 mV respectively. Both of the values are within 5 mV of the determined value for that of the wild-type and therefore are not considered to be significantly different than the wild-type. A comparison of the 3 values, wild-type, Y1F, and Y9F is shown on a graph of half cell potential (Eh) vs the log of the fraction oxidized / fraction red in Figure 4.2.1.

The $E_{m,7}$'s for mutants of the Y160 residue were also determined and found to be 377 ± 9 mV for the mutation of the residue to phenylalanine and 357 ± 3 mV for the leucine mutant. The value determined for the Y160F mutation is not considered different from the wild-type value, however, the value determined for the Y160L mutant showed a decrease of about 20 mV from the wild-type and the Y160F mutant. The difference, being greater than a 5 mV, is considered significant. The reduction in potential is seen in the Y160L mutant yet is not present in the Y160F mutant indicating the retention of the aromatic character of the Y160 residue is necessary to maintain the midpoint potential that is seen in the wild-type protein and the hydrogen bond of the phenolic hydrogen of Y160 with the heme propionate is not important. The data for the Y160L is also consistent with previous values determined in our lab (Bhise 2006). The half cell potential (Eh) against the log of the fraction oxidized / fraction reduced plots for the wild-type protein along with the Y160F and the Y160L mutants depicting the midpoint potentials at pH 7 are shown in Figure 4.2.2.

The potentials for both of the R156 mutants were conducted anaerobically due to the fact that both of the mutants were easily oxidized in the presence of oxygen. Placing the samples under nitrogen allowed for the midpoint potentials to be measured. The potentials measured at pH 7 varied from that of the wild-type and even more significantly than the Y160L mutant. The $E_{m,7}$ value for the R156K mutant was determined to be 325 ± 5 mV which is about a 55 mV decrease from the value of the wild-type, and the value for the R156L mutant was found to be 291 ± 6 mV showing a decrease from the R156K value of about 35 mV and from the wild-type value of 90 mV. This indicates that the arginine in the position accounts for 90 mV of the potential of the protein and when altered even to another positive residue greatly affects the midpoint potential. The values for the R156 mutants in comparison to the wild-type are presented in Figure 4.2.3.

Table 4.2.1: Cytochrome f wild-type and mutants values of the averaged midpoint potential at pH 7 with standard deviation and calculated value for the number of electrons transferred (n) for the potentials measured.

Protein	$E_{m,7}$ (mV)	n
wild-type	380 ± 4	0.99 ± 0.17
Y1F	384 ± 10	0.77 ± 0.06
Y9F	379 ± 1	0.91 ± 0.03
Y160F	377 ± 9	0.83 ± 0.12
Y160L	357 ± 3	0.83 ± 0.05
R156L	291 ± 6	0.78 ± 0.06
R156K	325 ± 5	0.72 ± 0.004

Figure 4.2.1: Plot of log [(red)/(ox)] vs. Eh showing the midpoint potential where the line intersects log [(red)/(ox)] = 0.0 for Wild-type cytochrome f (solid line, black squares), Y1F (dashed line, black circles), and Y9F (dotted line, gray triangles) at pH 7.

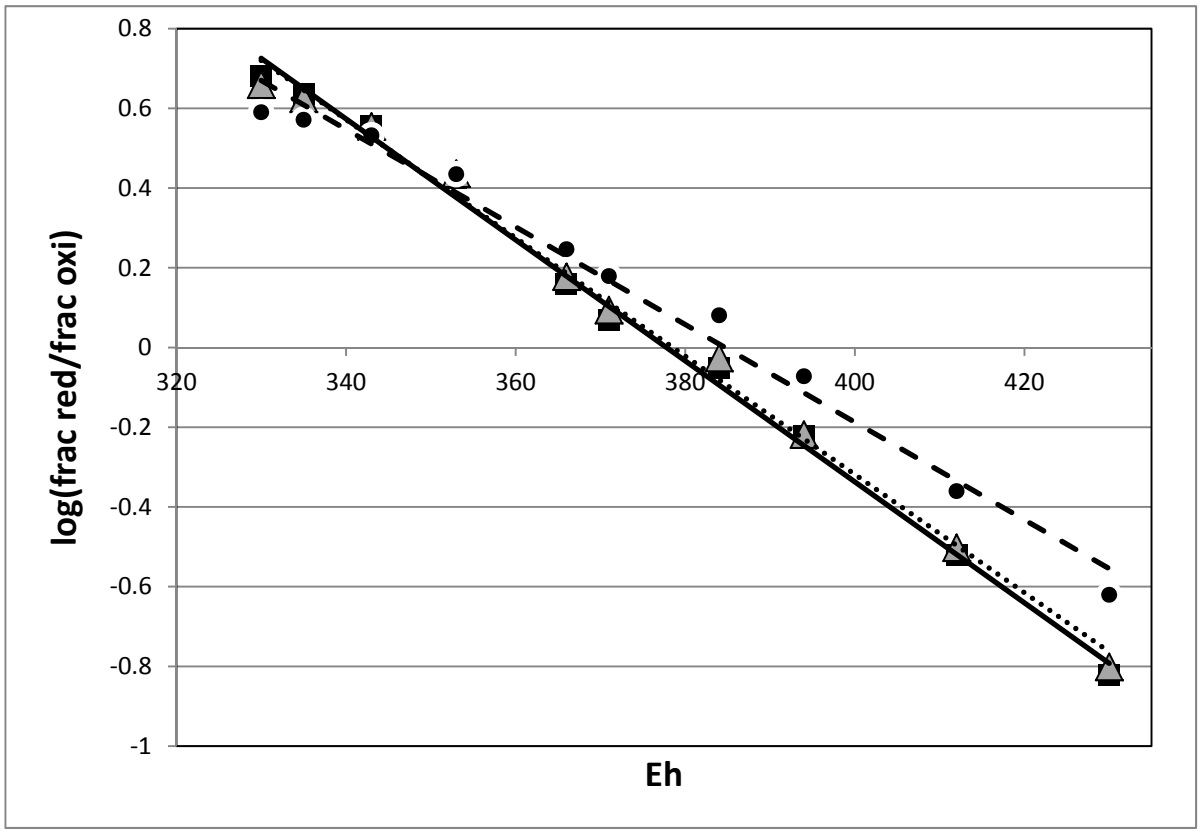
0.8
0.6
0.4
0.2
0
-0.2
-0.4
-0.6
-0.8
-1
320
340
360
380
400
420
log(frac red/frac oxi)
Eh

Figure 4.2.2: Plot of log [(red)/(ox)] vs. Eh showing the midpoint potential where the line intersects log [(red)/(ox)] = 0.0 for Wild-type cytochrome f (solid line, black squares), Y160F (dashed line, gray triangles), and Y160L (dotted line, black circles) at pH 7.

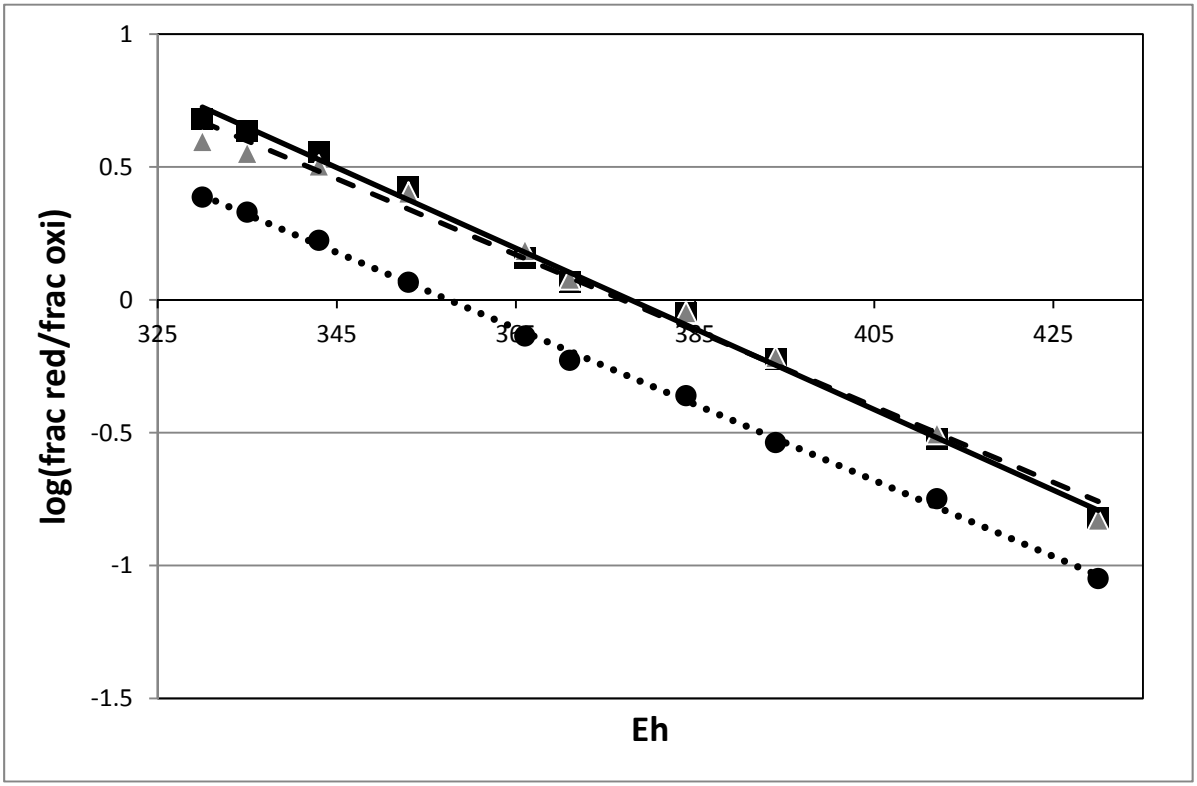
1
0.5
0
-0.5
-1
-1.5
325
345
405
425
log(frac red/frac oxi)
Eh

Figure 4.2.3: Plot of log [(red)/(ox)] vs. Eh showing the midpoint potential where the line intersects log [(red)/(ox)] = 0.0 for Wild-type cytochrome f (solid line, squares), R156K (dashed line, circles), and R156L (dotted line, triangles) at pH 7.

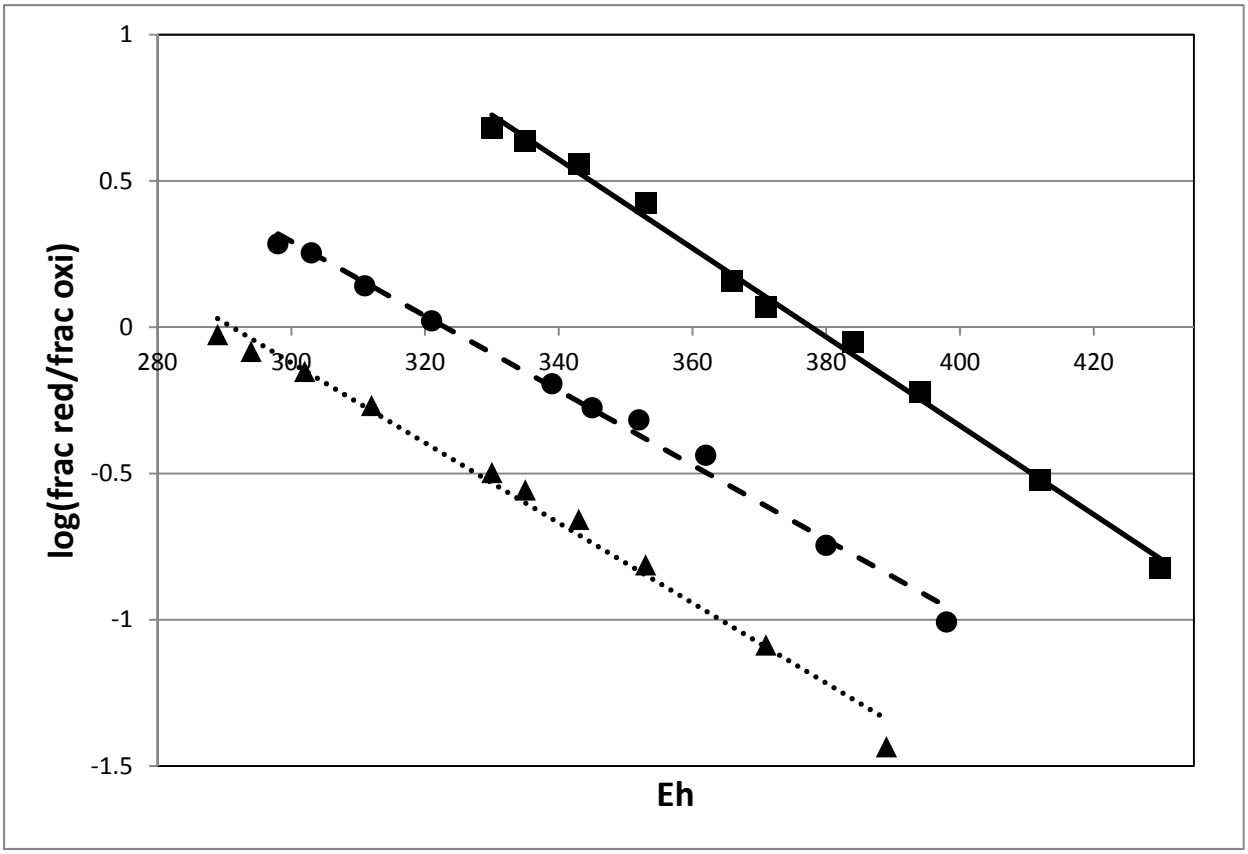
1
0.5
0
-0.5
-1
-1.5
280
300
320
340
360
380
400
420
log(frac red/frac oxi)
Eh

The midpoint potentials for the wild-type and mutant proteins were also determined across a range of pH from pH 6.0 to pH 10.5. By looking at the midpoint potential across a range of pH one can determine whether the potential drops as the pH increases, illustrating a pH dependence, or if the potential remains constant across the range of pH which is indicative of a potential that is independent of pH. If a decrease is seen the pKa for the protein can be determined by graphing pH vs E_m and drawing a straight line through the values for the midpoint potential that are consistent and another line through those where the midpoint potential drops. The pH indicated by the intersection of these lines defines the value for the pKa of transition for that protein.

Both the wild-type protein and the mutants Y1f, Y9F, Y160F, and Y160L show a decrease in the potential of the protein at higher pH's and therefore are considered to be pH dependent. The wild-type pKa was determined to be 9.3 ± 0.2. The pKa's found for the Y1F and Y9F mutants were found to be 9.3 ± 0.2 and 9.2 ± 0.2 respectively and are not significantly different from that of the value determined for the wild-type protein. The graphs showing the determinations of the pKa's for the Y1F and Y9F mutants are found along with those for the wild-type in Figures 4.2.4 and 4.2.5.

The pKa's were also determined for the Y160 mutants. The pKa found for the Y160F mutant was found to be 9.2 ± 0.2 and is shown on the graph in Figure 4.2.6 along with the graph of the wild-type. There is no significant difference for the pKa determined for the Y160F mutant and the pKa of the wild-type protein. The Y160L mutation, however, with a determined pKa of 8.8 ± 0.2 is significantly different from that of the wild-type protein. The determination of the value for the pKa of the Y160L mutant is found in Figure 4.2.7 and is shown along with that of the wild-type. The averages used along with the standard deviations and sample size values for the data for the wild-type and the Y1F, Y9F, Y160F, and Y160L mutants presented in the aforementioned figures are found in Table 4.2.2.

The pKa was not able to be determined for the mutants of the R156 residue. Mutations made to this residue have caused the protein to be unsuitable to undergo titrations throughout the range of pH needed to determine the value of the pKa. Titrations at higher pH do not give consistent midpoint potentials even with titrations conducted under anaerobic conditions with the samples being under nitrogen. It was noted however for the R156L mutant that the percent of the protein population reducible by ascorbate decreased as the pH increased, and from pH 9.5 to pH 10.5 the percent not reducible

accounted for more than half of the population. A depiction of the percent not reducible by ascorbate is presented in a graph in Figure 4.2.8. The R156K mutant was not able to be examined over the entire range of pH because of the low yield of the protein able to be obtained from the growth and purification procedures.

Figure 4.2.4: Graph of pH vs Eo showing the determinations of the pKa's of wild-type cytochrome f (black diamonds, solid black lines) and the Y1F mutant (grey dots, dashed grey lines).

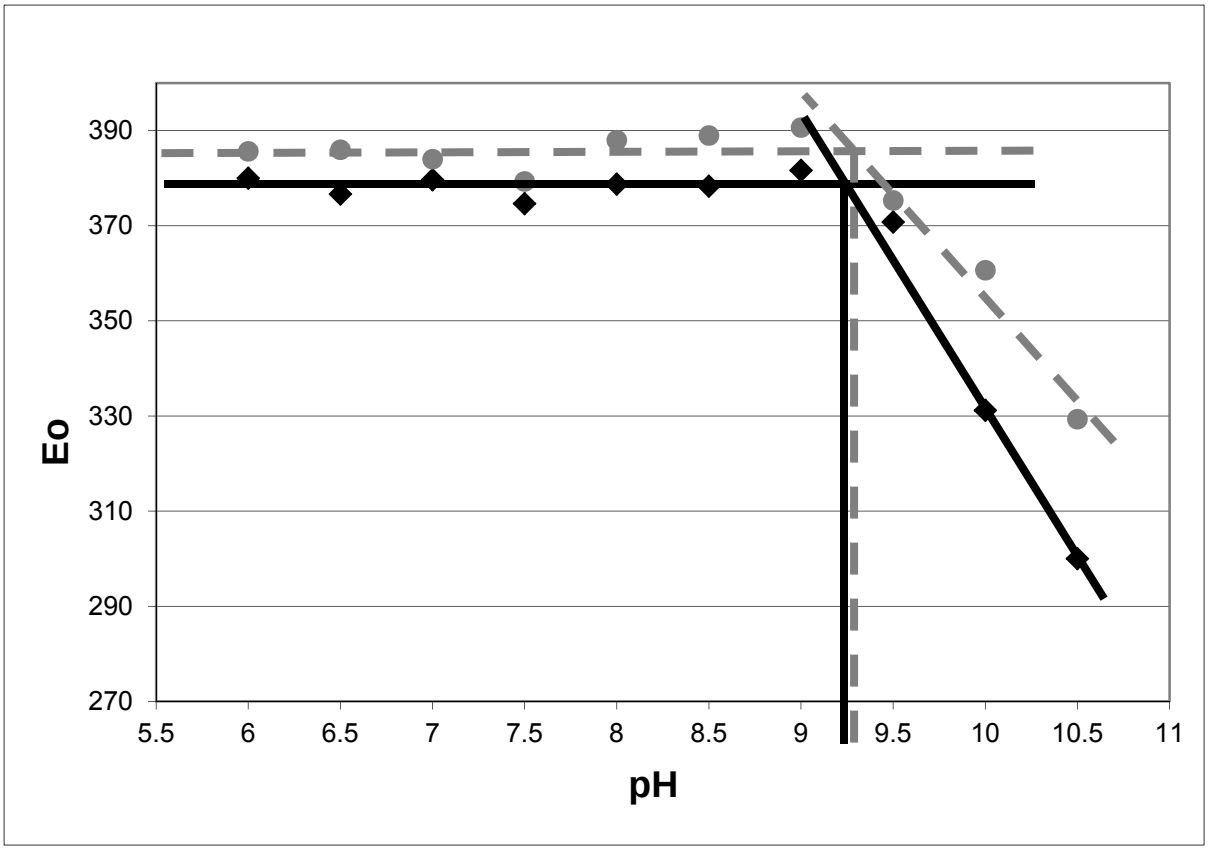
390
370
350
330
310
290
270
Eo
5.5
6
6.5
7
7.5
8
8.5
9
9.5
10
10.5
11
pH

Figure 4.2.5: Graph of pH vs Eo showing the determinations of the pKa's of wild-type cytochrome f (black diamonds, solid black lines) and the Y9F mutant (grey dots, dashed grey lines).

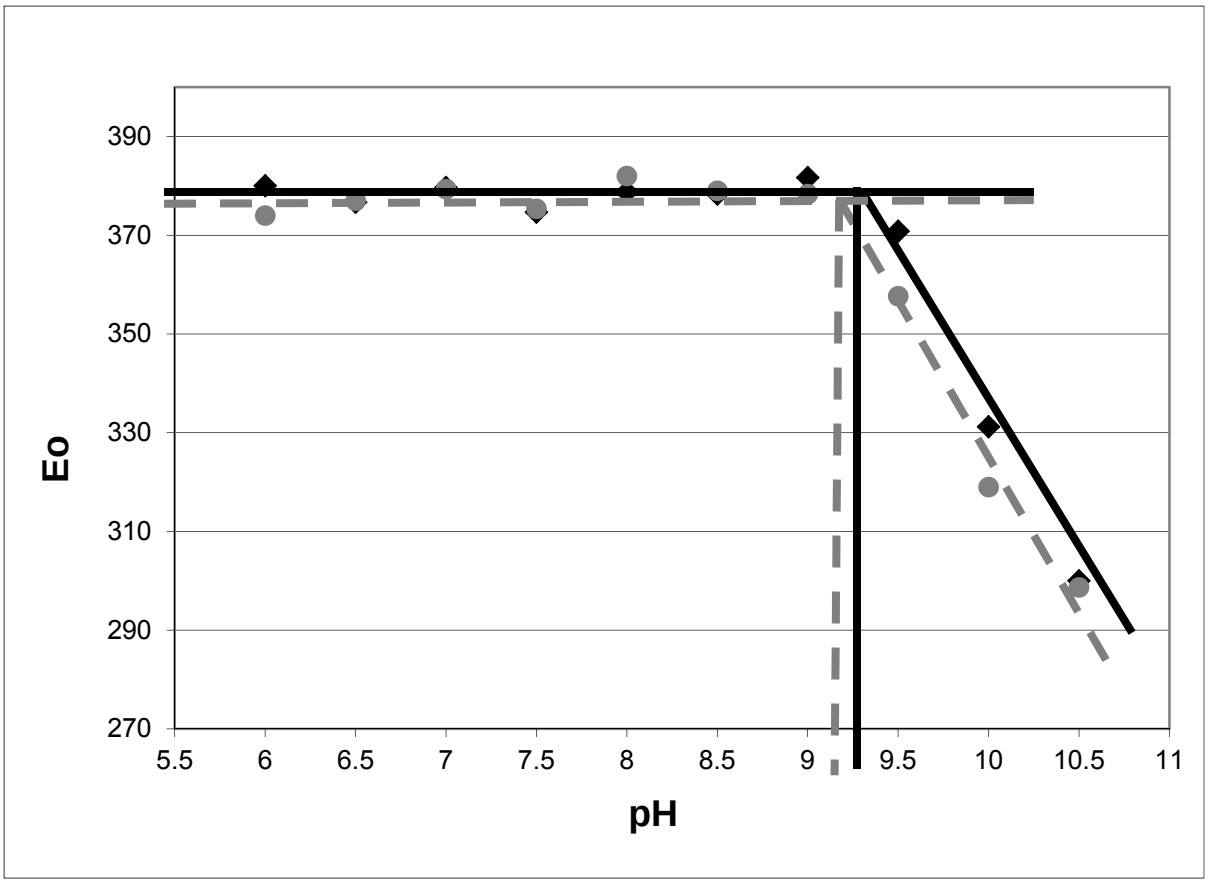
390
370
350
330
310
290
270
Eo
5.5
6
6.5
7
7.5
8
8.5
9
9.5
10
10.5
11
pH

Figure 4.2.6: Graph of pH vs Eo showing the determinations of the pKa's of wild-type cytochrome f (black diamonds, solid black lines) and the Y160F mutant (grey dots, dashed grey lines).

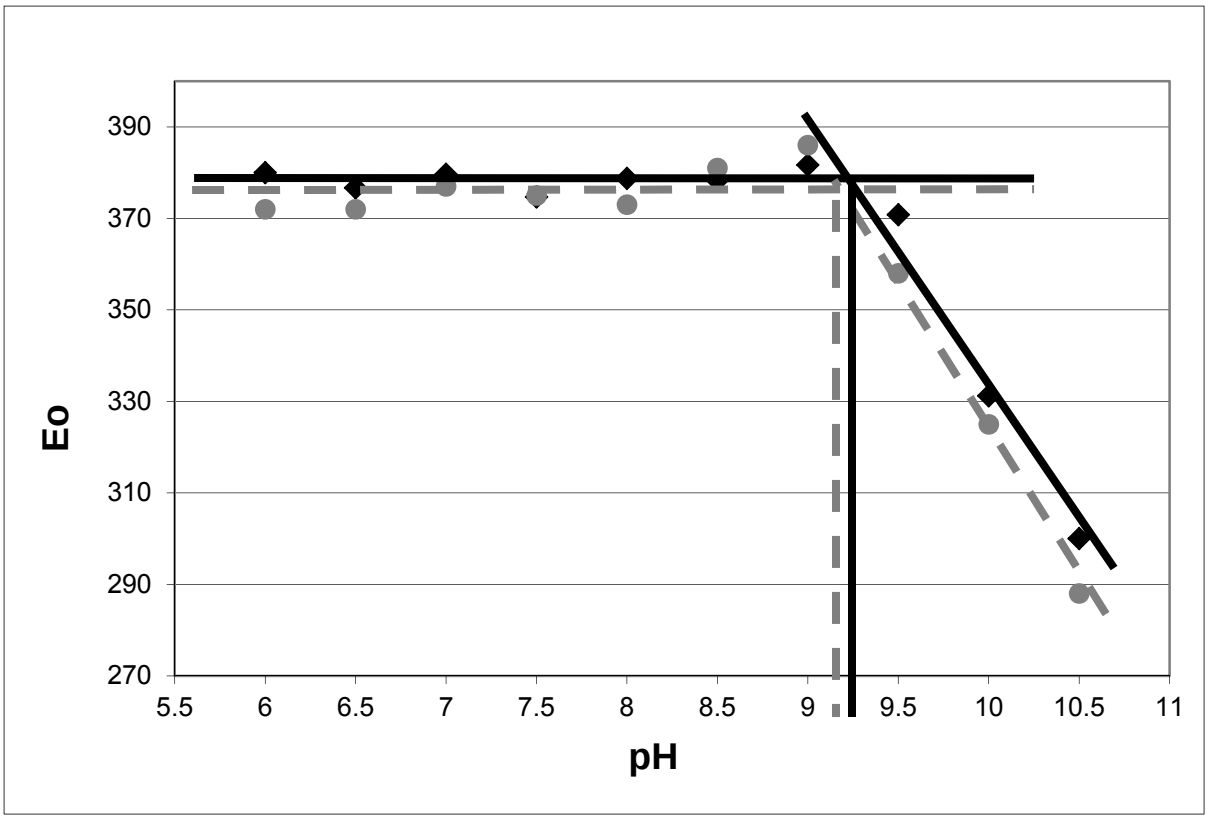
390
370
350
330
310
290
270
Eo
5.5
6
6.5
7
7.5
8
8.5
9
9.5
10
10.5
11
pH

Figure 4.2.7: Graph of pH vs Eo showing the determinations of the pKa's of wild-type cytochrome f (black diamonds, black solid lines) and the Y160L mutant (grey dots, dashed grey lines).

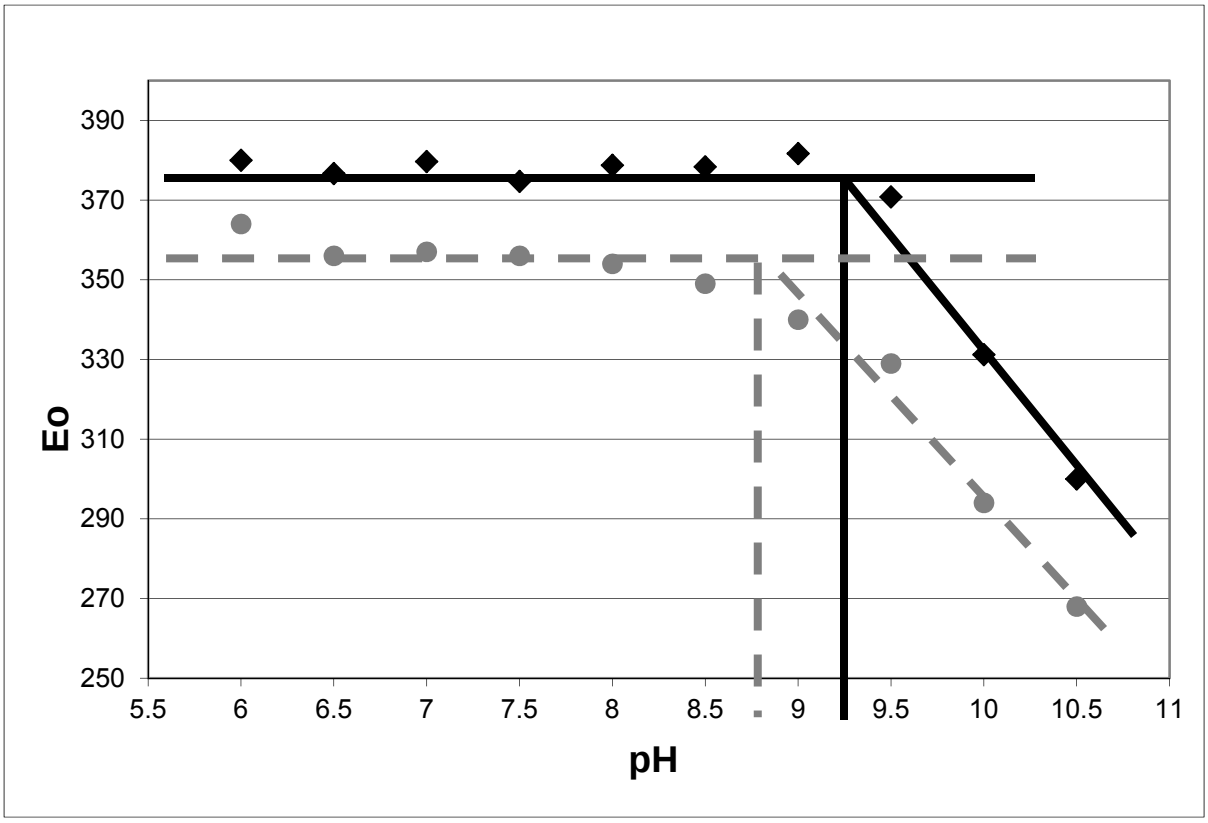
390
370
350
330
310
290
270
250
Eo
5.5
6
6.5
7
7.5
8
8.5
9
9.5
10
10.5
11
pH

Table 4.2.2: Table showing the averages, standard deviations, and sample size (n for the redox titrations at pH's 6.0 – 10.5 of the wild-type and mutants of cytochrome f corresponding to the data presented in Figures 4.2.4 through 4.2.7.

	Wild-type			Y1F			Y9F			Y160F			Y160L		
pH	AVG	SD	n	AVG	SD	n	AVG	SD	n	AVG	SD	n	AVG	SD	n
6.0	380	3	3	386	4	3	374	7	3	372	2	3	364	2	3
6.5	377	7	3	386	10	3	377	3	3	372	2	3	356	4	3
7.0	375	10	4	384	10	3	379	1	3	372	10	4	357	3	3
7.5	375	3	3	379	4	3	375	2	3	375	10	3	356	2	3
8.0	379	4	4	388	3	3	382	4	3	373	5	3	354	7	3
8.5	378	10	3	389	6	3	379	3	3	381	4	3	349	1	3
9.0	382	6	3	391	2	3	378	6	3	386	10	3	340	2	3
9.5	371	10	5	375	4	3	358	5	3	358	10	6	329	10	3
10.0	331	10	5	361	3	3	319	3	3	325	3	3	294	10	3
10.5	300	3	4	329	4	3	299	1	3	288	10	3	268	20	4

Figure 4.2.8: Graph of pH vs percent of protein not reducible by ascorbate for the cytochrome f R156L mutant (grey dots) vs the wild-type (black diamonds).

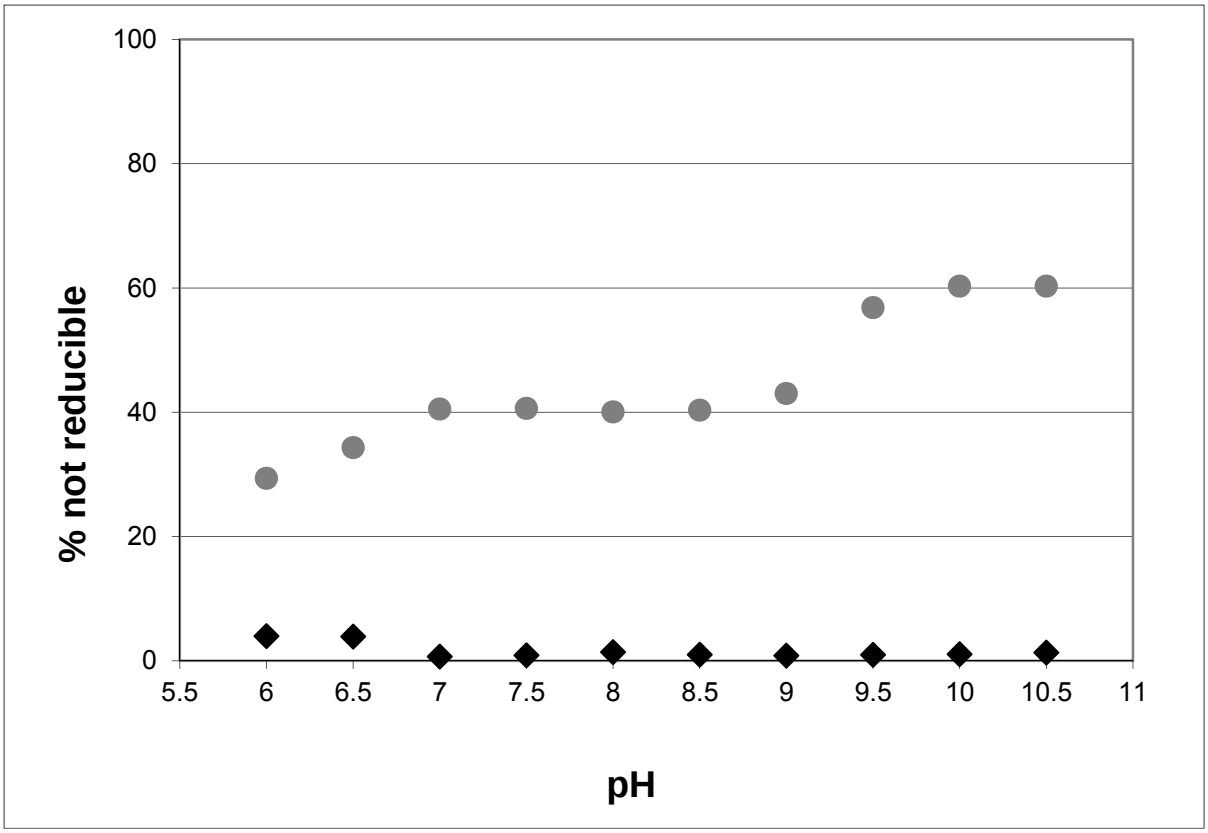
100
80
60
40
20
0
% not reducible
5.5
6
6.5
7
7.5
8
8.5
9
9.5
10
10.5
11
pH

4.3 DIFFERENTIAL SCANNING CALORIMETRY STUDIES OF CYTOCHROME F

Differential scanning calorimetry was used to establish the thermodynamic parameters of unfolding and the stability for cytochrome f from *C. reinhardtii*. When a protein folds reversibly this technique is able to provide values such as ΔS, ΔH, and melting temperature (T_m). These values can then be compared to values previously obtained for a wide range of other proteins. However, the folding of cytochrome f was found to be irreversible. The only value that was able to be obtained reproducibly was the melting temperature of the protein. The melting temperature is determined by looking at the graph of excess heat capacity vs. temperature. The melting temperatures determined for the runs conducted using oxidized wild-type cytochrome f and mutants thereof are displayed in Table 4.3.1. Initially runs were conducted on 0.5 to 1.0 mg/mL protein at 2°C/min. The profiles obtained for the oxidized wild-type protein contained one peak whose position averaged to be 49 ± 0.8°C. An example is shown in Figure 4.3.1. The reduced profile for the wild-type cytochrome f shown in Figure 4.3.2 also had one peak around 73°C. This profile shows the aggregation of the protein immediately upon unfolding indicated by the plummeting post transitional baseline.

When the mutant runs at 2°C/min were analyzed it was found that the profiles displayed multiple peaks. Runs were conducted using a slower scan rate of either 0.5 or 1°C/min in an attempt to resolve the profiles further. The Figure 4.3.3 is a profile from the Y160F mutant that was partially reduced before the run was conducted. The profile shows three peaks. The first peak is located where the oxidized peak for the mutant is typically located and the third peak is located where the reduced peak is expected to be found. The middle peak is therefore not representative of the reduced state being present in the population. This type of profile was found for all of the other mutants as well and is documented in Table 4.3.1. None of the values for any of the mutants of cytochrome f were found to be significantly different from that of the wild-type protein indicating that the mutations made did not specifically affect the stability of the protein.

Table 4.3.1: T_m values obtained from oxidized DSC experiments listing the peak heights from cytochrome f wild-type and mutants. Runs 1 and 2 were run at 2ºC/min, runs 3 and 4 at 1ºC/min, and run 5 at 0.5ºC/min. All samples were between 0.5 and 1.0 mg/mL.

Run	Wt	Y1F	Y9F	Y160F	Y160L
1	48	49, 59	47, 67	47, 67	47
2	50	49, 60		48, 58	49, 62
3		48, 61	47, 60	47, 60	48, 61
4			47, 60	47, 59	49, 61
5	48				
AVG	49	49, 60	47, 62	48, 59	48, 61

Figure 4.3.1: Oxidized DSC run for wild-type cytochrome f run at 2ºC/ min on a sample of 1 mg/mL showing a peak at 49°C. Baseline corrected using Microsoft Excel.

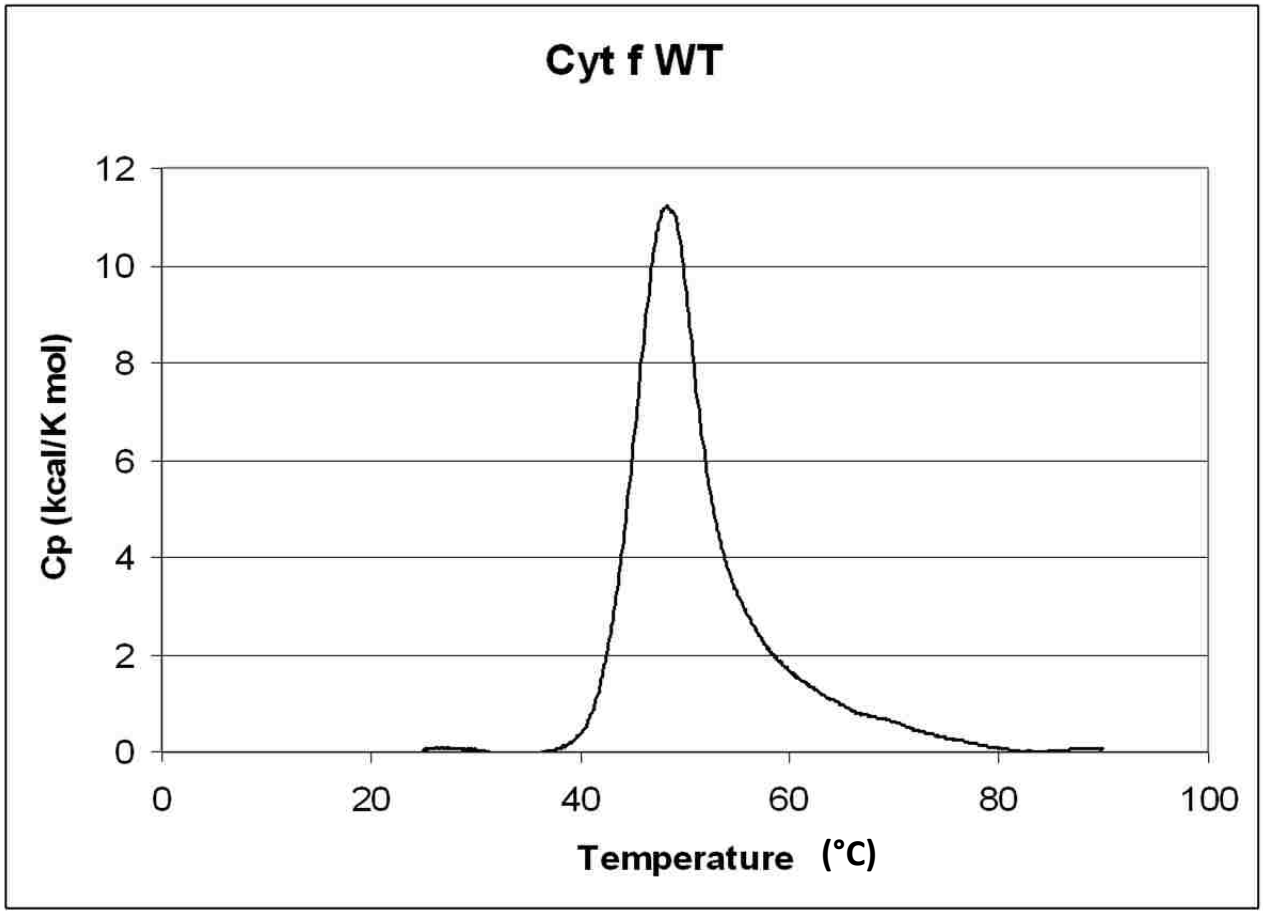
Cyt f WT
Cp (kcal/K mol)
12
10
8
6
4
2
0
0
20
40
60
80
100
Temperature (°C)

Figure 4.3.2: Reduced DSC run for wild-type cytochrome f run at 2ºC/min on a sample of 1 mg/mL showing a peak at 73°C.

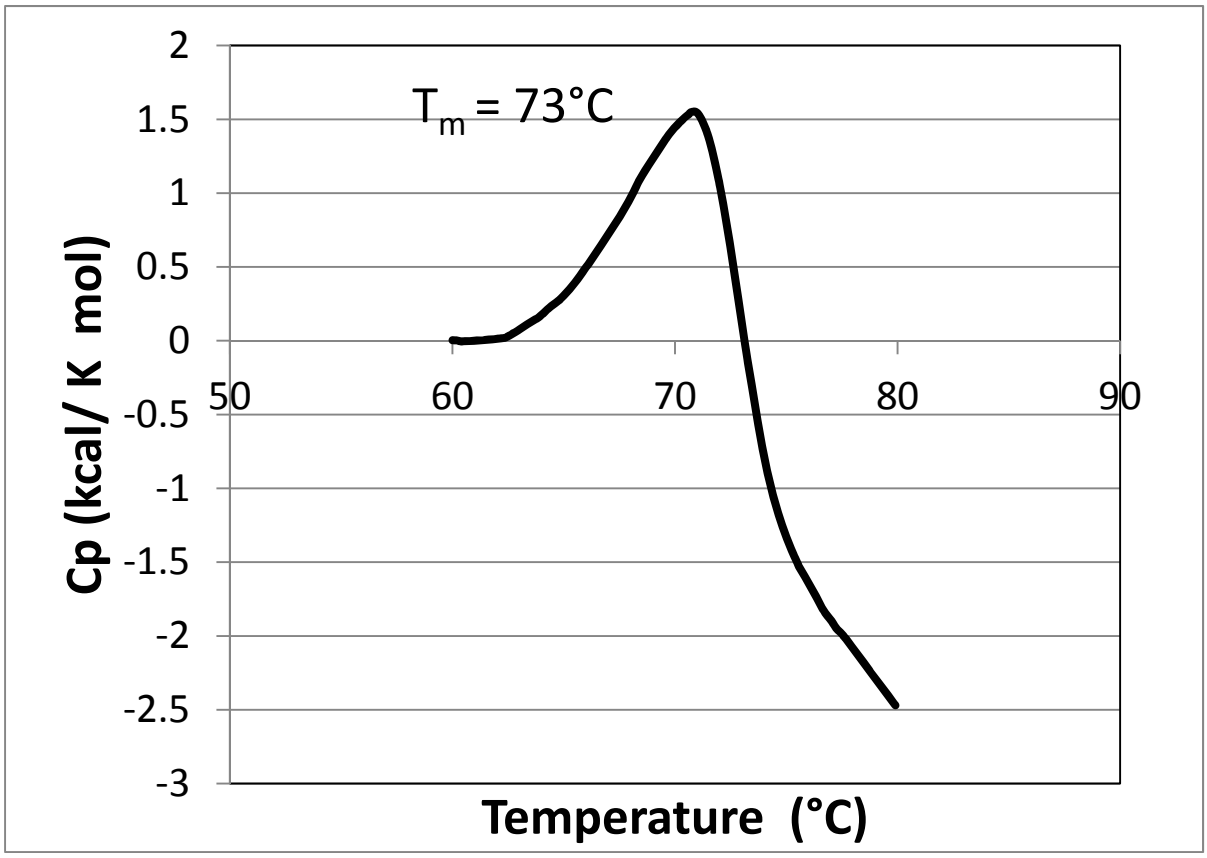
T_m = 73°C
2
1.5
1
0.5
0
-0.5
-1
-1.5
-2
-2.5
-3
50
60
70
80
90
Cp (kcal/ K mol)
Temperature (°C)

Figure 4.3.3: DSC run for cytochrome f mutant Y160F run at 2ºC/min on a sample of 1 mg/mL. This profile shows the 3 peaks. The reduced peak is present at 48°C, the oxidized at 73°C, and the 3rd peak at 58°C.

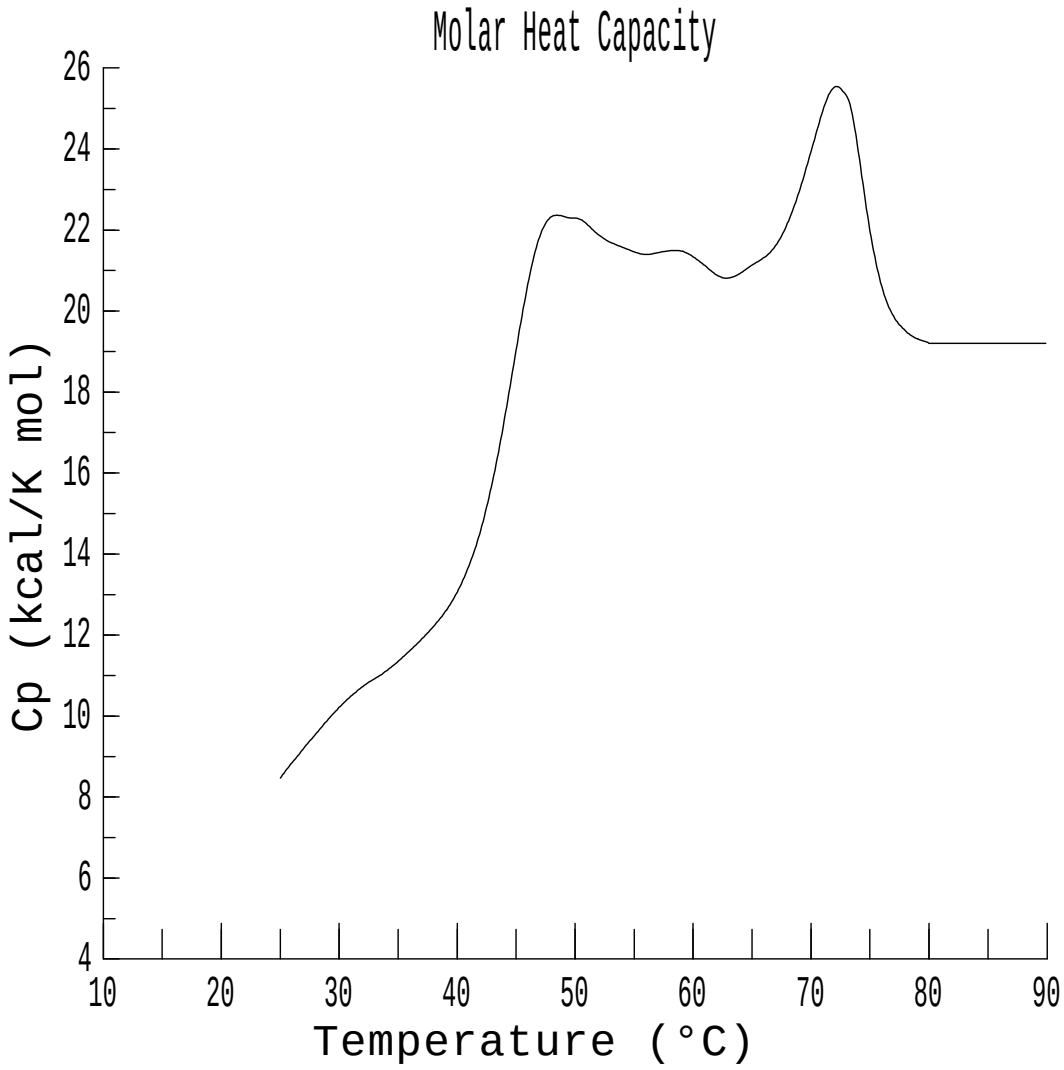
Molar Heat Capacity
Cp (kcal/K mol)
26
24
22
20
18
16
14
12
10
8
6
4
10
20
30
40
50
60
70
80
90
Temperature (°C)

4.4 PLASMID CREATION, GROWTH, AND EXPRESSION OF CYTOCHROME C_6 WILD-TYPE AND MUTANTS

In order to investigate the properties of cytochrome c_6 from *C. reinhardtii* a designer gene for the protein was incorporated into the cytochrome f expression system for ease of expression and purification. The synthetic gene constructed was based on the gene sequence in Hill et al. 1991. The leader sequence and introns were removed, and the codons were substituted to reflect codon bias of *E. coli*. NcoI, EcoR1, and Kpn1 restriction sites were also added for the use in introducing the sequence into the plasmid. The success of the cytochrome c_6 gene insertion into the expression system utilizing the *C. reinhardtii* cytochrome f gene-containing plasmid pUCF2 was confirmed by DNA sequencing. Both mutations, K29I and K57I, were also confirmed by the use of DNA sequencing.

The protein was expressed in *E. coli* (XL1B or MV1190 strain) and harvested from the E. coli by osmotic shock using the same parameters previously described for the cytochrome f protein. The process of purification using anion exchange (DE-53), gel filtration (G-100), and HPLC (Q-12 anion exchange) was also the same as the purification procedures used for cytochrome f. Throughout the process of purification the height of the alpha peak (553 nm) of the absorbance spectra, which indicates the presence of the cytochrome c_6, was monitored and compared to that of the 280 nm peak which accounts for the entire population of protein. The spectra taken after the crude protein was extracted and after the purifications steps are shown in Figure 4.4.1. The sample was considered pure when the $A_{553}/A_{280} \geq 0.8$. Typical growth and purification of both the wild-type protein and both mutants yielded between 0.5 and 2 mg/L of protein.

The identification of the protein was achieved by examination of the spectral characteristics (presented in the section 4.5) and N-terminal sequencing. The N-terminal sequencing provided a 27 amino acid sequence of D L A L G A Q V F N G N (C A A C H) M G G R N S V M P E. This sequence matches exactly that of the expected sequence based on the construction of the plasmid. The heme binding motif (CXXCH) is present in the sequence.

Figure 4.4.1: The absorbance spectra of wild-type *C. reinhardtii* cytochrome c_6 in 10 mM Tris buffer at pH 7 showing the increase in the absorbance at the alpha peak at 553 nm relative to that of the 280 nm peak from crude 6 μM protein (thin black line), 3 μM protein after DE-53 anion exchange, 3 μM protein after G-100 gel filtration columns (dashed line), and 5 μM protein after the Q-12 HPLC anion exchange column (dark black line).

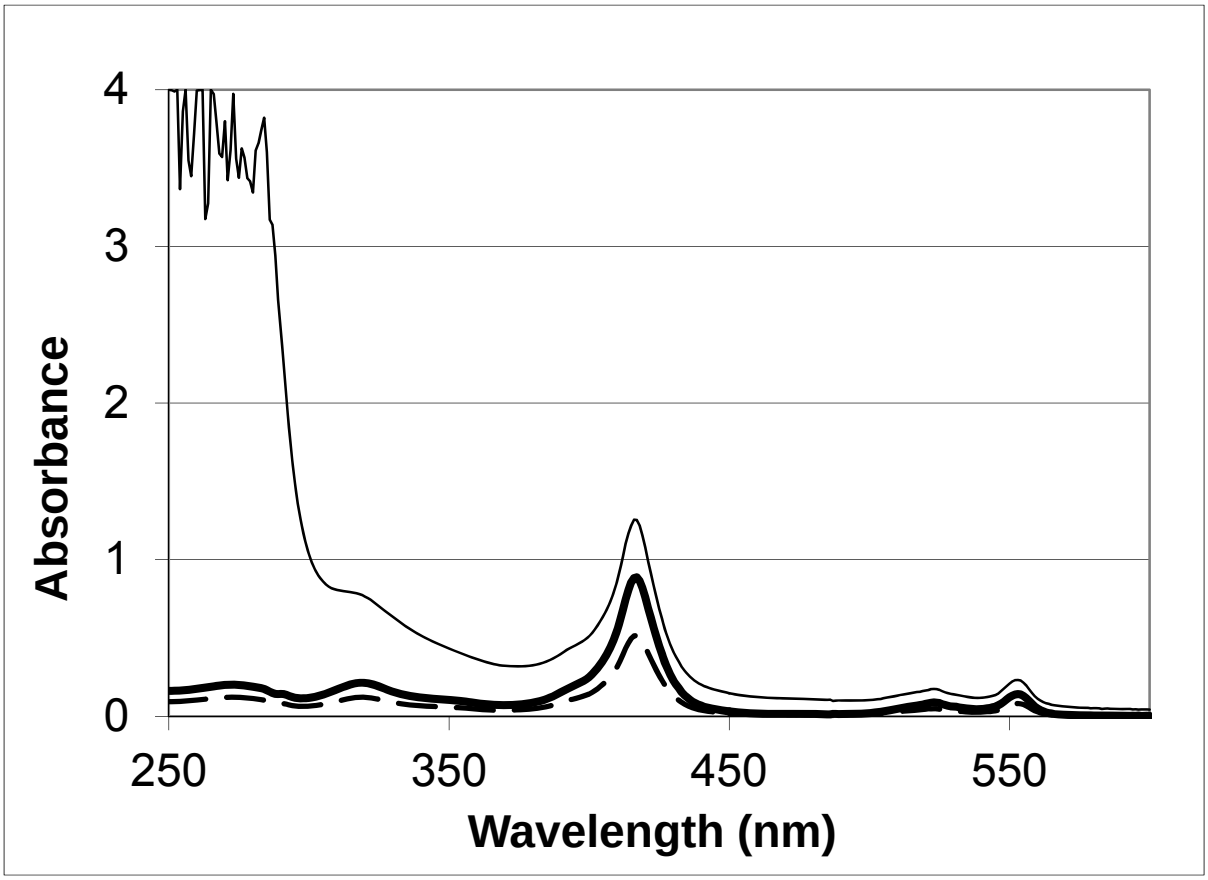
4
3
2
1
0
Absorbance
250
350
450
550
Wavelength (nm)

4.5 SPECTRAL CHARACTERISTICS OF MUTANT AND WILD-TYPE CYTOCHROME C_6

The spectrum for the wild-type *C. reinhardtii* cytochrome c_6 in the reduced state was found to include an alpha peak at 553 nm, a beta peak at 523 nm, and a Soret peak at 417 nm. In the spectrum of the oxidized protein the broadening of the alpha and beta peaks is observed compared to that of the reduced spectrum and the Soret peak is located between 411 nm and 412 nm. Due to the limitations imposed by the resolution of the instrument we can only observe the spectrum at every nm; because of the constant shift in the Soret peak between 411 nm and 412 nm it is suspected to perhaps fall between the two values. There is also peak located at 689 nm in the oxidized spectrum as seen in other c-type cytochromes as depicted in Figure 4.5.2. This 689 nm band is indicative of a histidine-methionine coordination of the heme as expected for *C. reinhardtii* cytochrome c_6. An example of the reduced and oxidized spectra may be seen in Figure 4.5.1. The spectra for the mutants are slightly different from that of the wild-type. The K29I mutant reduced spectrum includes an alpha peak between 552 nm and 553 nm, a beta peak at 523 nm, and a Soret peak at 417 nm. In the spectrum of the oxidized protein the Soret peak is located between 411 nm and 412 nm. The K57I mutant reduced spectrum includes an alpha peak at 552 nm, a beta peak at 523 nm, and a Soret peak between 416 nm and 417 nm. In the spectrum of the oxidized protein the Soret peak is located between 411 nm and 412 nm.

The peaks of the spectra tended to shift towards lower wavelengths at higher pH. For the wild-type protein there were shifts seen in the beta peak and both the oxidized and reduced Soret peaks. Both mutants showed shifts in peaks primarily at pH 9.0 and above. The K29I mutant showed shifts in all peaks with the most substantial changed in both the oxidized and reduced Soret peaks. The K57I mutant has shifts in the beta peak and the oxidized Soret peak. The peaks are shown in Tables 4.5.1 through 4.5.3.

Figure 4.5.1: The absorbance spectra of 11 μM wild-type *C. reinhardtii* cytochrome c_6 in 10 mM Tris buffer at pH 7 showing the reduced spectrum (black) with the alpha peak at 553 nm, the beta peak at 523 nm, and the Soret peak at 417 nm along with the oxidized spectrum (grey) showing the Soret peak at 412 nm along with the broadened alpha and beta peaks.

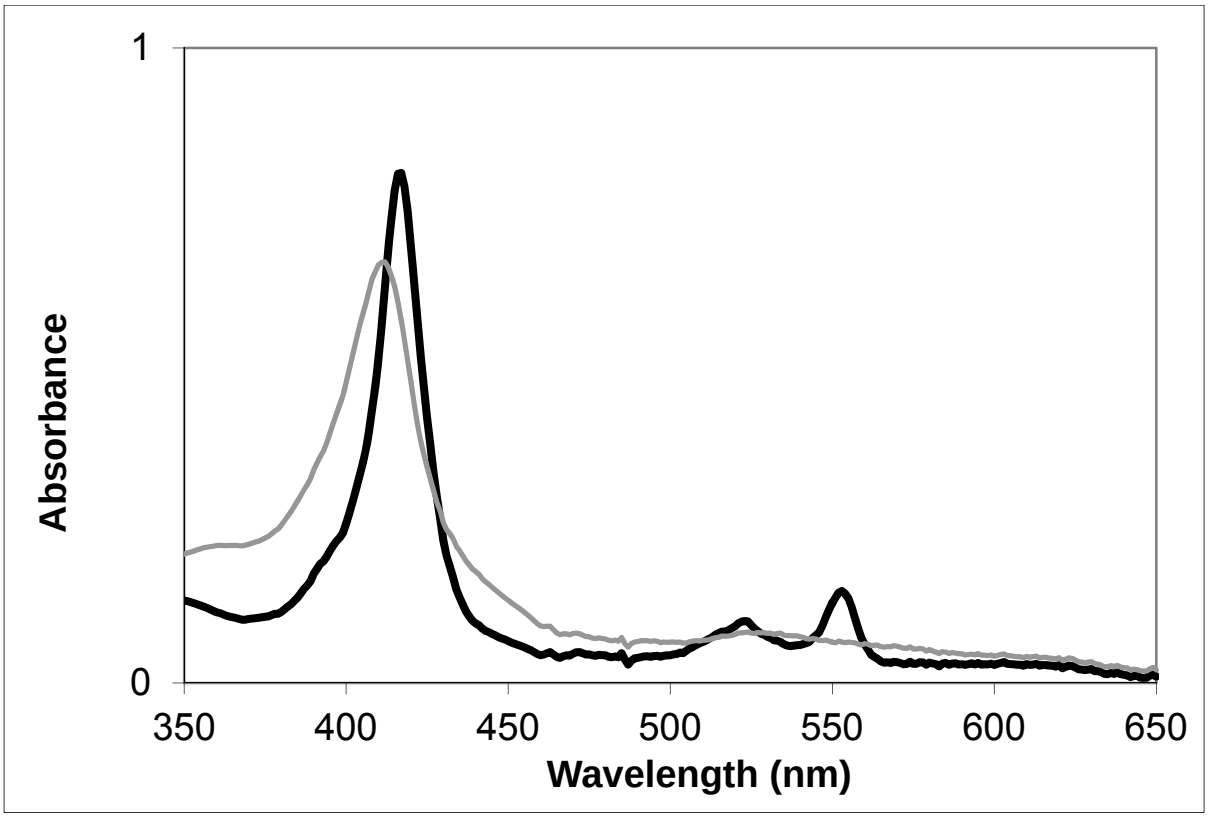
1
0
Absorbance
350
400
450
500
550
600
650
Wavelength (nm)

Figure 4.5.2: The absorbance spectrum of 0.7 mM oxidized wild-type *C. reinhardtii* cytochrome c_6 in 10 mM Tris buffer at pH 7 showing the peak at 689 nm indicative of a His-Met ligation of the heme.

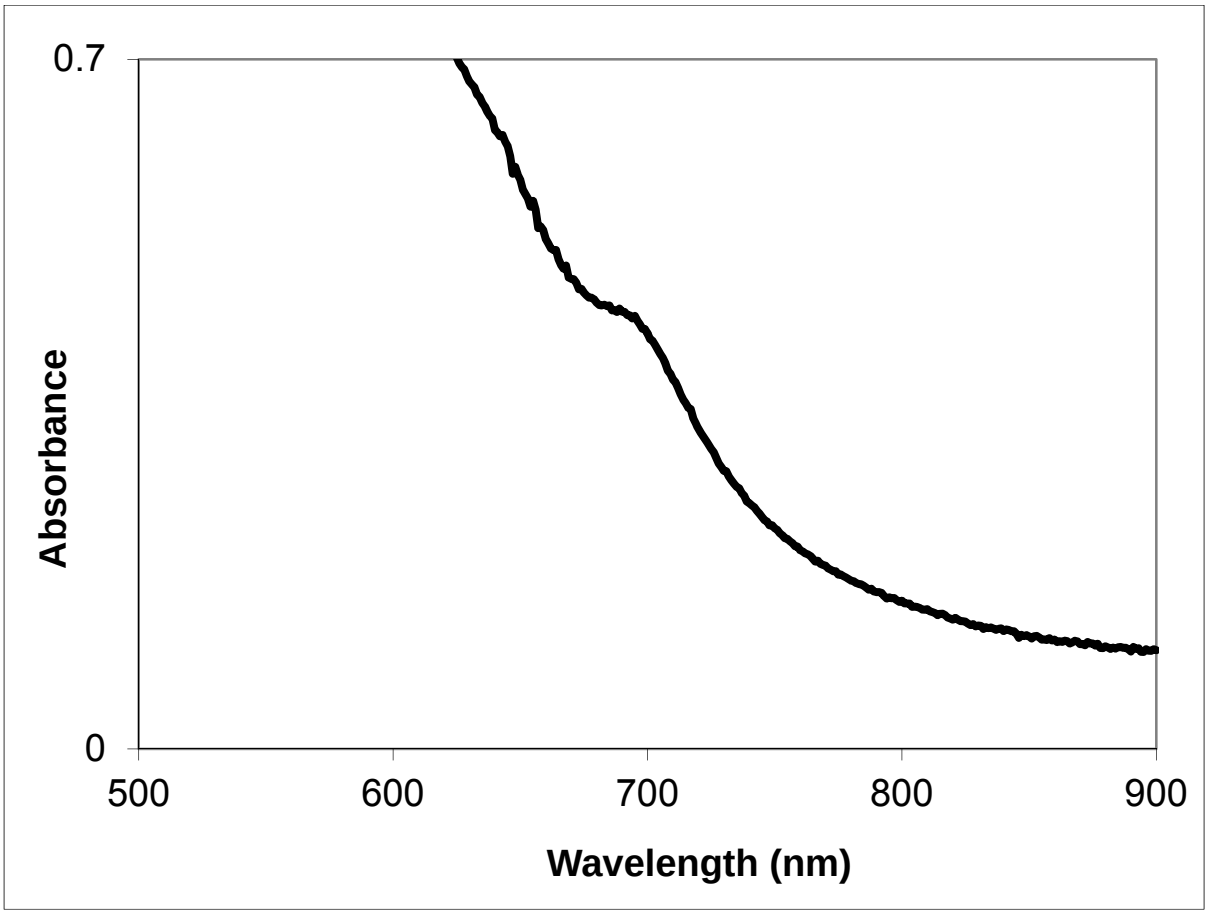
0.7
0
Absorbance
500
600
700
800
900
Wavelength (nm)

Table 4.5.1: Peaks of the cytochrome c_6 wild-type as observed during redox titrations with shifted peaks in bold. Multiple entries are due to different value being observed during different titrations.

	alpha peak (nm)	beta peak (nm)	reduced Soret peak (nm)	oxidized Soret peak (nm)
pH 6.0	553	523	417	411, 412
pH 6.0 + Dithionite	553	523	417	
pH 6.5	553	523	417	411, 412
pH 6.5 + Dithionite	553	**523, 524**	417	
pH 7.0	553	523	417	411, 412
pH 7.0 + Dithionite	553	523	417	
pH 7.5	553	523	417	**411, 412, 413**
pH 7.5 + Dithionite	553	523	417	
pH 8.0	553	523	417	412
pH 8.0 + Dithionite	553	523	417	
pH 8.5	553	523	417	412
pH 8.5 + Dithionite	553	523	417	
pH 9.0	553	**523, 524**	417	411
pH 9.0 + Dithionite	553	523	417	
pH 9.5	553	523	417	411
pH 9.5 + Dithionite	553	523	417	
pH 10.0	553	**523, 524**	417	**410, 411**
pH 10.0 + Dithionite	553	523	417	
pH 10.5	553	523	**416, 417**	**406, 407, 408, 411, 412**
pH 10.5 + Dithionite	553	523	417	
pH 10.5 (Phosphate)	553	523	417	**406, 407**
pH 11.0 (Phosphate)	553	523	**416**	**405**
pH 11.0 + Dithionite (Phosphate)	553	523	417	
pH 11.0 (CAPS)	553	523	**416**	**405**
pH 11.0 + Dithionite (CAPS)	553	523	417	

Table 4.5.2: Peaks of the cytochrome c_6 mutant K29I as observed during redox titrations with shifted peaks in bold. Multiple entries are due to different value being observed during different titrations.

	alpha peak (nm)	beta peak (nm)	reduced Soret peak (nm)	oxidized Soret peak (nm)
pH 6.0	553	**523, 524**	417	411
pH 6.0 + Dithionite	553	523	417	
pH 6.5	553	523	417	411, 412
pH 6.5 + Dithionite	553	**524**	417	
pH 7.0	552, 553	523	417	412
pH 7.0 + Dithionite	552, 553	523	417	
pH 7.5	553	523	417	411
pH 7.5 + Dithionite	553	523	417	
pH 8.0	552, 553	523	417	411, 412
pH 8.0 + Dithionite	552, 553	523	417	
pH 8.5	553	523	417	411
pH 8.5 + Dithionite	553	523	417	
pH 9.0	552, 553	523	417	**410, 411**
pH 9.0 + Dithionite	552,553	**523, 524**	417	
pH 9.5	552	523	**416**	**408, 409**
pH 9.5 + Dithionite	**554**	**524**	**419, 421, 422**	
pH 10.0	552, 553	523	**416**	**410**
pH 10.0 + Dithionite	553	523	**417, 418**	

Table 4.5.3: Peaks of the cytochrome c_6 mutant K57I as observed during redox titrations with shifted peaks in bold. Multiple entries are due to different value being observed during different titrations.

	alpha peak (nm)	beta peak (nm)	reduced Soret band (nm)	oxidized Soret peak (nm)
pH 6.0	552	523	416, 417	411, 412
pH 6.0 + Dithionite	**552, 553**	523	417	
pH 6.5	552	523	417	412
pH 6.5 + Dithionite	552	523	416, 417	
pH 7.0	552	523	416, 417	411, 412
pH 7.0 + Dithionite	552	523	416, 417	
pH 7.5	552	523	416	412
pH 7.5 + Dithionite	552	523	417	
pH 8.0	552	523	416	411, 412
pH 8.0 + Dithionite	552	523	417	
pH 8.5	552	523	416	411
pH 8.5 + Dithionite	552	523	416, 417	
pH 9.0	552	**522**	416, 417	**410, 411**
pH 9.0 + Dithionite	552	**522**	416, 417	
pH 9.5	552	**522, 523**	416	**409**
pH 9.5 + Dithionite	552	**522, 523**	417	
pH 10.0	552	**522, 523**	416	**410, 411**
pH 10.0 + Dithionite	552	523	417	

4.6 REDOX POTENTIALS OF MUTANT AND WILD-TYPE CYTOCHROME C_6 AND THEIR DEPENDENCE UPON PH

The midpoint potentials were determined for the wild-type and K29I and K57I mutants of cytochrome c_6 by conducting titrations with a ferricyanide/ ferrocyanide couple of known potential using the same methods and parameters that were used for wild-type cytochrome f. A straight line plot was generated by plotting the half cell potential (Eh) against the log of the fraction oxidized divided by the fraction reduced. The point at which the line crosses the X-axis gives the value for the midpoint potential of the protein. A summary of the average values at pH 7 and the number of calculated electrons transferred are displayed in Table 4.6.1. The wild-type cytochrome c_6 was found to have a midpoint potential at pH 7 of 367 ± 10 mV.

The K29I mutant was found to have an $E_{m,7}$ of 322 ± 5 mV at pH 7. This value is 45 mV lower than that of the wild-type and being more than a 5 mV difference is considered significantly different. The K57I $E_{m,7}$ value was also significantly different from that of the wild-type and was found to be 335 ± 2 mV at pH 7, a decrease of about 30 mV. The plot of the half cell potential against the log of the fraction oxidized divided by the fraction reduced for the K29I mutant alongside that of the K57I mutant and the wild-type protein is shown in Figure 4.6.1. When examining the midpoint potential for both the wild-type cytochrome c_6 and the K29I and K57I mutants across the range of pH it was noticed that neither the wild-type nor either mutant has a decrease in the mid-point potential at higher pH's. The midpoint potential of the wild-type protein was able to be measured reproducible up to pH 10 without a drop in the midpoint potential at any of the measured pH's using either a phosphate buffer or a CAPS buffer. This indicates that the either the protein is pH independent or that the pKa lies above 10.0. Both of the mutants were also able to be examined up to the point of pH 10.0, and like the wild-type protein both of the mutants were independent of pH up to pH 10.0. Either the mutants are truly pH dependent or the pKa's lie somewhere above 10.0. A plot depicting the data for the wild-type along with both mutants is present in Figure 4.6.2 in a plot of the midpoint potential vs. pH. The averages used along with the standard deviations and sample size values for the data for the wild-type and the K29I and K57I mutants presented in the Figure 4.6.2 are found in Table 4.6.2.

Table 4.6.1: Cytochrome c_6 wild-type and mutants values of the averaged midpoint potential at pH 7 with standard deviation and calculated value for the number of electrons transferred (n) for the potentials measured at pH 7 with standard deviation.

Protein	Em,7 (mV)	n
wild-type	367 ± 10	0.97 ± 0.14
K29I	322 ± 5	0.89 ± 0.10
K57I	335 ± 2	0.93 ± 0.07

Figure 4.6.1: Plot of log [(red)/(ox)] vs. Eh showing the midpoint potential where the line intersects log [(red)/(ox)] = 0.0 for Wild-type cytochrome c_6 (solid line, black triangles), K57I (dashed gray line, gray squares), and K29I (dotted line, black circles) at pH 7.

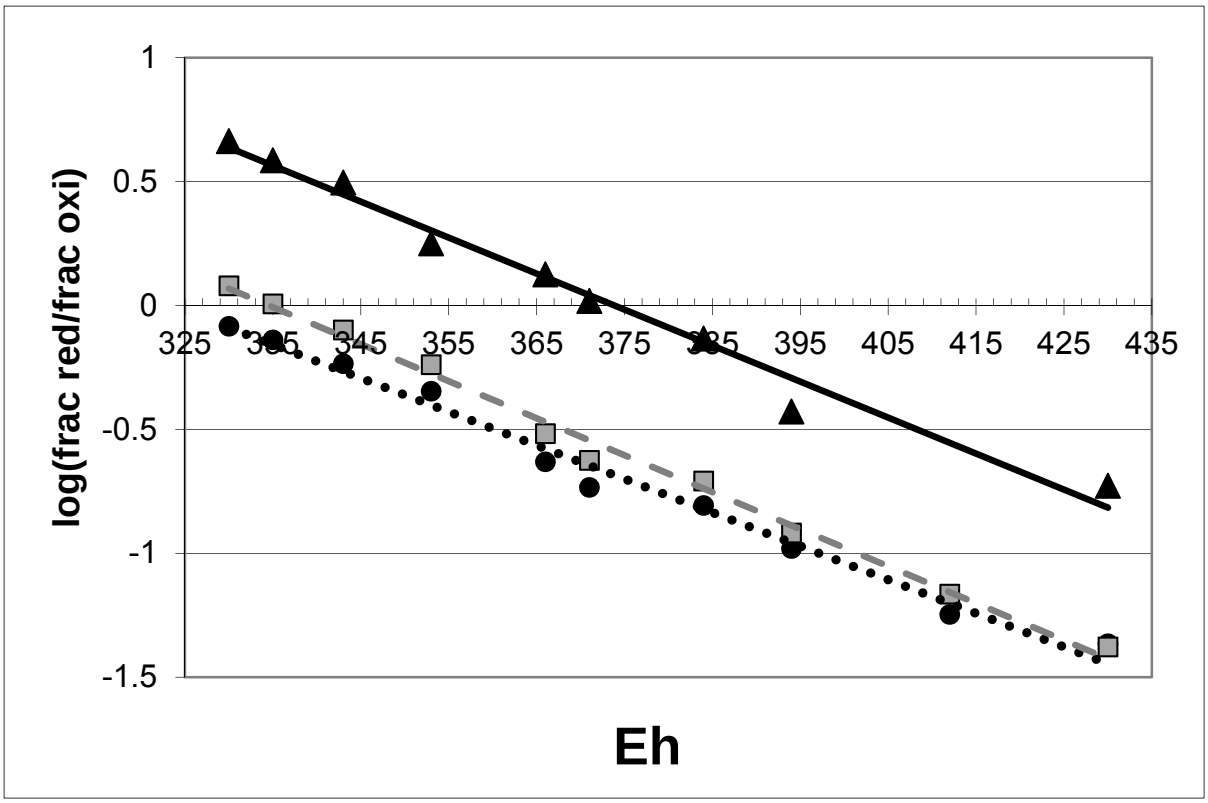
1
0.5
0
-0.5
-1
-1.5
325
345
355
365
375
395
405
415
425
435
log(frac red/frac oxi)
Eh

Figure 4.6.2: Graph of pH vs Eo showing the lack of dependence of the redox potentials on pH for the wild-type cytochrome c_6 (black squares), the K57I mutant (light gray triangles), and the K29I mutant (dark gray triangles).

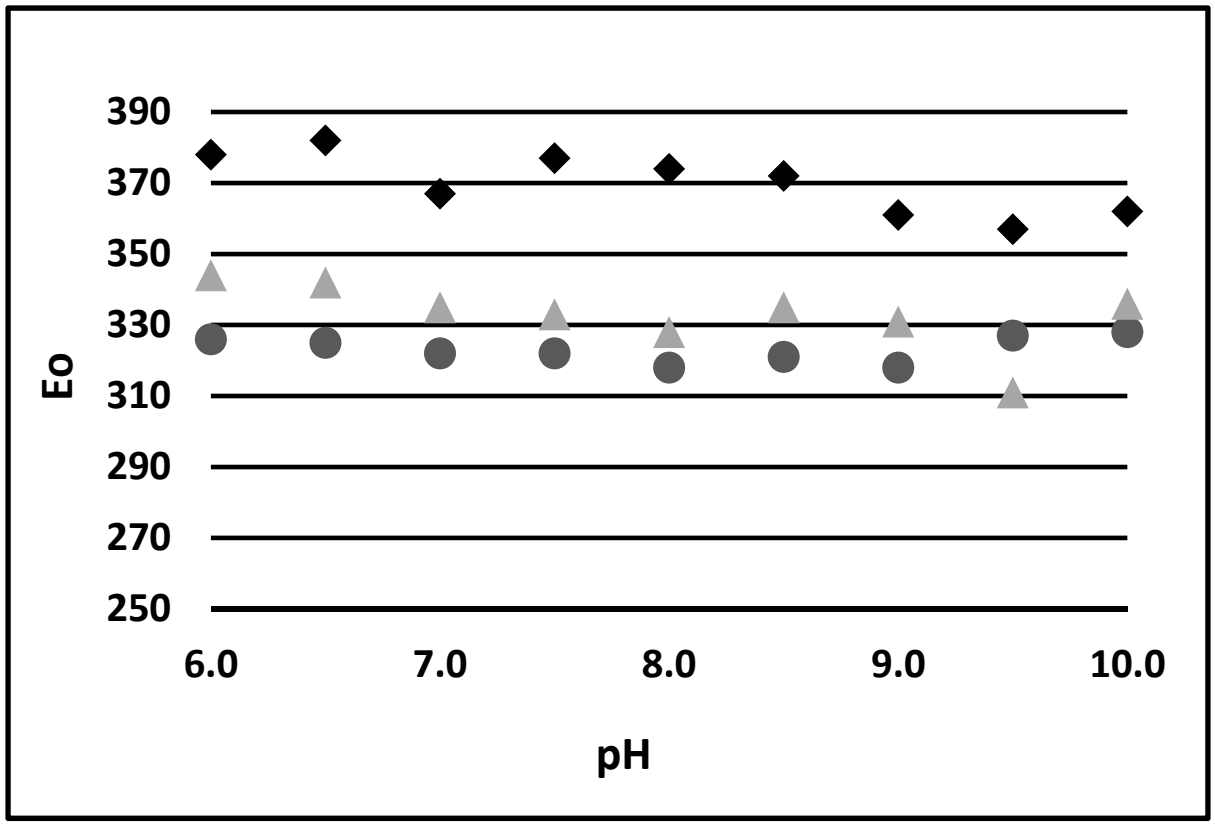
390
370
350
330
310
290
270
250
Eo
6.0
7.0
8.0
9.0
10.0
pH

Table 4.6.2: Table showing the averages and standard deviations for the redox titrations at pH's 6.0 – 10.5 of the wild-type and mutants of cytochrome c_6 corresponding to the data presented in Figure 4.6.2.

	Wild-type			K29I			K57I		
pH	AVG	SD	n	AVG	SD	n	AVG	SD	n
6.0	378	3	3	326	4	3	344	3	3
6.5	382	7	3	325	3	3	342	2	3
7.0	367	10	3	322	5	3	335	2	3
7.5	377	4	3	322	1	3	333	1	3
8.0	374	6	3	318	4	3	328	5	3
8.5	372	4	3	321	1	3	335	5	3
9.0	361	10	3	318	2	3	331	3	3
9.5	357	10	3	327	7	3	311	4	3
10.0	362	9	3	328	2	3	336	1	3
10.5	292	60	4	-----	--		----	--	

4.7 DIFFERENTIAL SCANNING CALORIMETRY STUDIES ON CYTOCHROME c_6

In an attempt to define the thermodynamic parameters of unfolding and the stability of cytochrome c_6 from *C. reinhardtii*, differential scanning calorimetry was utilized. In a system where the protein folds reversibly this technique is able to provide a number of thermodynamic parameters. Values such as ΔS and ΔH and melting temperature (T_m) can be determined and compared to values previously obtained for a wide range of other proteins. However, the folding of cytochrome c_6 was found to be irreversible based on the second up-scan of the DSC run showing no unfolding profile. The only value that was able to be obtained reproducibly was the melting temperature of the protein. The melting temperature is determined by identifying the temperature that corresponds to the highest point of the peak on the graph. The average T_m for the oxidized wild-type protein was found to be 78 ± 0.1°C and 110 ± 0.3°C for the reduced protein. The oxidized and reduced profiles are represented by the peak in the graph of heat capacity vs. temperature in Figures 4.7.1 and 4.7.2 respectively.

The oxidized DSC profiles for the cytochrome c_6 mutants reveal the average T_m's to be lower than that of the wild-type protein. The T_m values were determined to be 70 ± 0.7°C for the K29I mutant and 71 ± 0.2°C for the K57I mutant and are represented on the graphs shown in Figures 4.7.3 and 4.7.4 respectively. Figure 4.7.4, representing the DSC profile for the K57I mutant, shows aggregation of the sample upon unfolding indicated by the plummeting baseline. The significant reduction of the melting temperature of the mutants, 8°C for the K29I mutant and 7°C for the K57I mutant, relative to that of the wild-type protein, indicates a reduction in the stability of the mutant proteins when compared to the wild-type.

Figure 4.7.1: Oxidized DSC run for wild-type cytochrome c_6 run at 2ºC/min on a sample of 1 mg/mL showing a peak at 78°C.

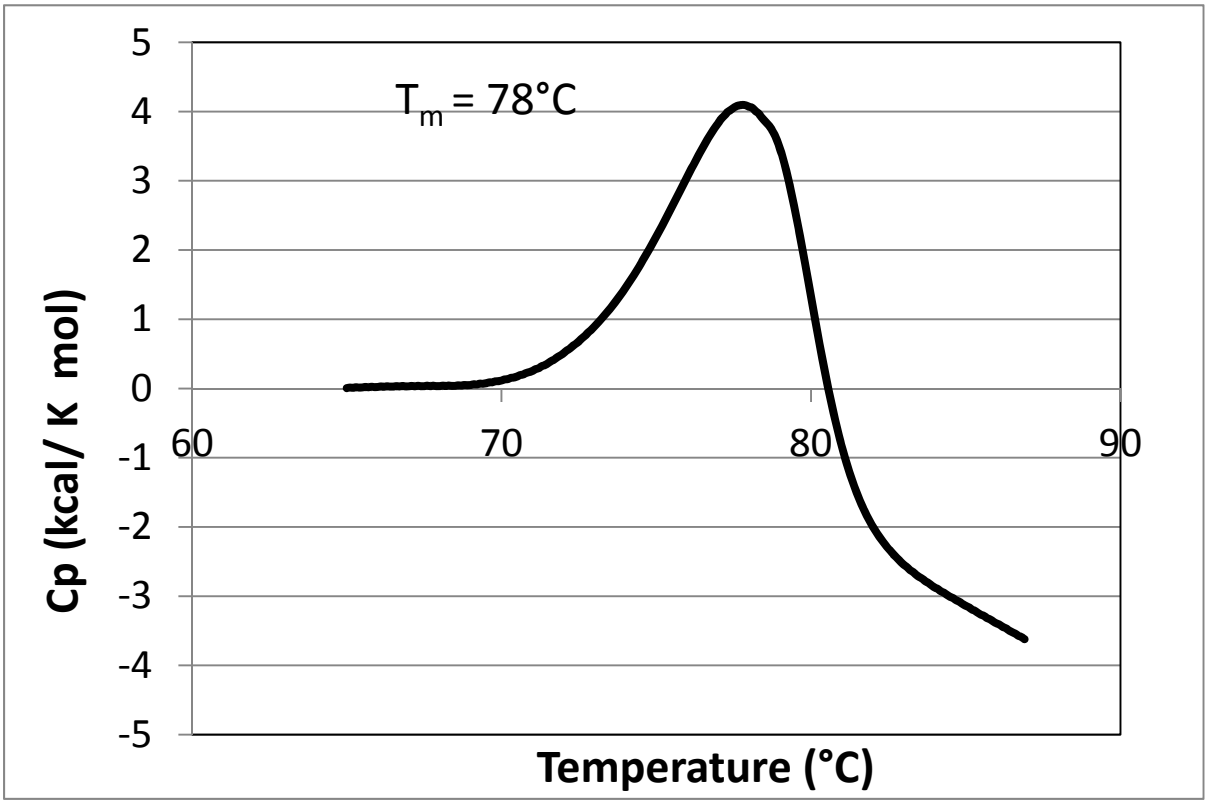
5
4
3
2
1
0
-1
-2
-3
-4
-5
60
70
80
90
T_m = 78°C
Cp (kcal/ K mol)
Temperature (°C)

Figure 4.7.2: Reduced DSC run for wild-type cytochrome c_6 run at 2ºC/min on a sample of 1 mg/mL showing a peak at 70°C. Baseline corrected using Microsoft Excel.

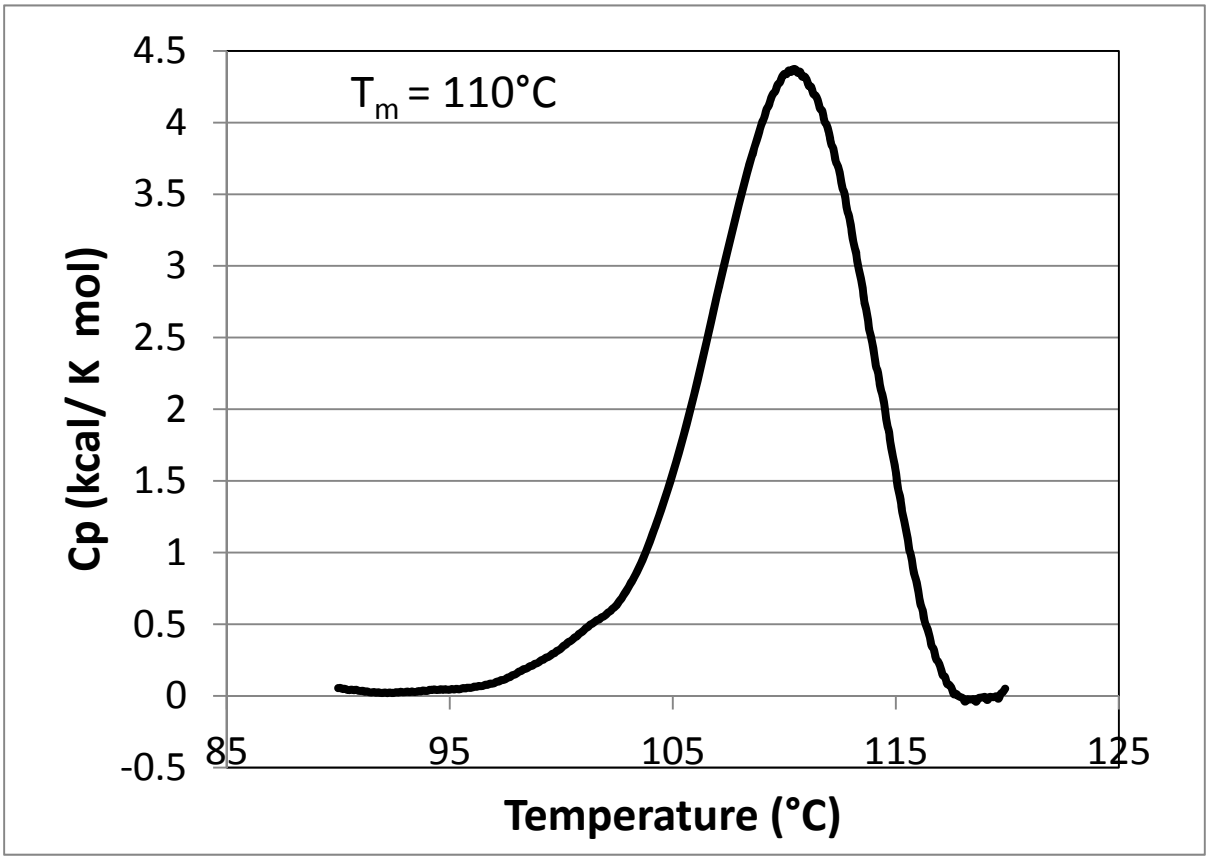
T_m = 110°C
Cp (kcal/ K mol)
4.5
4
3.5
3
2.5
2
1.5
1
0.5
0
-0.5
85
95
105
115
125
Temperature (°C)

Figure 4.7.3: Oxidized DSC run for cytochrome c_6 mutant K29I run at 2ºC/min on a sample of 1 mg/mL showing a peak at 70°C. Baseline corrected using Microsoft Excel.

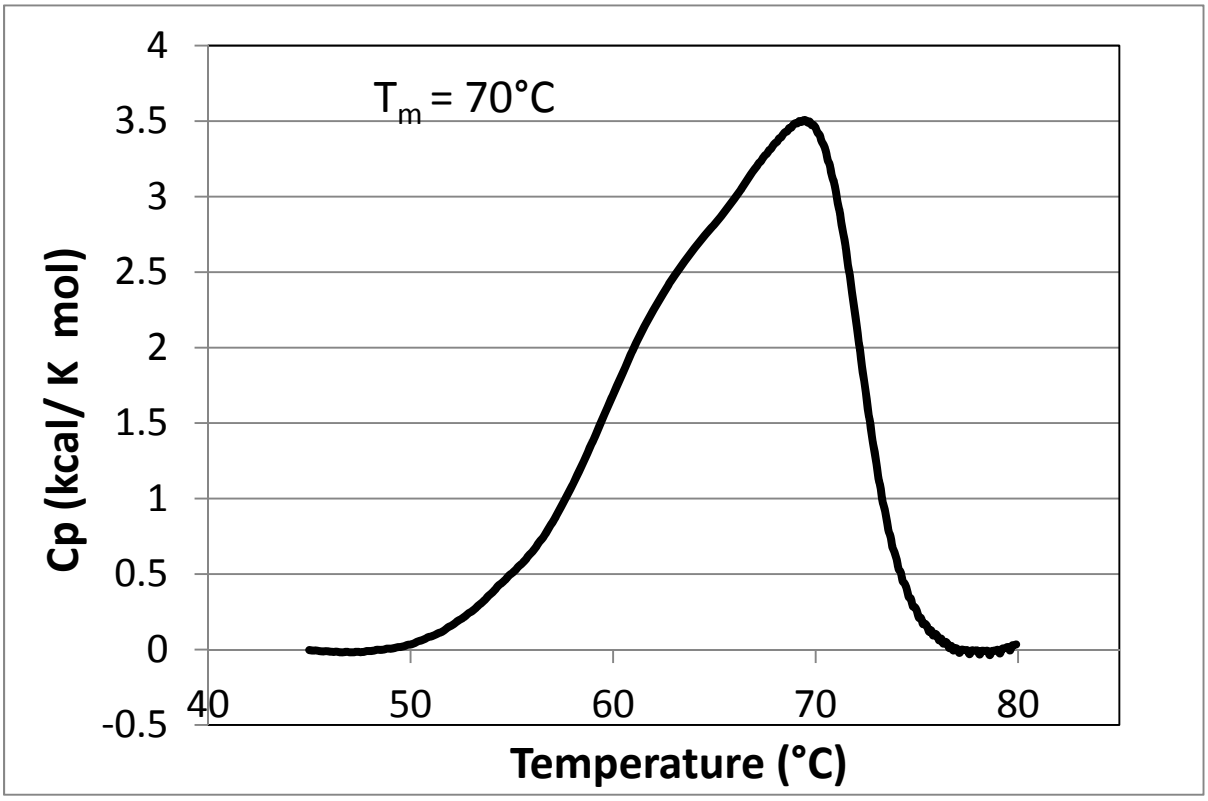
T_m = 70°C
Cp (kcal/ K mol)
Temperature (°C)
4
3.5
3
2.5
2
1.5
1
0.5
0
-0.5
40
50
60
70
80

Figure 4.7.4: Oxidized DSC run for cytochrome c_6 mutant K57I run at 2ºC/min on a sample of 1 mg/mL showing a peak at 70°C. Baseline corrected using Microsoft Excel.

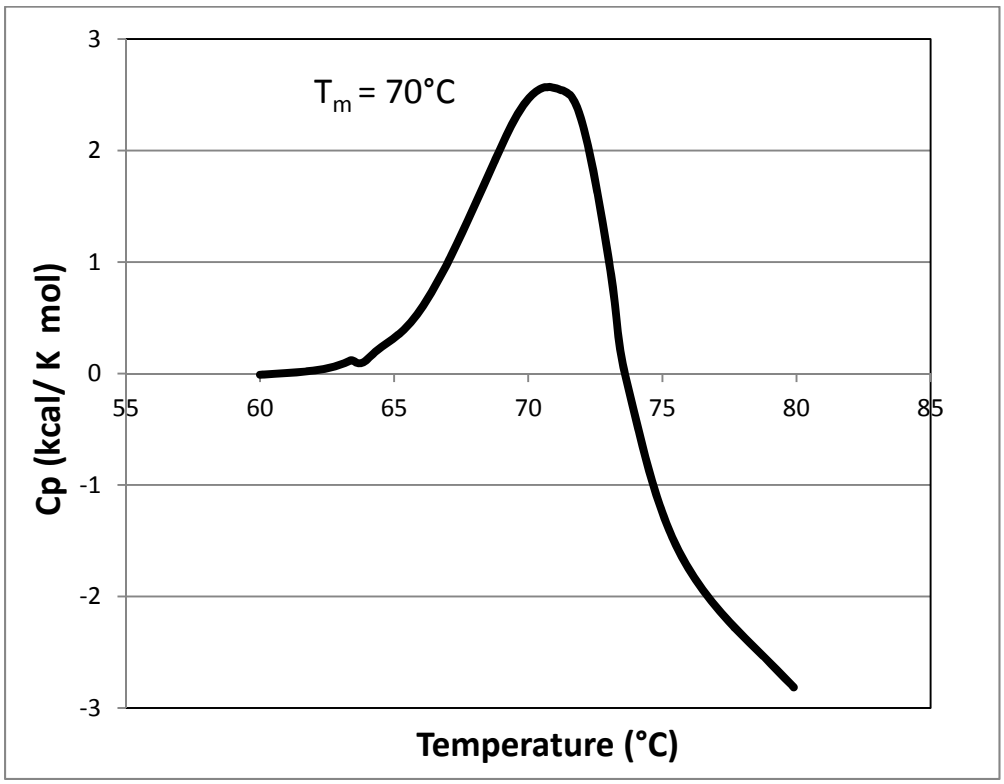
T_m = 70°C
3
2
1
0
-1
-2
-3
55
60
65
70
75
80
85
Cp (kcal/ K mol)
Temperature (°C)

4.8 CD SPECTRAL ANALYSIS OF CYTOCHROME C_6

In a number of recorded CD spectra previously obtained for different cytochromes a negative peak or negative Cotton effect has been observed in the oxidized CD spectrum and is located around 419 nm. It has been suggested that a conserved aromatic amino acid residue in the vicinity of the heme and its orientation with respect to the heme of the cytochromes may be the reason for this negative Cotton effect commonly seen in the oxidized CD spectra (Vinogradov and Zand 1968, Bullock and Mayer 1978, Rafferty et al. 1990, Scharlau 1998).

Tryptophan 88 in *C. reinhardtii* cytochrome c_6 is found in an equivalent position to the conserved amino acid that is supposedly responsible for the observed negative Cotton effect in the oxidized CD spectrum. Both the reduced and oxidized CD spectra for the wild-type cytochrome c_6 of *C. reinhardtii* are shown in Figure 4.8.1. There is an observed positive peak in the reduced spectrum located at 414 nm. The oxidized spectrum shows a positive peak located at 405 nm. Unlike many of the spectra seen previously for other cytochromes, cytochrome c_6 of *C. reinhardtii* has no negative peak in the oxidized CD spectrum.

Figure 4.8.1: CD spectra of 5 μM wild-type cytochrome c_6 in 10 mM Phosphate buffer at pH 7 showing the oxidized spectra in black with a positive peak at 405 nm and the reduced spectra in gray with a peak at 414 nm.

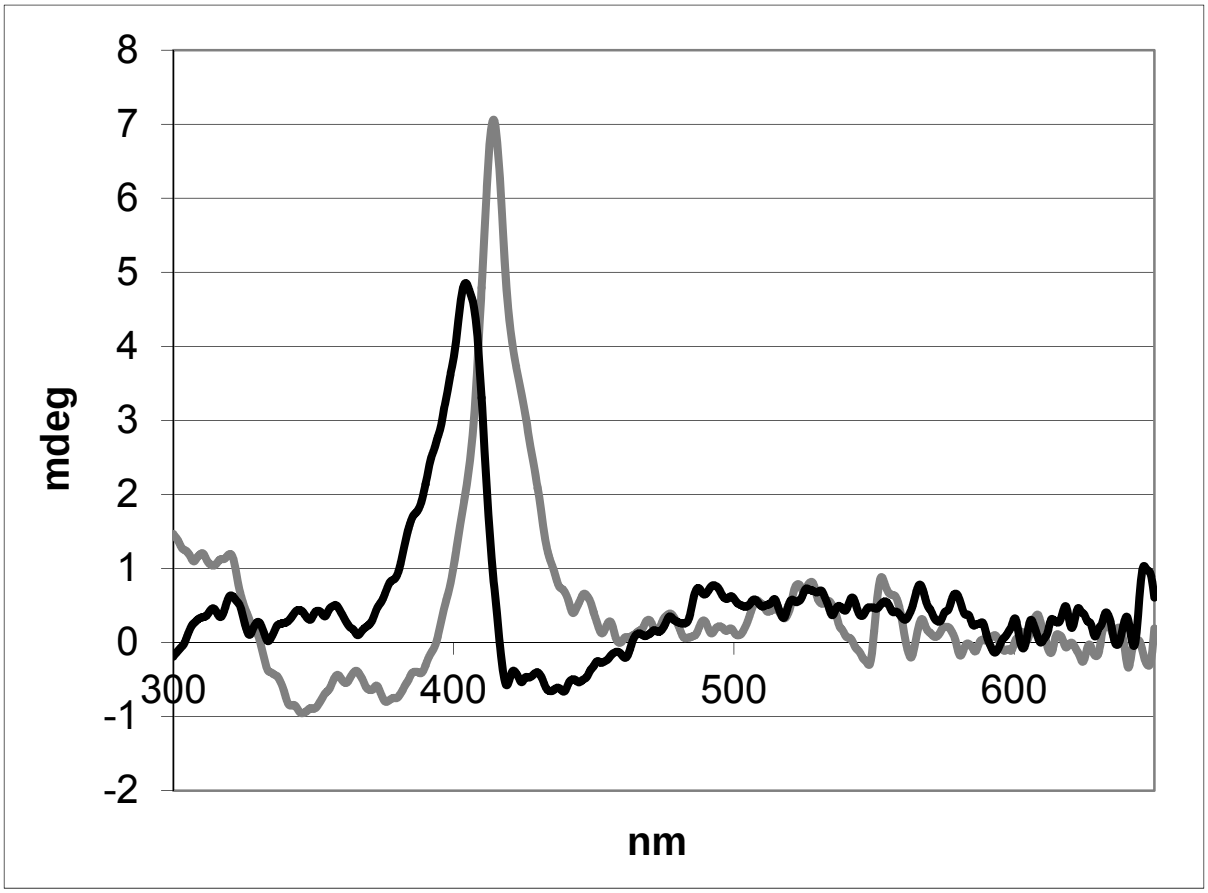
8
7
6
5
4
3
2
1
0
-1
-2
mdeg
300
400
500
600
nm

CHAPTER 5 – DISCUSSION

Cytochrome f plays an important role in photosynthesis acting as the electron donor to a mobile electron carrier either plastocyanin or cytochrome c_6 (Kerfeld and Krogmann 1998, Gorman and Levine 1965). Even though cytochrome f is considered a c-type cytochrome, it differs from other proteins of the same category because of its unique structure and axial ligation of its heme. Cytochrome f is a two domain protein that has a secondary structure primarily composed of beta sheets whereas most cytochromes in its class are alpha helical proteins of one domain. The ligation of the heme is also different from other c-type cytochromes having the alpha amino group of the N-terminal residue function as one of the axial ligands to the heme as opposed to a methionine residue as typically seen (Chi et al. 2000). The protein has been well characterized; however there have not been a lot of studies examining the control of the redox potential. In the studies presented in this volume of work, multiple mutations have been made to the residues surrounding the heme of cytochrome f from *Chlamydomonas reinhardtti*. This allows us to observe the differences between the properties of the wild-type and mutant proteins. By doing so, we can identify the effect of the mutated residues on the heme environment in terms of the redox potential of the protein, its dependence on pH, and the thermal stability of the protein.

Cytochrome c_6, an interaction partner of cytochrome f in photosynthesis, shuttles electron between cytochrome f and photosystem I (Kerfeld and Krogmann 1998). Cytochrome c_6, which is not found in higher plants, is a class I, c-type cytochrome. Cytochrome c_6, unlike cytochrome f, shows more characteristic features of its class of proteins. It has an alpha helical secondary structure and histidine and methionine serve as the axial ligands to the heme as seen in cytochrome c of the mitochondria (Kerfeld et al. 1995). In this body of work we examined the cytochrome c_6 from *Chlamydomonas reinhardtii*. Even though the protein is similar in its classification to cytochrome c, this particular cytochrome c_6 shows a number of characteristics that differ from the classic model of cytochrome c. The protein has been examined with regard to the redox potential and its dependence on pH, its thermal stability, and its CD spectra for the Soret region.

5.1 DESIGN OF WILD-TYPE CYTOCHROME F MUTANTS

Mutations made to the PUCF2 plasmid coding for cytochrome f were made to investigate the effects of alterations made to the heme environment. The mutations were made to residues in the heme vicinity and include: Y1F, Y9F, Y160F, Y160L, R156L, and R156K. The Y1 and Y9 residues are ionizable residues found in close vicinity to the heme and are depicted in Figure 5.1 in green and blue respectively (Chi et al. 2000). The Y1F and Y9F mutants remove the ability of the residues to be ionizable by replacing the tyrosine residue with a phenylalanine residue which does not contain an ionizable hydroxyl group. The Y160 residue, depicted in cyan in Figure 5.1, is within hydrogen bonding distance of a heme propionate and contains an ionizable hydroxyl group. The Y160L mutant removes both the aromatic character of the residue and the ability to hydrogen bond to a propionate group of the heme, and the Y160F mutant retains the aromatic character of the residue but eliminates its capacity to form a hydrogen bond with a propionate of the heme. The positively charged R156 residue near the heme interacts electrostatically with the negative charge of the heme propionate and is pictured in yellow in Figure 5.1. The R156L mutation removes the positive charge of the residue so that it no longer can interact with the heme propionate, and the R156K mutant reinstates the positive charge to allow an electrostatic interaction but removes the specificity of the residue conformation.

5.2 SPECTRAL CHARACTERISTICS OF WILD-TYPE CYTOCHROME F AND MUTANTS

The peak positions of the spectrum of the wild-type and the mutants were monitored throughout the redox measurements. Shifts were seen in the peaks of all the examined proteins and are represented in Tables 4.1.1, 4.1.2, and 4.1.3. on pages 59, 61, and 63. The oxidized Soret peak tends to shift at high pH in both the wild-type and Y160F mutant. Shifts are also seen is the oxidized Soret peak in the Y1F and Y9F mutants as low as pH 7.0 and pH 8.5 respectively. The Y160L mutant shown in the next table 4.1.2 shows shifts in the oxidized Soret peak at lower pH, shifts in the reduced Soret band at higher pH, shifts in the alpha band at extremely high pH, and shifts in the beta band throughout the entire range of pH's examined. All four peaks of the R156L mutant shown in table 4.2.3 also shift throughout the entire range of pH examined. The R156K mutant was not looked at over a range of pH, but its spectra are

similar in nature to that of the other R156 mutant R156L. Shifts seen in the experiments are indicative of a change in the environment surrounding the heme. The only change examined in peak position with the wild-type protein is a high pH. Such is the case for the Y160F mutant showing that the alteration of the heme environment in the case of the Y160F mutant may not be as intensive as that in the Y160L mutant which shows a change across the entire range of pH. The Y1F and Y9F also show more of an alteration of peak position at a wider range of pH. Both of the R156 mutants show changes across the entire range of pH and a repositioning of the alpha peak from 554 nm to 553 nm. This shows that there is an alteration of the heme environment in each of mutants (Ponamarev et al. 2000).

Figure 5.2.1: *Chlamydomonas reinhardtii* cytochrome f: file 1CFM downloaded from the Protein Data Bank edited in DS ViewerPro 5.0 by Accelrys Inc. The heme portion and residues Y160 (cyan), Y1 (green), Y9 (blue), and R156 (yellow) shown in ball and stick format.

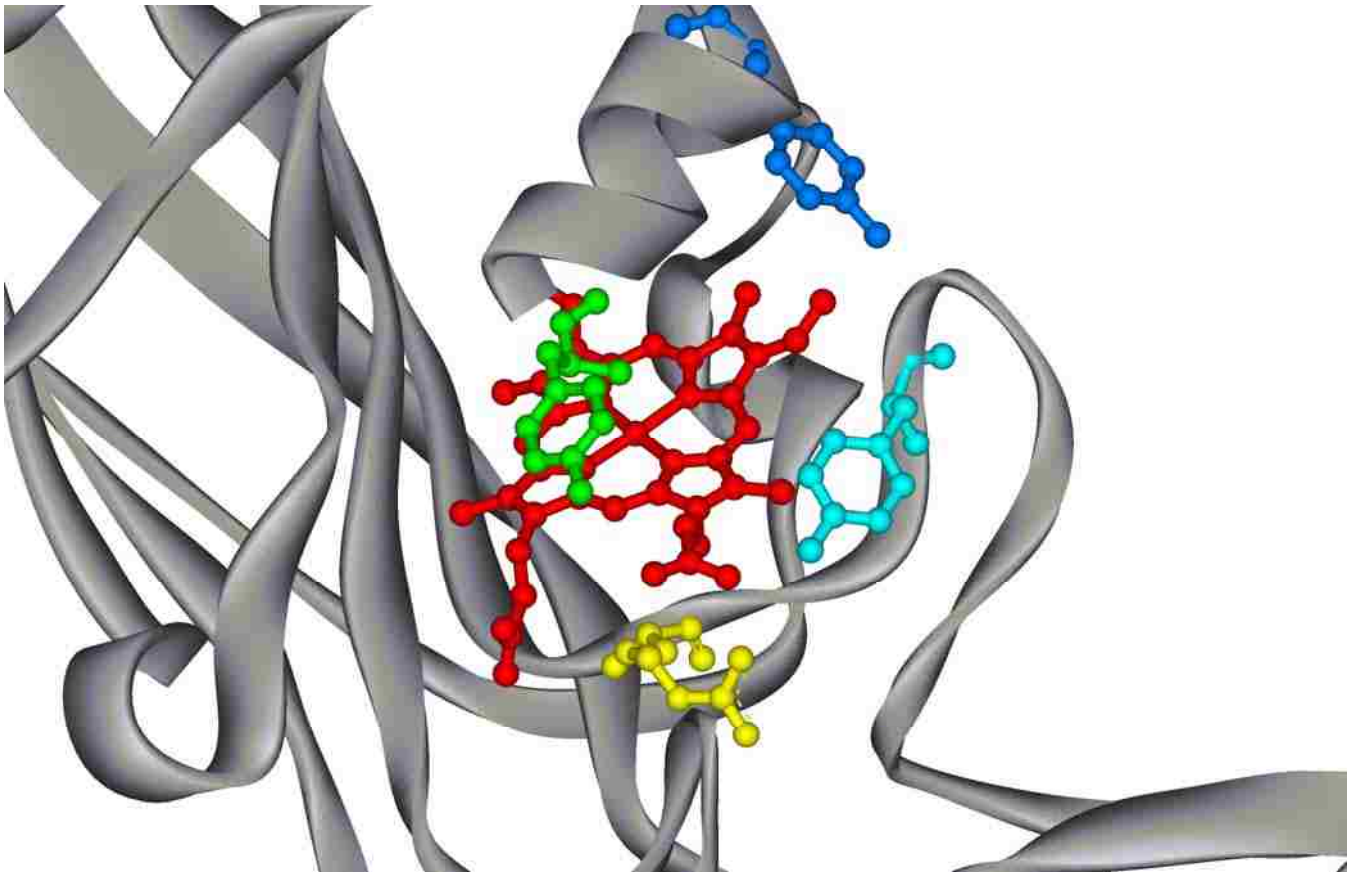

5.3 THE REDOX POTENTIALS OF THE TYROSINE MUTANTS AND WILD-TYPE CYTOCHROME F

The redox potential of a heme protein is a value that is dependent on the heme environment. The redox potential of the iron heme alone is measured to be -200 mV (Shifman et al. 2000). However, the potential of the heme that is bound to protein can range 800 mV spanning from -400 mV up to about 400 mV. It is the specific conformation of the residues around the heme that control the redox potential. The character of each residue in the heme environment and the way it interacts with the heme or nearby residues can affect the redox potential by either stabilizing or destabilizing the oxidized form or the reduced form. Lower potentials can be the result of either a decrease in the stability of the oxidized state or the stabilization of the reduced state. The value of the redox potential is represented by the relative stability between the reduced and oxidized states of the protein (Pettigrew and Moore 1990).

The mutations to both the Y1 and Y9 residues to phenylalanine did not result in significant changes in the measured redox potentials and therefore are not essential in creating the specific environment around the heme that give the protein is specific redox potential. The Y160L mutant, which shows a redox potential of 357 ± 3 mV, does show a significant variation from the wild-type value of 380 ± 4 mV. An earlier study noted the drop in the potential of the Y160L mutant and the lack of a drop in potential of the Y160F mutant. These indicate that the interaction of the propionate group with the protein residue at position 160 has an effect on the redox potential of the protein. The mutation of residue 160 from tyrosine to leucine mutant removes both the hydrogen bonding ability and aromatic characteristic of the Y160 residue. It is unclear as to which of these characteristics of the Y160 residue is important to maintain the stability of the heme environment. However, the replacement of the tyrosine at position 160 with a phenylalanine, which leaves the aromaticity and removes only the hydrogen bonding capabilities of the residue, resulted in an experimentally obtained value of 377 ± 9 for the redox potential. This value is not significantly different from the value found for the wild-type protein. The absence of a significant difference between the wild-type potential and that of Y160F indicates that the aromaticity of the residue and not its hydrogen bonding capability is important for the stabilization of the heme environment and the redox potential of the protein.

5.4 THE DEPENDENCE OF THE REDOX POTENTIALS OF THE TYROSINE MUTANTS AND WILD-TYPE CYTOCHROME F

The pKa of a residue in a protein may change due to other residues in the area being protonated or deprotonated, small conformational shifts in the protein, or conformations of flexible hydroxyl groups. In cytochrome c the alkaline transition is accompanied by ligand replacement where the methionine ligand to the heme is replaced by a lysine in the vicinity of the heme (Smith and Millett 1980, Gadsby 1987, Ying et al. 2009). Cytochrome f however doesn't have an alkaline transition marked by ligand replacement seeing as the sixth ligand to the heme is not a methionine but the α-amino group of the n-terminal residue (Chi et al. 2000) although there is an alkaline transition defined by pH dependence of redox potential. Previous studies have examined the dependence of redox potential on pH of wild-type cytochrome f from turnip (Metzger et al. 1997, Martinez et al. 1996). Both of these studies used potentiometric titration to determine the redox potential of cytochrome f at various pH's. The studies conducted in 1996 and 1997 showed that the cytochrome f from turnip is pH dependent and has a pKa value around 8.5. In their discussion of their results they predicted that residues Y1, Y160, and R156 would not contribute to the pKa value of around 8.5. We investigated the redox potential and its pH dependence in our mutants in an attempt to elucidate the reason for the presence of an alkaline transition in the unique cytochrome f.

In computational studies conducted in 2004, M. Gunner attempted to incorporate factors such as flexibility into the computations of protein residue pKa's whereas all prior studies have treated proteins as rigid bodies with the particular conformations based on the crystal structure (Hauser et al. 2004). Her work has focused on accounting for the variable pKa's of particular residues based on the distinct environment in which they are found. Our study is based in part on the predictions made by M. Gunner's calculations which suggest that the residues Y1 and Y9 may play a role in the pH dependence and pKa of transition for cytochrome f (Hauser et al. 2004, Alexov and Gunner 1997). The Y160 and R156 residues which both interact with surface exposed heme propionates are also considered in this study. The Y160 residue interacts with a heme propionate group via a hydrogen bond involving the phenolic hydrogen of the residue (Chi et al. 2000). The interaction between the propionate group and R156 is an electrostatic

interaction between the positively charged residue and the negatively charged propionate group. These residues are of interest in this study to due to their proximity and interaction with the heme, and though not specifically predicted to have an effect on the pH dependence of the redox potential or the pKa of transition by M. Gunner, may influence the redox potential and its pH dependence (Hauser et al. 2004, Alexov and Gunner 1997).

All of the tyrosine mutants that were made in this study resulted in proteins that had redox potentials that were dependent on pH. Because the alkaline transition is present in all the mutants and they have nearly identical pKa's when compared to that of the wild-type, it can be concluded that none of the mutated residues are responsible for the dependence on pH seen for the redox potential. The Y1 and Y9 residues that were of pointed interest in the studies conducted by Gunner were shown to have redox potentials that were dependent on pH indicating that the current computations can not accurately account for the flexibility of proteins in the calculation of pKa's of transition. Also, because we see the presence of the dependence of the redox potential on pH with each of the mutants it is implied that none of the residues mutated is responsible for the alkaline transition that is seen in cytochrome f in which case the dependence would be absent.

5.5 THE REDOX POTENTIALS OF THE ARGININE MUTANTS AND WILD-TYPE CYTOCHROME F AND THEIR DEPENDENCE ON PH

In contrast to the wild-type or the tyrosine mutants in which the reduced form is stable in air, the R156L mutation resulted in a protein which still contained heme but was highly susceptible to air oxidation. Although reducible by ascorbate or dithionite, the protein was rapidly re-oxidized once such reductants were consumed. Because of this, the previous method utilizing aerobic titrations was insufficient to measure the redox potentials of the R156L mutant. This means that in each of the spectra taken the extent of reduction of the sample was not accurately represented because of an unknown amount of protein that will be converted back to the oxidized state. In order for the redox potentials of R156L to be accurately measured anaerobic titrations were conducted to eliminate the samples exposure to oxygen. The adjustment to the previous experiments was that the titrations were performed in a sealed

cuvette after the oxygen above the sample is displaced by nitrogen gas. Even with adjustments to titration conditions, potentials were only able to be reproducibly measured between pH 5 and pH 9. The pKa of transition for the R156L mutant was therefore not able to be determined. It was noted however that as pH increases the percent reducible by ascorbate decreases as seen in Figure 4.2.8 on page 89 of this work. The midpoint potential of the mutant also differs greatly from the wild-type with a value of 291 ± 6 mV as compared to 380 ± 4 mV of the wild-type at pH 7. The loss of the electrostatic interaction between R156 and the heme propionate thus appears to result in significant alteration of the protein's redox properties. This could be due to either the loss of the electrostatic interaction or a conformational change affecting the heme environment.

The R156K mutant was designed to investigate if the loss of positive charge caused the observations seen with the R156L mutant. Anaerobic titrations were used to determine the potential for the mutant seeing as though it behaved similar to the R156L mutant with respect to them both being susceptible to air-oxidation. The absorbance was measured at 553 nm seeing as this mutant also shows a shift in the alpha peak as did the R156L mutant. A redox potential of 325 ± 5 mV was measured for the R156K mutant. This value is about a 55 mV decrease from the value of the wild-type yet recovers 35 mV of potential that was lost with the mutation of the residue to a leucine eliminating the positive charge completely. Therefore, reinstatement of the positive charge at position 156 only partially recovered the midpoint potential indicating that the specificity of the arginine residue found in the wild-type is critical at position 156 to obtain the wild-type midpoint potential of 375mV. The exact position of the positive charge due to the length and conformation of the arginine residue may be necessary in order to stabilize the reduced state of the iron of the heme. The loss of the exact positioning of this positive charge would afford the reason for the drop seen in both of the arginine mutants. The pH dependence of the redox potential was not examined because of the low yield of protein after growth and purification.

5.6 DIFFERENTIAL SCANNING CALORIMETRY STUDIES OF CYTOCHROME F

Differential scanning calorimetry was used to establish the thermodynamic parameters of unfolding and the stability for cytochrome f from *C. reinhardtii*. When a protein folds reversibly this technique is able to provide values such as ΔS, ΔH, and melting temperature (T_m). These values can be compared to values previously obtained for a wide range of other proteins. However, the folding of cytochrome f was found to be irreversible. The only value that was able to be obtained reproducibly was the melting temperature of the protein

Irreversibility can be due to a number of things including hydrolysis of peptide bonds, deamidation, cysteine oxidation, loss of cofactors, and other factors. When data is collected after conducting a run with an irreversible system the melting point value is determined by identifying the temperature where the plot of the change in heat capacity vs. temperature is the highest.

It has been reported that with the addition of a nondetergent sulfobetaine (NDSB) the process of protein folding may become reversible for some proteins (Collins et al. 2006). MOPS is a standard buffer that has been found to reduce the extent of aggregation seen with the denaturation of large proteins. The NDBS is a molecule that closely resembles the MOPS buffer and has been shown to protect large proteins against aggregation caused by thermal denaturation by heat. NDSB at 0.5-1 M final concentration was added to the sample, and the same concentration was added to the buffer used to determine the baseline. The addition of NDSB (3-(1-pyridinio)-1-propanesulfonate), seen in Figure 5.6.1, to a number of different proteins has either allowed the process of unfolding to become reversible or has delayed the aggregation to higher temperatures (Collins et al. 2006, D'Amico et al. 2009). The folding of *Chlamydomonas reinhardtii* cytochrome f, however, was found to be irreversible even with the addition of 1M NDBS. It has been seen previously that the refolding of the two domain hen egg lysozyme protein has been assisted in refolding by NDSB. However, only 2% refolding was achieved at concentrations of 1 mg /mL which is the concentrations used in the experiments for DSC (Goldberg et al. 1996).

Figure 5.6.1 Structures of the nondetergent sulfobetaine 3-(1-pyridinio)-1-propanesulfonate (NDSB) and of the buffer 3-(N-morpholino)propanesulfonic acid (Mops)(D'Amico et al. 2009).

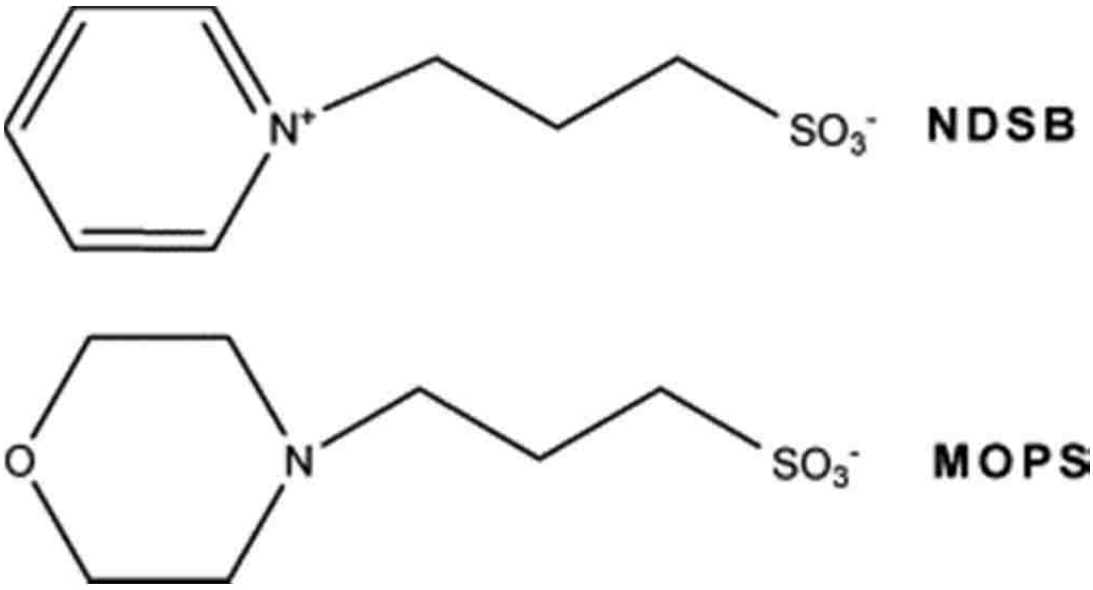
N+
SO3-
NDSB
O
N
SO3-
MOPS

The melting temperature of the wild-type protein was found to be 49°C for the oxidized protein and 73°C for the reduced protein. With all of the mutants of cytochrome f including Y1F, Y9F, Y160F, and Y160L two peaks have been noted on the DSC unfolding profile for the oxidized protein. The first peak is similar to that of the wild-type peak around 49°C. The second peak, however, is not seen in the wild-type profiles. This second peak cannot be accounted for by a reduced fraction of the sample seeing as though the spectra were recorded before the runs to ensure full oxidation of the samples and the peak is found lower than where the reduced peak would be present around 73°C.

Freezing-induced heterogeneity has been seen in turnip and spinach cytochrome f after extended storage at -20°C (Metzger et al. 1997). This heterogeneity may be the reason two peaks show up in the DSC profiles for cytochrome f. To eliminate the possibility of insufficient purification and presence of other molecules in the sample the purity was confirmed by running the sample on an SDS-PAGE gel after the samples have been put through the Q-12 anion exchange column on the HPLC for a second time. The gel showed only one band for the protein.

It is possible that the two peaks seen in the tyrosine mutant profiles reflect the unfolding of each domain of the protein. Cytochrome f has a large domain and a small domain. It may be that the mutations made to the protein cause a conformational shift in the protein that allows us to see the unfolding of each domain separately in the DSC profiles.

The profiles of the R156L and R156K mutants are not sufficient to draw any conclusions. The R156L mutant failed to give a profile with any distinct peaks to analyze, and the R156K mutant couldn't be produced in enough yield to run the experiment. It appears that the mutants are not stable enough to undergo examination by DSC.

5.7 PLASMID CREATION, EXPRESSION, AND PURIFICATION OF CYTOCHROME C_6

The cytochrome c_6 gene insertion into the expression system utilizing the *C. reinhardtii* cytochrome f gene-containing plasmid pUCF2 allowed for the utilization of the same expression, harvesting, and purification techniques as cytochrome f. Once the cytochrome f gene was removed and replaced by that of cytochrome c_6 the expression was conducted by the co-transformation of the pUCF2 plasmid along with the pEC86 plasmid containing the genes that code for the molecular machinery that covalently attaches the heme to the apo-protein. The pelB leader sequence incorporated into the pUCF2 plasmid directs the exportation of the protein to the periplasm of the cell. Harvesting by osmotic shock allows only the release of the contents of the periplasm of the cell. The initial harvest yields about 1 - 2 mg protein/ L media on average per growth. Because the overall charge of the protein is negative, the first step in purification of the protein is a DE-53 anion exchange column. After the soluble fraction recovered from the osmotic shock is run bound to the column and eluted off with a salt gradient, the yield of the protein remains close to 1 - 2 mg protein / L media. The next step in the purification is a gel filtration column after which not much of the yield is lost. The final step in purification is another anion exchange column (Q-12) on an HPLC. This step in purification reduces the yield to about half the original concentration resulting in the final yield of the wild-type protein after expression and purification of about 0.5 - 1.0 mg / L.

5.8 DESIGN OF WILD-TYPE CYTOCHROME C_6 MUTANTS

The two mutants constructed were K29I and K57I. The K29 residue is a highly conserved (Kerfeld et al. 1995). This residue H-bonds to an oxygen atom of a heme propionate and so counter balances the negative charge of the propionate (Beissinger et al. 1998, Sawaya et al. 2001). It is considered a possible candidate for ligand replacement at high pH as seen in the alkaline transition of cytochrome c (Campos et al. 1993, Kerfeld et al. 1995) . It has also been suggested that mutation of this residue may lower the redox potential (Kerfeld et al. 1995). This residue is 10.0 angstroms from the heme iron and so would be a possible replacement considering cytochrome c's ligand replacements have been documented at 8.9 for horse c and 10.9 for human c (Ying et al. 2009). The K57 residue is also

highly conserved (Kerfeld et al. 1995). This residue flanks the heme crevice and H-bonds to a buried water molecule. It also serves to counter balance to the negative charge of the propionate (Beissinger et al. 1998). It is considered to be a possible candidate for ligand replacement at high pH (Campos et al. 1993, Dikiy et al. 2002). This residue is 10.4 angstroms from the heme iron and so would be a possible consideration for replacement (Ying et al. 2009). The mutations made were from positive lysine residues to neutral and non-titratable isoleucine residues.

5.9 SPECTRAL CHARACTERISTICS OF MUTANT AND WILD-TYPE CYTOCHROME C_6

Spectral characteristics of the wild-type cytochrome c_6 include a reduced α peak at 553nm which is indicative of a c-type cytochrome where the alpha peak typically lies between 549 and 556 nm (Pettigrew and Moore 1987). The oxidized spectrum reveals a peak at 693nm which is characteristic of methionine and histidine serving as axial ligands as typically seen in class I c-type, cytochromes (Pettigrew and Moore 1987). The mutants show a slight shift of the alpha peak to 552 nm. The spectrum for the wild-type *C. reinhardtii* cytochrome c_6 in the reduced state also includes a beta peak at 523 nm, and a Soret peak at 417 nm. In the spectrum of the oxidized protein the broadening of the alpha and beta peaks is observed compared to that of the reduced spectrum and the Soret peak is located between 411 nm and 412 nm. The K29I mutant reduced spectrum includes an alpha peak between 552 nm and 553 nm, a beta peak at 523 nm, and a Soret peak at 417 nm. In the spectrum of the oxidized protein the Soret peak is located between 411 nm and 412 nm. The K57I mutant reduced spectrum includes an alpha peak at 552 nm, a beta peak at 523 nm, and a Soret peak between 416 nm and 417 nm. In the spectrum of the oxidized protein the Soret peak is located between 411 nm and 412 nm. The difference between the spectrum of the wild-type and mutants indicates an alteration in the heme environment of the protein with the alteration of the residues (Ponamarev et al. 2000).

The peak positions of the spectrum of the wild-type and the mutants were monitored throughout the redox measurements which are represented in Tables 4.51, 4.5.2, and 4.5.3 on pages 107, 109, and 111. Peak shifts to higher wavelengths are noticed and are primarily at pH 9.0 and above. The wild-type shifts were seen in beta and Soret peaks in the reduced spectra and the Soret peak in the oxidized

spectra. The K29I mutant showed shifts in all peaks with the most substantial changed in both the oxidized and reduced Soret peaks. The K57I mutant has shifts in the beta peak and the oxidized Soret peak. The shifts being present at higher pH indicate that the environment around the heme is changed. This could be due to conformational shifts or partial unfolding of the protein.

5.10 MIDPOINT POTENTIALS OF MUTANT AND WILD-TYPE CYTOCHROME C_6 AND THE ABSENCE OF THE ALKALINE TRANSITION

The redox potential of cytochrome c_6 has been found to range from 340 - 390 mV throughout a range of species (Kerfeld et al.1995). The wild-type cytochrome c_6 was found to have a midpoint potential at pH 7 of 367 ± 10 mV. The K29I mutant was found to have an $E_{m,7}$ of 322 ± 5 mV. This value is 45 mV lower than that of the wild-type and being more than a 5 mV difference is considered significantly different indicating that the electrostatic interaction with the heme propionate functions to stabilize the reduced state of the protein relative to the oxidized state. The K57I $E_{m,7}$ value was also significantly different from that of the wild-type and was found to be 335 ± 2 mV, a decrease of about 30 mV. Since the midpoint potential of the mutant is lower when compared to the wild-type it can be concluded that the residues electrostatic interaction with the heme propionate serves to stabilize the reduced state of the heme iron in relation to the oxidized state.

Cytochrome c, exhibits an alkaline transition in which the redox potential becomes pH dependent at high pH. In the case of cytochrome c this has been attributed to replacement of the methionine sulfur serving as the sixth iron ligand by a deprotonated amino group (Smith and Millett 1980, Gadsby 1987, Ying et al. 2009). Previous studies also examined the dependence of the midpoint potential on pH for cytochrome c_6. The first study, conducted in 1993, examined the cytochrome c_6 from *Monoraphidium braunii*. In the study it was found that the midpoint potential of the protein is pH dependent and has an apparent pKa of about 9 (Campos et al. 1993). In 1997 the pH dependence of cytochrome c_6 from *Chlorella fusca* was examined, and it was found that the midpoint potential of the protein was also pH dependent with an apparent pKa of 8.7 (Inda et al. 1997). Another study conducted in 2002 examining

the cytochrome c_6 of *Cladophora glomerata* also found that the midpoint potential was dependent on pH and had an apparent pKa of 7.9 (Dikiy et al. 2002).

However, in examining the midpoint potential for both the wild-type cytochrome c_6 and the K29I and K57I mutants across the range of pH it was noticed that neither the wild-type nor either mutant has a decrease in the mid-point potential at higher pH's. The proteins were not able to be further reduced by latter additions of FoCN during titrations conducted at pH 10 and above. A buffer change was made to 100mM phosphate buffer at pH 10.0 with the wild-type to investigate if the lack of reduction could have been due to a buffer affect, but no difference was found in the titrations whether conducted aerobically or anaerobically. Data cannot be reproducibly collected using the current methods past pH 10. These results indicate that either the midpoint potentials of the proteins is pH independent or the pKa of the protein is above 10.

A comparison of the sequences of the protein to those known to be pH dependent reveals no clues to the reason for the difference. The amino acid sequence for *Chlamydomonas reinhardtii* shows five residues that vary from both the sequences of *Chlorella vulgaris/ fusca and Cladophora glomerata*. All five of these residues are highlighted in red in the sequence alignment given in Figure 5.10.1 and are highlighted in red. Each of these residues is located on the surface of the protein away from the heme. Because the residues are far enough away from the heme so as not to be able to interact with it or have an effect on the environment created around it, they are unlikely the cause for the lack of the alkaline transition.

Figure 5.10.1 Sequence alignment of cytochrome c_6 from *Chlamydomonas reinhardtii*, *Chlorella vulgaris* with the first 30 residues of *Chlorella fusca* substituted in, and *Cladophora glomerata* using ClustalW (Oku et al. 2002, Inda et al. 1997, Hill et. al. 1991, Dikiy et. al. 2002).

```
C. reinhardtii       -ADLALGAQVFNGNCAACHMGGRNSVMPEKTLDKAALEQYLDGGFKVESIIYQVENGKGA 59
C. vulgaris          RADLALGKQVFDGNCAACHAGGNNCVIPDHTLQKAALEQYLEGGFSVASIITQVENGKGA 60
C. glomererata       AELLADGKKVFAGNCAACHLGGNNSVLADKTLKKDAIEKYLEGGLTLEAIKYQVNNGKGA 60
                      ** * :** ******* **.*.*:.::**.* *:*:**:**:.: :*  **:*****

C. reinhardtii       MPAWADRLSEEEIQAVAEYVFKQATDAAWKY 90
C. vulgaris          MPAWSGRLDSDEIESVAEYVFKQAEGNLW-- 89
C. glomerata         MPAWADRLDEDDIEAVSNYVYDQAVNSKW-- 89
                     ****:.**..::*::*::**:.** .  *
```

5.11 DIFFERENTIAL SCANNING CALORIMETRY STUDIES ON CYTOCHROME C_6

The thermal stability of cytochrome c_6 was examined using differential scanning calorimetry. Since the protein folds irreversibly the only value able to be obtained was the melting temperature of the protein. The average T_m for the oxidized wild-type protein was found to be 78 ± 0.1°C. The reduced form of the protein had a melting temperature of 110 ± 0.3°C. Iso-1-cytochrome c from *Saccharomyces cerevisiae* has been found to have a T_m between 50 and 60°C at pH 6 according to studies conducted on the oxidized form of the protein (Liggins et al. 1994, Liggins et al. 1999). The T_m value given for the reduced state protein was given as 80°C at pH 4.7 (Lett et al. 1996). Both the values for the oxidized and reduced states of the iso-1-cytochrome c are lower than that the values established for the cytochrome c_6 of *Chlamydomonas reinhardtii* indicating that the cytochrome c_6 is more stable in both states than the iso-1-cytochrome c. This may be due in part to the relative content of glycine and alanine in the proteins. The small glycine and alanine residues comprise about 18% (18 of 103 residues) of the primary structure of iso-1-cytochrome c whereas the make up around 26% (23 of 90 residues) of the structure of cytochrome c_6. Proteins containing a higher percentage of small residues can have a more compact tertiary structure and as a result can be more thermally stable than proteins with a smaller percentage as seen here in the difference between iso-1-cytochrome c and cytochrome c_6. A sequence alignment of the two proteins can be seen in Figure 5.11.1.

The mutant average T_m's are lower at 70 ± 0.7°C for the K29I mutant and 70 ± 0.2°C for the K57I mutant. The significant reduction of the melting temperature of the mutants, 8°C for the K29I mutant and 7°C for the K57I mutant, relative to that of the wild-type protein indicates a reduction in the stability of the mutant proteins when compared to the wild-type. It is possible that the difference in stability between the mutants and the wild-type c_6 can be accounted for by the loss of electrostatic interaction with the heme propionate by each of the residues when mutated to isoleucine. Another possible contributing factor to the lower T_m of the mutants could be the loss of hydrogen bonds, K29 with the propionate of the heme and K57 with a buried water molecule found within the structure (Campos et al. 1993, Sawaya et al. 2001).

Figure 5.11.1 Sequence alignment of iso-1-cytochrome c from *Saccharomyces cerevesia* and cytochrome c_6 from *Clamydomonas reinhardttii* using ClustalW (Ernst et. al. 1985, Hill et. al. 1991).

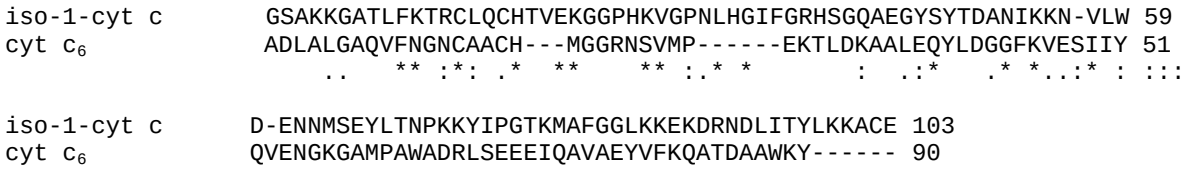
iso-1-cyt c GSAKKGATLFKTRCLQCHTVEKGGPHKVGPNLHGIFGRHSGQAEGYSYTDANIKKN-VLW 59
cyt c6 ADLALGAQVFNGNCAACH---MGGRNSVMP------EKTLDKAALEQYLDGGFKVESIIY 51
iso-1-cyt c D-ENNMSEYLTNPKKYIPGTKMAFGGLKKEKDRNDLITYLKKACE 103
cyt c6 QVENGKGAMPAWADRLSEEEIQAVAEYVFKQATDAAWKY------ 90

5.12 CD SPECTRAL ANALYSIS OF CYTOCHROME C_6

Circular dichroism has classically been used to elucidate secondary structure in proteins by examining the far UV region between 190nm and 250nm. However, this technique can also be utilized to observe alterations in the heme environment by focusing on the Soret or gamma-band region of 380nm – 440nm (Myer 1985). A number of cytochromes have been investigated with respect to their CD characteristics in the Soret region. This characterization is of particular interest because of the presence or absence of a negative Cotton effect seen in the oxidized spectra of a number of previously investigated cytochromes including *Spirulina maxima* cyt c_6, *Aphanzomenon flos-aquae* c_6, *Euglena gracilis* c_6, *Pseudomonas aeroginosa* c551, *Rhodospirillum rubrum* c_2, and *Escherichia coli* cytochrome 562 (Eades 1996).

It has been found that a conserved aromatic amino acid residue in the vicinity of the heme may be the reason for the negative Cotton effect seen in a number of recorded CD spectra previously obtained for different cytochromes as seen in Table 5.12.1. Tryptophan 88 in *C. reinhardtii* cytochrome c_6 is found to be in an equivalent position. Studies on mitochondrial ferri-cytochrome c have shown a presence of the negative peak and have conducted mutational studies in which the conserved phenylalanine 82 residue was mutated to the aromatic residue tyrosine and also to non-aromatic amino acids. The retention of the aromaticity of the residue resulted in a CD spectrum showing the negative Cotton effect. When the residue was mutated to a non-aromatic residue the negative peak disappeared (Rafferty et al. 1990, Zheng et al. 2000). Of the investigated cytochromes, it has been found that an aromatic amino acid in the vicinity of the heme, if it is oriented co-facially so that the π to π^* transition of the aromatic ring interacts directly with the π to π^* transition of the heme group, may be responsible for the intense negative Cotton effect seen around 419nm in the oxidized CD spectrum (Pielak et al. 1986). The oxidized CD spectra of *Euglena* does not show a negative Cotton effect and is the only previously examined cytochrome c_6 wild-type protein that does not contain a phenylalanine in the suspect position. The orientation of the tryptophan residue found in its place, however, is not known. The residue in *C. reinhardtii* is a tryptophan, and the crystal structure indicates that the residue is not co-facially oriented with respect to the heme (Kerfeld et al. 1995). This would lead us to expect to see no negative Cotton

effect in the CD spectrum of the ferri-cytochrome c_6 (Scharlau 1998).

In the CD spectra for the wild-cytochrome c_6 of *C. reinhardtii* there is an observed positive peak in the reduced spectrum located at 405 nm. The oxidized spectrum shows a positive peak located at 414 nm. Unlike many of the spectra seen previously for other cytochromes like those in Table 5.12.1, cytochrome c_6 of *C. reinhardtii* has no negative peak in the oxidized CD spectra. This implies the aromatic amino acid in the vicinity of the heme does in fact need to be co-facially oriented to be able to observe the negative Cotton effect around 419 nm.

Table 5.12.1 Invested cytochrome list indicating the presence or lack of the negative band and the orientation of the amino acid that may be responsible for the effect.

Source	Cytochrome	Aromatic amino acid in heme vicinity	Cofacial Orientation	Presence of negative peak	Reference
Saccharomyces cerevisiae	iso-1-c	Phe	yes	yes	Zheng et al. 2000, Pielak et al. 1986, Rafferty et al. 1990
Escherichia coli	c562	Phe	yes	yes	Bullock and Myer 1978
Spirulina maxima	c6	Phe	unknown	yes	Scharlau 1998
Aphanzomenon flos-aquae	c6	Phe	unknown	yes	Scharlau 1998
Pseudomonas aeroginosa	c551	none	N/A	no	Vinogradov and Zand 1968
Rhodospirillum rubrum	c2	Phe	no	no	Flatmark et al. 1968
Euglena gracilis	c6	Trp	unknown	no	Scharlau 1998
Chlamydomonas reinhardtii	c6	Trp	no	no	This work

CHAPTER 6 – CONCLUSION

In this work, two c-type cytochromes were investigated with respect to their midpoint potentials, the dependence of that midpoint potential on pH, and the thermal stability of the proteins. Residues surrounding the heme of the proteins, Y1, Y9, Y160, and R156 in cytochrome f and K29 and K57 in cytochrome c_6, were mutated to alter their interaction with the heme and to establish their contribution to the characteristics of the wild-type proteins.

Cytochrome f has a distinct fold when compared to cytochrome c of the mitochondria. It is primarily comprised of beta sheets and contains two domains. The ligation of the heme is also different having the alpha amino group of the n-terminal residue function as one of the axial ligands instead of a methionine residue as seen in mitochondrial cytochrome c. The redox potential of the cytochrome f for Chlamydomonas reinhardtti was found to be around 380 mV. The Y1F and Y9F mutations did not alter the redox potential neither did the Y160F mutant. A lower redox potential was observed for the Y160L mutant. This indicated that the aromaticity of the residue in the vicinity of the heme helps contribute to the more positive potential by either destabilization of the reduced state of the protein or the stabilization of the oxidized state. The R156 mutations to both leucine and lysine significantly lowered the redox potential. Because the mutation to lysine maintains the positive charge of the residue and in theory would not alter the interaction between the positive residue and the negative propionate one wouldn't expect to see a drop in the midpoint potential. The decrease in the potential indicates that the residue 156 must be maintained as an arginine in order to maintain the value of the potential. The redox potentials of the lysine mutants of cytochrome c_6 also varied from the wild-type. Either the removal of a positive charge and therefore the interaction of the residues with the negative propionate of the heme, or the loss of the residues abilities to hydrogen bond, K29 to the heme propionate and K57 to a buried water molecule, caused the redox potential of each of the mutants to be lower than that of the wild-type indicating either the stabilization of the oxidized state or the destabilization of the reduced state.

The pH dependence of the redox potential was examined for both proteins. In the case of cytochrome f where the midpoint potential of the wild-type protein is dependent on pH there is no ligand replacement as seen in cytochrome c. The residue responsible for the pH dependence of the potential

was not identified in these studies because all of the mutants that were able to be examined with the current methods had midpoint potentials that were dependent on pH. In the case of cytochrome c_6 it was found that the midpoint potential of the wild-type protein along with those of the mutants was independent of pH as far as pH 10. If there is a dependence of the potential then it must fall above pH 10.

The thermal stability of the oxidized and reduced forms of the wild-type proteins was examined using differential scanning calorimetry. The wild-type form of cytochrome f was found to be no different than the mutants thereof. The mutant profiles for the DSC runs showed two peaks around the T_m of the oxidized and the reduced state of the protein that can possibly be accounted for by either a freeze-induced heterogeneity of the sample or the unfolding of each domain of the protein separately. The melting temperatures for cytochrome c_6 wild-type were found to be higher than that those of cytochrome f indicating that in relation to cytochrome f cytochrome c_6 is more thermally stable. Both of the lysine mutants of the cytochrome c_6 had lower observed melting temperatures than the wild-type.

Cytochrome c_6 was also examined by CD spectroscopy in order to determine if there was negative Cotton effect in the spectra of the oxidized protein. The spectra, showing an absence of the negative peak around 419 nm, provides further evidence that the Cotton effect is a result of the co-facial orientation of an aromatic amino acid residue in the vicinity of the heme and not merely its proximity to the heme.

CHAPTER 7 – REFERENCES

Alexov, E. G., Gunner, M. *Biophysical Journal*. **1997**. 74: 2075-2093.

Akazaki, H., Kawai, F., Chida, H., Matsumoto, Y., Hirayama, M., Hoshikawa, K., Unzai, S., Hakamata, W., Nishio, T., Park, S.Y., Oku, T. *Acta Crystallogr Sect F Struct Biol Cryst Commun*. **2008**. 64: 674-80.

Baniulis, D., Yamashita, E., Zhang, H., Hasan, S. S., Cramer, W. A. *Photochemistry and Photobiology*. **2008**. 84: 1349–1358.

Beissinger, M., Sticht, H., Sutter, M., Ejchart, A. Haehnel, W., Roesch, P. *The EMBO Journal*. **1998**. 17: 27-36.

Berg, J., Tymoczko, J.L., Stryer, L. *Biochemistry*. 5th Ed. **2002**. Freeman, New York.

Bhise, A. *Coupling of Site-Directed Mutagenesis and Photo-Initiated Electron Transfer Studies Involiving Cytochrome f*. **2006**.

Blankenship, R. *Photosynth Res*. **1992**. 33. 91-111.

Bullock, P.A., Mayer, Y.P. *Biochemistry*. **1978**. 17: 3084-3091.

Campos, A.P. Aguiar, A.P., Hervas, M., Regalla, M., Navarro, J.A., Ortega, J.M., Xavier, A.V., De la Rosa, M.A., Teixeira, M. *Eur. J. Biochem*. **1993**. 216: 329-341.

Choquet, Y., Stern, D. B., Wostrikoff, K., Kuras, R., Girard-Bascou, J., Wollman, F.A. *PNAS*. **1998**. 95: 4380-4385.

Chi Y.I., Huang L.S., Zhang Z., Fernández-Velasco J.G., Berry E.A. *Biochemistry*. **2000**. 26: 7689-7701.

Chida, H., Yokoyama, T., Kawai, F., Nakazawa, A., Akazaki, H., Takayama, Y., Hirano, T., Suruga, K., Satoh, T., Yamada, S., Kawachi, R., Unzai, S., Nishio, T., Park, S.Y., Oku, T. *FEBS Lett*. **2006**. 580: 3763-8.

Collins T., D'Amico S., Georlette D., Marx J.C., Huston A.L., Feller G. *Analytical Biochemistry*. **2006**. 352: 299-301.

Copeland,A., Lucas,S., Lapidus,A., Barry,K., Detter,J.C., Glavina,T., Hammon,N., Israni,S., Pitluck,S., Saunders,E.H., Schmutz,J., Larimer,F., Land,M., Kyrpides,N., Mavrommatis,K., Richardson,P. US DOE Joint Genome Institute. **2005**. <http://www.ncbi.nlm.nih.gov/nuccore/75906225>

Copeland,A., Lucas,S., Lapidus,A., Glavina del Rio,T., Dalin,E.,Tice,H., Pitluck,S., Chain,P., Malfatti,S., Shin,M., Vergez,L., Schmutz,J., Larimer,F., Land,M., Hauser,L., Kyrpides,N., Kim,E.,Meeks,J.C., Elhai,J., Campbell,E.L., Thiel,T., Longmire,J., Potts,M., Atlas,R. US DOE Joint Genome Institute. **2008**. <http://www.ncbi.nlm.nih.gov/protein/YP_001865484.1>

Cramer W.A., Soriano G.M., Ponomarev M., Huang D., Zhang H., Martinez S.E., Smith J.L. *Annu Rev Plant Physiol Plant Mol Biol*. **1996**. 47: 477-508.

D'Amico, S., Feller, G.. *Anal Biochem*. **2009**. 385: 389-91.

Dikiy, A., Carpentier, W., Vandenberghe, I., Borsari, M., Safarov, N., Dikaya, E., Van Beeumen, J., Ciurli, S. *Biochemistry***. 2002**. 41: 14689-14699.

Eades, C.A. *Electron Transfer Proteins Functioning on the Oxidizing and Reducing Sides of Photosystem I*. **1996**.

Ernst, J.F., Hampsey, D.M., Sherman, F. *Genetics*. **1985**. 111: 233-241.

Flatmark, T., Robinson, A.B, *Structure and Function of Cytochromes*. **1968**. Univ. Tokyo Press. 318-327.

Gadsby, P.M., Peterson, J., Foote, N., Greenwood, C., Thomson, A.J. *Biochem J.* **1987**. 246: 43-54.

Genoscope - Centre National de Sequencage. **2008**. <http://www.ncbi.nlm.nih.gov/protein/CAT18795.1>

Goldberg, M. E., Expert-Bezancon, N., Vuillard, L., Rabilloud, T. *Folding & Design*. **1996**. 1: 21-27.

Gorman, D.S., Levine, R.P. **1965**. *PNAS*. 54: 1665-1669.

Gupta, R., He, Z., Luan, S. *Nature*. **2002**. 417: 567-71.

Haddadian, E.J., Gross, E.L. *Biophys J*. **2005**. 88: 2323-39.

Hauser, K., Mao, J., Gunner, M.R. *Biopolymers*. **2004**. 74: 51-54.

Hervás, M., Navarro, J.A., De La Rosa, M.A.. *Acc Chem Res*. **2003**. 36: 798-805.

Hill, K.L, Li, H.H., Singer, J. Merchant, S. *The Journal of Biol. Chem.* **1991.** 266: 15060-15067.

Inda, L.A., Medina, M., Saraiva, L.M., Gomez-Moreno, C., Teixeira, M., Peleato, M.L. *Photosynthesis Research*. **1997**. 54: 107-114.

Kallas, T., Spiller, S., Malkin, R. *Proc Natl Acad Sci U S A*. **1988**. 85: 5794-8.

Kadokura,K., Nagai,J., Mizuno,N., Minegishi,A., Nishio,T., Oku,T. **1998**. <http://www.ncbi.nlm.nih.gov/protein/7430459>

Kerfeld, C.A., Haroon, P.A., Interrante, R., Merchant, S., Yeates, T.O. *J. Mol. Biol*. **1995**. 250: 627-647.

Kerfeld, C.A., Krogman, D.W., *Annu. Rev. Plant Physiol. Mol. Biol*. **1998**. 49: 397-425.

Kerfeld,C.A., Sawaya,M.R., Krogmann,D.W., Yeates,T.O. *Acta Crystallogr. D Biol. Crystallogr.* **2002**. 58: 1104-1110.

Kurisu, G., Zhang, H,. Smith, JL., Cramer, WA. *Science.* **2003**. 302: 1009–14.

Lett, M.C., Berghuis, A.M., Frey, H.E., Lepock, J.R., Guillemette, G.J. *The Journal of Biological Chemistry*. **1996**. 271: 29088-29093.

Li,T., Zhao,J., Zhao,C., Liu,Z., Zhao,F., Marquardt,J.,Nomura,C.T., Persson,S., Detter,J.Chris., Richardson,P.M., Lanz,C., Schuster,S.C., Wang,J., Li,S., Huang,X., Cai,T., Yu,Z., Luo,J., Zhao,J., Bryant,D.A. Dept. of Biochemistry and Molecular Biology, The Pennsylvania State University. **2008**. <http://www.ncbi.nlm.nih.gov/protein/YP_001735624.1>

Liggins, J.R., Sherman, F., Mathews, A.J., Nall, B.T. *Biochemistry*. **1994**. 33: 9209-9219.

Liggins, J.R., Terence, P.L., Brayer, G.D., Nall, B.T. *Protein Science*. **1999**. 8: 2645-2654.

Lucas,S., Copeland,A., Lapidus,A., Glavina del Rio,T., Dalin,E.,Tice,H., Bruce,D., Goodwin,L., Pitluck,S., Chertkov,O., Brettin,T.,Detter,J.C., Han,C., Larimer,F., Land,M., Hauser,L., Kyrpides,N.,Mikhailova,N., Liberton,M., Stoeckel,J., Banerjee,A., Singh,A.,Page,L., Sato,H., Zhao,L., Sherman,L., Pakrasi,H., Richardson,P. US DOE Joint Genome Institute. **2008**. <http://www.ncbi.nlm.nih.gov/protein/YP_002379589.1>

Martinez, S.E., Huang, D., Ponomarev, M., Cramer, W.A., Smith, J.L. *Protein Science*. **1996**. 5: 1081-1092.

Maeda,S., Sugita,C., Sugita,M., Omata,T. *J. Biol. Chem*. **2006**. 281: 37868-37876.

Mejean,A., Mazmouz,R., Mann,S., Calteau,A., Medigue,C., Ploux,O. *J. Bacteriol*. **2010**. 192: 5264-5265.

Metzger, S.U., Cramer, W.A., Whitmarsh, J. *Biochimica et Biophysica Acta*. **1997**. 1319: 233-241.

Molina-Heredia, F.P., Wastl, J., Navarro, J.A., Bendall, D., Hervás, M., Howe, C., De la Rosa, M.A. *Nature*. **2003**. 424: 33-34.

Myer,Y.P. *Current Top. Bioenergetics*. **1985**. 14: 149-188.

Nakamura,Y., Kaneko,T., Sato,S., Mimuro,M., Miyashita,H., Tsuchiya,T., Sasamoto,S., Watanabe,A., Kawashima,K., Kishida,Y., Kiyokawa,C., Kohara,M., Matsumoto,M., Matsuno,A., Nakazaki,N., Shimpo,S., Takeuchi,C., Yamada,M.,Tabata,S. *DNA Res*. **2003**. 10: 137-145.

Navarro, J.A., Hervás, M., De la Rosa, M.A.. *Methods Mol Biol*. **2004**. 274: 79-92.

Okamoto,Y., Minami,Y., Matsubara,H., Sugimura,Y. *J. Biochem*. **1987**. 102: 1251-1260.

Oku, T., Mitsuda, Y., Chida, H., Atoh, A., Nishio, T., Kawachi, R.,Tanaka, Y. and Nakamura, T. College of Bioresource Sciences, Nihon University. **2002**. <http://www.ncbi.nlm.nih.gov/protein/BAC54100.1>

Oku,T., Chida,H., Sekino,A., Nakazawa,A. Department of Agricultural and Biological Chemistry,College of Bioresource Sciences, Nihon University. **2003**. <http://www.ncbi.nlm.nih.gov/protein/BAC85100.1>

Paoli, M., Marles-Wright, J., Smith, A. *DNA and Cell Biology*. **2002**. 21: 271-280.

Pettigrew, G.W., Moore, G.R. *Cytochromes c: Biological Aspects*. **1987**. Springer-Verlag, 17-23.

Pettigrew, G.W., Moore, G.R. *Cytochromes c: Evolutionary, Structural, and Physiochemical Aspects*. **1990**. Springer-Verlag, 309-311.

Pielak, G.J., Oikawa, K., Mauk, A.G., Smith, M., Kay, C.M. *J. Am. Chem. Soc*. **1986**. 108: 2724-2727.

Ponamarev, M.V., Schlarb, B,G., Howe, C.J., Carrell, C.J., Smith, J.L., Bendall, D.S., Cramer, W.A. *Biochemistry*. **2000**. 39: 5971-6.

Promega. Wizard Plus Minipreps DNA Purification System, Technical Bulletin. **2002**.

Rafferty, S.P., Pearce, L.L., Barker, P.D., Guillemette, J.G., Kay, C.M., Smith, M., Mauk, A.G. *Biochemistry*. **1990**. 29: 9365-9369.

Rogers, N.K., Moore, G.R., *Federation of European Biochemical Societies*. **1988**. 228: 69-73.

Sainz, G., Carrell, C. J., Ponamarev, M. V., Soriano, G. M., Cramer, W. A., Smith, J. L. *Biochemistry*. **2000**. *39* : 9164-9173.

Sawaya, M.R., Krogmann, D.W., Serag A., Ho, K.K., Yeates, T.O., Kerfeld, C.A. *Biochemistry*. **2001**. 40: 9215-9225.

Scharlau, M. *Studies on Cytochrome c_6 and Plastocyanin, Two Interchangeable Proteins Functioning Between the Cytochrome b_6f Complex and Photosystem I.* **1998**.

Schnackenberg, J., Than, M.E., Mann, K., Wiegand, G., Huber, R., Reuter, W. *J Mol Biol*. **1999**. 290:1019-30.

Shifman, J.M., Gibney, B.R., Sharp, R.E., Dutton, P.L.. *Biochemistry*. **2000**. 39: 14813-21.

Smith, H.T., Millett, F. *Biochemistry*. **1980**. 19: 1117-20.

Soriano, G.M., Ponamarev, M.V., Piskorowski, R.A., Kramer, W.A. *Biochemistry*. **1998**. 37: 15120- 15128.

Staiger, J. *An Analysis of Cation-Pi interactions in Cytochrome f*. **2007**.

Steiner,J.M., Serrano,A., Allmaier,G., Jakowitsch,J., Loffelhardt,W. *Eur. J. Biochem*. **2000**. 267: 4232-4241.

Stratagene. Quickchange II Site-Directed Mutagenesis Kit, Instruction Manual. **2004**.

Stroebel, D.; Choquet, Y.; Popot, J.L.; Picot, D. *Nature*. **2003**. 426: 413–8.

Taiz, L., Zeiger, E. *Plant Physiology* (4 ed.). **2006**. Sinauer Associates.

Vinogradov, S., Zand, R. *Archives of Biochem. Biophys*. **1968**. 125: 902-910.

Vuillard, L., Rabilloud, T., Goldberg, M.E. *Eur J Biochem*. **1998**. 256: 128-35.

Wastl, J., Bendall, D.S., Howe, C.J. *Trends Plant Sci*. **2002**. 7: 244-5.

Wastl, J., Purton, S., Bendall, D.S., Howe, C.J. *Trends Plant Sci*. **2004**. 9: 474-6.

Whitmarsh J., Govindjee, *The Photosynthetic Process in "Concepts in Photobiology: Photosynthesis and Photomorphogenesis*". **2001**. 11-51.

Worrall, J.A., Schlarb-Ridley, B.G., Reda, T., Marcaida, M.J., Moorlen, R.J., Wastl, J., Hirst, J., Bendall, D.S., Luisi, B.F., Howe, C.J. *J Am Chem Soc*. **2007**.129: 9468-75.

Yamada, S., Park, S.Y., Shimizu, H., Koshizuka, Y., Kadokura, K., Satoh, T., Suruga, K., Ogawa, M., Isogai, Y., Nishio, T., Shiro, Y., Oku, T. *Acta Crystallogr D Biol Crystallogr*. **2000**. 56: 1577-82.

Ying, T., Zhong, F., Xie, J., Feng, Y., Wang, Z., Huang, Z., Tan, X. J *Bioenerg Biomembr*. **2009.** 41: 251-257.

Zheng, J., Ye, S., Lu. T., Cotton, T.M., Chumanov, G. *Biopolymers*. **2000**. 57: 77-84.